# SPARGER DESIGN AS A CRITICAL COMPONENT OF A MILITARY FIELD-DEPLOYABLE AUTOTRANSFUSION SYSTEM


**BY**

**Tiffany Ethridge**


**This dissertation was submitted in part fulfillment of requirements for the degree of MSc Biomedical Engineering**

**in the**


**Department of Biomedical Engineering**

**UNIVERSITY OF STRATHCLYDE**


AUGUST 2015

This thesis is the result of the author's original research. It has been composed by the author and has not been previously submitted for examination which has led to the award of a degree.



Signed: Date:

FOR LANELL & DEAN, WITH LOVE

MANY THANKS TO TERRY GOURLAY AND HIS TEAM—
CRAIG ROBERTSON, CRAIG SIMPSON, AND MONICA HOPKINS

Uncontrolled haemorrhage is the primary cause of combat-related death, with most injured patients dying before reaching a medical facility. Most deaths due to haemorrhage occur within 10 minutes, and volume expanding fluids carried by field medics can be detrimental in cases involving massive blood loss. Currently the military utilises blood banking and buddy systems for whole blood transfusion; however the donor is limited to light duty post-donation, and whole donor blood is a limited resource. An ideal fluid resuscitation technique would involve autologous blood transfusion taken directly from a haemorrhaging wound. Current autotransfusion systems are not field-deployable due to size and electrical power requirements, and the larger project goal is to develop a field-deployable military autotransfusion system which is lightweight, compact, and manually operable. Beyond this project remit, a hand-crank pump has been developed to extract blood from the wound and transmit a blood-air mixture to a collection bag for initial blood processing. The current project aim is to design and fabricate a technology allowing the collection bag to remove air from the blood and filter larger sediment using a defoamer and filter sock device. This bag-attached flow device needs to (1) hold the defoamer and filter in place, (2) slow incoming fluid velocity, (3) disperse flow across the inner surface of the sock, and (4) direct flow without inducing haemolysis. A hemispherically-shaped sparger mechanism was developed over multiple design iterations to slow and radially disperse the flow. Hoods were used to hold the vertically hanging sock away from the sparger and assist in directing flow. Following a series of design modifications and laboratory testing, a successful design iteration was devised which acceptably slows flow and disperses it outward in all directions; future alterations and testing will be performed to improve flow direction and evaluate complete system functionality.

# Table of Contents

# List of Figures

# List of Tables

# Introduction

The treatment of haemorrhage on the battlefield is limited by what a medic can carry; currently the only first-line solutions for non-compressible haemorrhage are to contain the blood within a body cavity using wraps functionally similar to 'cling wrap,' or to intravenously infuse haemodiluting volume-expander solutions. The types of battlefield wounds, urgency of immediate haemorrhage care, and high prevalence of non-compressible haemorrhage in preventable deaths outline the importance of attempting to better address traumatic haemorrhage in the field. Fresh whole blood is a useful and therapeutic fluid in traumatic haemorrhage and is easier to locate and provide in austere situations compared to alternative treatments such as component therapy. Whole blood directly from the wound site is immediately available, immune-compatible, and capable of being autotransfused. These subjects will be discussed, along with reasoning and discussion of components in a novel field autotransfusion system. The component of the subsystem developed in this thesis will assist in removing air and contamination from blood.

## Types of Battlefield Wounds

Wound type prevalence is dependent on military branch. Each branch uses different weaponry, employs different tactics, and fights on different battlefields. Table 1 below outlines the injury distribution amongst the branches existing in wartime through the end of the Vietnam War in 1975. Ballistics, or penetrating missiles, were the cause of over 90% of infantry wounds. Soldiers riding in armoured vehicles such as tanks endured primarily ballistics and thermal injury at rates of 50% and 25% respectively. The naval branch experienced ballistic and thermal injury at rates of 25% and 30% respectively. Military air forces suffered a high rate of blunt trauma at 50% and also a significant amount of thermal injuries. Higher thermal injury rates are generally attributed to the soldiers' environments—being located in confined areas such as tanks, ships, and planes. (Champion, Bellamy, Roberts, & Leppaniemi, 2003)

**DISTRIBUTION OF INJURY MECHANISMS BY MILITARY BRANCH***

| | Infantry (%) | Armour (%) | Sea (%) | Air (%) |
|---|---|---|---|---|
| **BALLISTIC** | 90 | 50 | 25 | 5 |
| **BLUNT** | 2-3 | 5 | 10 | 50 |
| **BLAST** | 2-3 | 5 | 10 | <5 |
| **THERMAL** | 2-3 | 25 | 30 | 25 |
| **COMBINED** | <5 | 15 | 25 | 10 |

*statistics taken from data acquired through end of Vietnam War

**Table 1: Distribution of injury mechanisms by military branch (Champion, Bellamy, Roberts, & Leppaniemi, 2003)**

The highest blast injury rate is seen in the navy, but at a rate of 10% this made blast injury relatively uncommon. It is important to note a large portion of secondary blast injuries—those due to smaller pieces of debris propelled by an explosion—are grouped with ballistic injury because these fragments exert damage similar to bullets. Today blast wounds—any wounds from explosion—rival or supersede the number of bullet wounds due to evolving explosive weaponry and ever-improving armour. As shown in Table 2, using cavalry scout data taken from Afghanistan and Iraq between 2003 and 2011, explosives were responsible for 70% of casualties. (Schoenfeld, Dunn, Bader, & Belmont Jr, 2013)

| Injury Mechanism | Iraq, n (%) | Afghanistan, n (%) | Total (%) |
|---|---|---|---|
| *Gunshot wound* | 103 (17) | 26 (33) | 129 (18) |
| *Explosion* | 439 (71) | 49 (61) | 488 (70) |
| *Other* | 79 (13) | 5 (6) | 84 (12) |
| *Total* | 721 (100) | 80 (100) | 701 (100) |

**Table 2: Mechanisms of injury from 2003-2011 in cavalry scouts by location (Schoenfeld, Dunn, Bader, & Belmont Jr, 2013)**

The Wound Data and Munitions Effectiveness Team (WDMET) database is comprised of data from 7,989 patients in Vietnam. Distribution of injury mechanisms from the study is shown in Figure 1. (Champion, Bellamy, Roberts, & Leppaniemi, 2003)

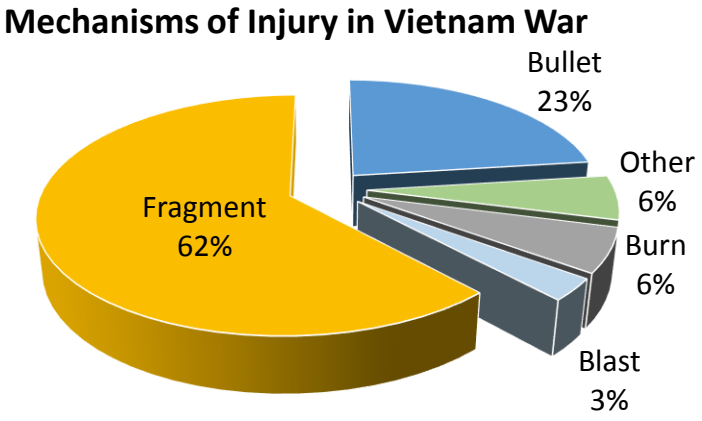


**Figure 1: Mechanisms of Injury in Vietnam War (Champion, Bellamy, Roberts, & Leppaniemi, 2003)**

Although explosive fragments were the primary cause of injury in the Vietnam War, the percentages of injury mechanisms change with each new conflict. Bullets were most common in the Northern Ireland and Somalia conflicts at 45% and 55% respectively.

Alternatively in Desert Storm, fragments were the cause of an overwhelming 95% of penetrating battlefield wounds. (Mabry, et al., 2000)

The most survivable wounds are those to the soft tissue and extremities, while wounds to the head and torso are predominantly fatal. Figure 2 below from the WDMET study outlines the sites and prevalence of fatal wounds. Ballistic injuries to the head and torso have lethality of 78% and 72% respectively. (Champion, Bellamy, Roberts, & Leppaniemi, 2003)

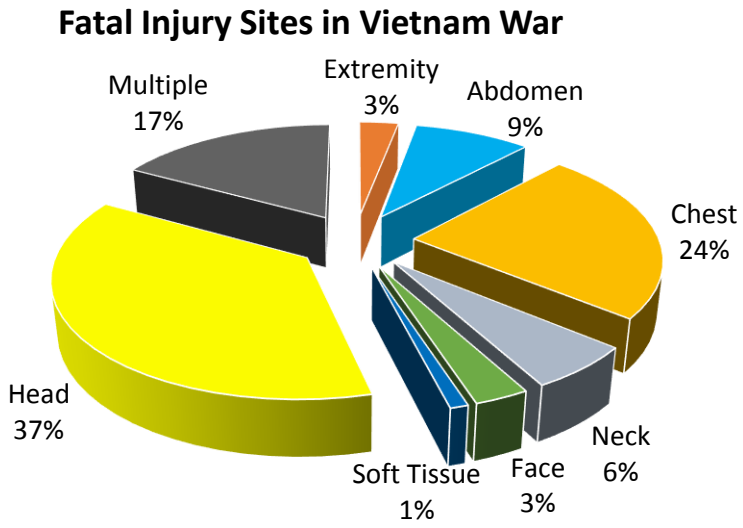


**Figure 2: Sites of Fatal Injuries in Vietnam War (Champion, Bellamy, Roberts, & Leppaniemi, 2003)**

Approximately 50% of mortal penetrating wounds are fatal due to excessive haemorrhage, with central nervous system damage being the other primary cause of mortality. The cessation of bleeding, commonly termed haemostasis, has been and continues to be a primary focus of military combat care. The WDMET database findings suggest approximately half of preventable battlefield deaths are due to haemorrhage from extremities. Consequently the military has invested significant time and money in developing more effective haemostatic agents. (Lawton, Granville-Chapman, & J, 2009)

## Urgency of Haemorrhage Management

A clinical trial run in the final 6 months of World War II in Italy involved both haemodynamic and biochemical measurements in critically wounded patients approximately 6.5 hours post-injury. Another term for shock is hypoperfusion—inadequate tissue perfusion causing oxygen and nutrient deficiency. Some pertinent results from this study are shown below in Table 3. Lethality rates more than double when blood loss increases from 34% to 46%. (Champion, Bellamy, Roberts, & Leppaniemi, 2003)

| **Correlations Among Blood Loss, Haemodynamic, and Outcome** | | | | |
|---|---|---|---|---|
| **Grade of Shock** | Blood Pressure Systolic/Diastolic (mmHg) | Heart Rate (beats/min) | Blood Loss (% blood vol.) | Lethality (%) |
| **None** | 126/75 | 103 | 14 | 16 |
| **Slight** | 109/66 | 111 | 21 | 12 |
| **Moderate** | 95/58 | 113 | 34 | 25 |
| **Severe** | 49/25 | 116 | 46 | 66 |

**Table 3: WWII findings showing correlations among haemodynamics, blood loss, and outcome (Champion, Bellamy, Roberts, & Leppaniemi, 2003)**

It is generally accepted 25% blood loss with systolic blood pressure (SBP) around 85 mmHg induces shock, and 60% blood loss with SBP under 50 mmHg leads to cerebral perfusion and death. Blood volumes less than 50% are usually fatal, as shown in the World War II study and again in studies as recent as 2003. (Champion, Bellamy, Roberts, & Leppaniemi, 2003)

Death due to haemorrhage is directly related to blood loss rate. U.S. soldiers have haemorrhaged to death in a combat zone over hours, but death generally occurs within 5 to 10 minutes. There is a very brief window to save patients with uncontrolled

haemorrhage and an SBP falling below 90 mmHg; this finding is backed up by the World War II study findings shown in Table 3. Controlling the rate of blood loss to avoid massive drops in blood pressure would be a valuable immediate tactic to increase survival chances. Patients undergoing slower rates of blood loss could possibly undergo tactics to prolong the "golden hour"—the time in which medical treatment is most likely to prevent death—until more comprehensive care can be provided. Military doctors suggest at least 10% of soldiers who die from truncal haemorrhage have wounds correctable with surgery. (Champion, Bellamy, Roberts, & Leppaniemi, 2003)

Soldiers killed in action (KIA) die before reaching medical care at an aid station, while those listed as dying of wounds (DOW) die after arrival. A retrospective study of 4,596 fatalities in Operations Iraqi and Enduring Freedom between 2001 and 2011 was published by Eastridge *et al.* It focused primarily on casualties who died before reaching a support hospital. 'Potentially survivable' (PS) is defined in the military as a wound or condition which the casualty has survival potential under ideal conditions; ideal conditions involve availability of all the proper equipment and facilities, and use of latest techniques. The study revealed 87.3% of fatalities were KIA; additionally 24.3% of these KIA deaths were classified as PS (Figure 3).

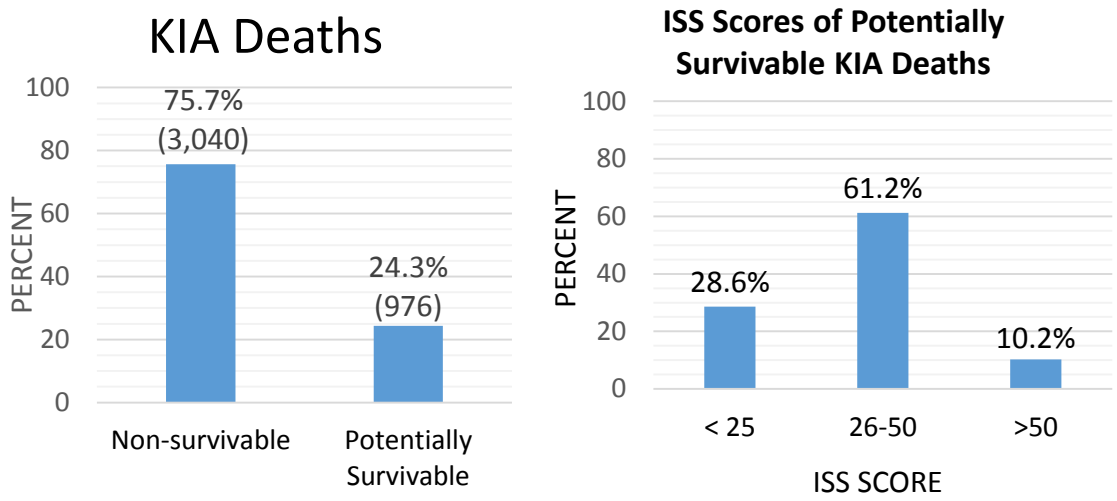


**Figure 3: Survivability of KIA casualties (left) and ISS scores of potentially survivable subset (Eastridge, et al., 2012)**

A majority of these potentially survivable KIA deaths involved wounds with an injury severity score (ISS) between 26 and 50. (Eastridge, et al., 2012) The ISS is one of the most-used measures of injury severity and is considered the 'gold standard' in trauma grading; a score over 15 is broadly considered major trauma. (Palmer, 2007)

## Truncal Haemorrhage

A large majority (80%) of excessive haemorrhage deaths occur from torso wounds, and only 20% of these involve potentially compressible vessels coming from the neck or limbs. (Champion, Bellamy, Roberts, & Leppaniemi, 2003) Truncal, or non-compressible, haemorrhage accounts for over two-thirds of haemorrhagic deaths. (Holcomb, et al., June 2007) Much research is being done regarding methods and materials to decrease uncontrollable haemorrhage. (Lawton, Granville-Chapman, & J, 2009) Currently field medics have no real solutions for addressing non-compressible haemorrhage beyond administrating intravenous fluids (volume-expanders) and attempting to confine bleeding with compression wraps.

Killed-in-action rates have remained fairly steady around 20% for the last 150 years. (Champion, Bellamy, Roberts, & Leppaniemi, 2003) Many soldiers with non-compressible haemorrhage are KIA due to failure to control bleeding and lack of tactics to sustain the body until reaching a facility. Evacuation to surgical care typically takes 6 or more hours in urban conflicts due to buildings and nearby combatants. Armoured vehicles on city streets can easily be struck by antitank rockets or RPGs, while crossing streets and moving through debris on foot is dangerous and difficult. (Mabry, et al., 2000)

The 2002 urban combat situation of Israeli Defence Force (IDF) operations in West Bank Palestinian refugee camps revealed an increase from 13% to 48% in bullet wounds and an increase in chest and abdominal wounds from 19% to 27% compared to earlier urban combat in Lebanon. Death from or related to blood loss also increased from 41% to 56% even though evacuation times averaged an expeditious 53 minutes. (Champion, Bellamy, Roberts, & Leppaniemi, 2003) This data is evidence the urban landscape is a unique and

exceptionally deadly battlefield, and it also emphasises the need for immediate haemorrhage control in the field.

Truncal haemorrhage is the principal source of potentially survivable battlefield deaths. Figure 4 below from the Eastridge *et al.* 2012 study shows haemorrhage as the predominant cause of death in PS battlefield casualties with truncal haemorrhage consisting of 67.3% of this subset. These wounds cannot be treated with tourniquets or compression, and the patient generally dies from blood loss within minutes.

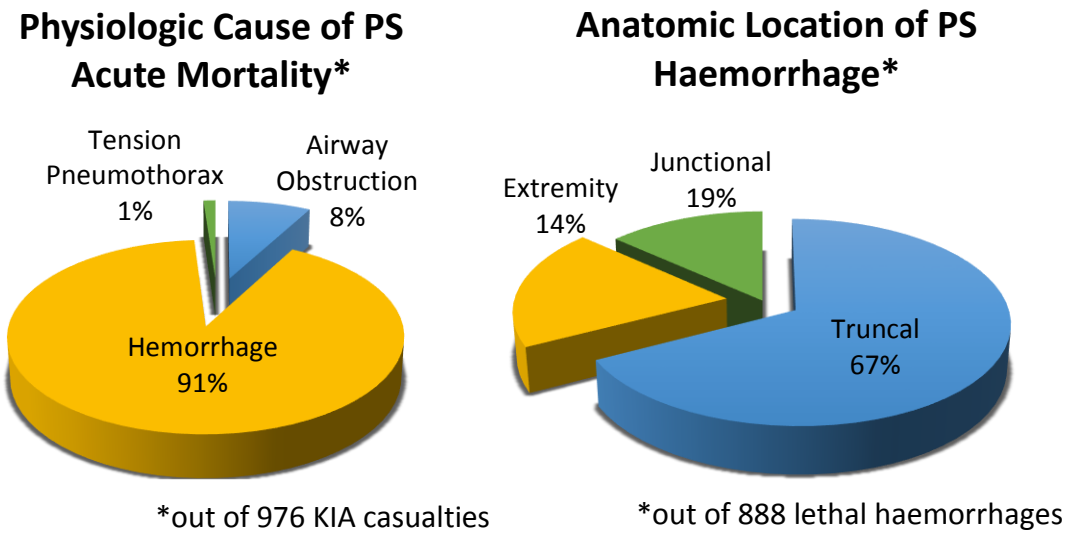


**Figure 4: Physiologic causes of PS battlefield deaths (left) and location of lethal haemorrhages (right) (Eastridge, et al., 2012)**

A study published in 2008 regarding medical statistics from Operations Iraqi Freedom and Enduring Freedom re-emphasised the impact of truncal haemorrhage in battle. Iraqi Freedom and Enduring Freedom fatality records for this study revealed potentially survivable cases to comprise 19% (out of 486) and 28% (out of 496) of fatalities. Truncal haemorrhage was found to be the largest contributor to cause of death in these cases at 87% and 83% respectively. (Kelly, et al., 2008) These findings closely resemble study results in a previous U.S. Special Operations Forces (SOF) study. (Holcomb, et al., June 2007)

## Fluid Resuscitation: Colloids & Crystalloids

Severe haemorrhage is the primary cause of acute intravascular volume loss and can lead to traumatic shock. Fluids must be transfused in large quantities, a process termed aggressive fluid resuscitation, to combat this volume loss. Volume loss can trigger a widespread and complex variety of physiologic regulatory responses as the body attempts to maintain adequate flow to the vascular beds of the most essential organs—heart, brain, and kidneys. (Phillips & Davis, 2014) Fragments propelled by explosions can cause significant tissue damage, massive haemorrhage and death in minutes without fluid resuscitation. (Rose & Grande, 1998)

Fluids used for resuscitation are separated into two primary categories, colloids and crystalloids. Colloids can either be natural—primarily blood or its primary protein albumin—or synthetic; synthetic colloids include gelatine, dextran solutions, and hydroxyethyl starches. Colloids have high molecular weight and remain in the intravascular space, preserving high osmotic pressure in the blood. In contrast crystalloids are water-based solutions containing mineral salts or other water-soluble molecules which lead to haemodilution; they increase interstitial and extracellular volume, and they are much cheaper to produce than colloids. (Gan, 2011)

In the military the two primary crystalloids primarily used for initial resuscitation are 0.9% sodium chloride (NaCl) and lactated Ringer's. NaCl is an isotonic crystalloid chosen for fluid resuscitation whenever a head injury may have occurred. Lactated Ringer's is more physiologic, as it contains both calcium and potassium electrolytes and more closely mimics the body's sodium and chloride ion concentrations. However lactated Ringer's can activate the coagulation cascade leading to clot formation, so it is avoided if blood or blood products are administered simultaneously. Crystalloids with glucose can cause cerebral oedema and also trigger increased urination so they are generally avoided. Hypertonic saline and more recently hypertonic saline with 6% dextran have met with mixed success involving small volume resuscitation; large volume resuscitation

still presents the unavoidable issue of haemodilution due to the volume expanders' water-based nature. (Rose & Grande, 1998)

Oedema, or excess water in body tissues and cavities, is a central issue in the debate between colloids versus crystalloids. Crystalloid fluids can induce oedema, which in turn can damage haemostatic capabilities and trigger anaphylaxis (whole-body allergic reaction) amongst other undesired consequences. (Gan, 2011) Most clinicians prefer to use a combination of blood or blood products and crystalloids; in the field blood components are hard to come by and medics are limited in the amount of crystalloids they can carry while responding.

Multiple studies have found aggressive crystalloid fluid therapy increases risk of re-bleeding and can lend to uncontrolled haemorrhage. One study involved a sample of 1,754 patients with moderate to severe blunt trauma requiring significant transfusion due to haemorrhage within 12 hours post-incident. Figure 5 shows the incidence of complications versus crystalloid volume within the first 24 hours post-injury.

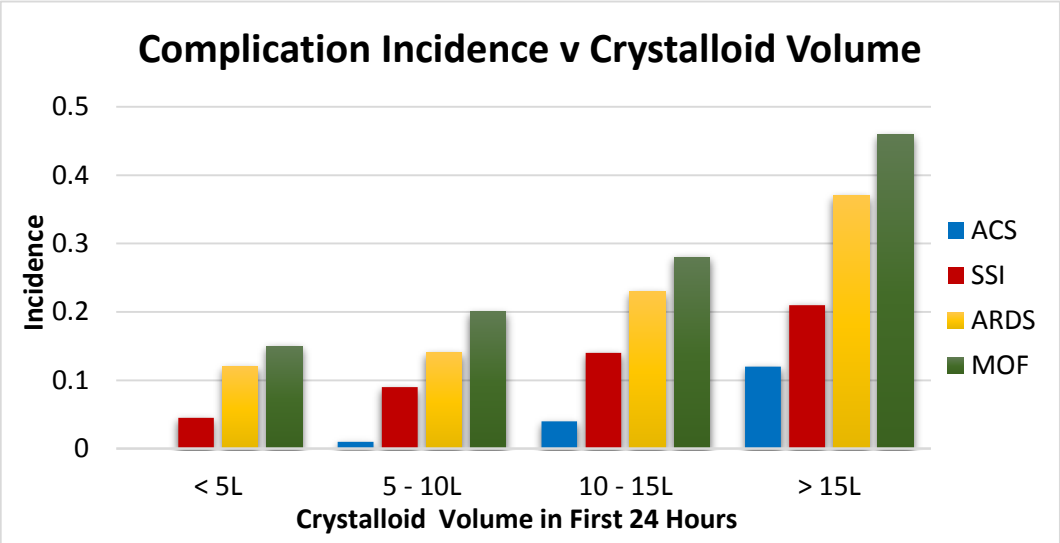


**Figure 5: Crystalloid transfusion volume and incidence (shown by ratio of probability) of ARDS, multiple organ failure, abdominal compartment syndrome, and surgical site infection (Kasotakis, et al., 2013)**

Crystalloid volume was linked to increased days on a mechanical ventilator, in the ICU, and in the hospital. Patients receiving 10-15L crystalloid in the first 24 hours were five times more likely to develop abdominal compartment syndrome (organ dysfunction due to increased abdominal pressure); those receiving more than 15L were nine times more likely compared to patients who received 5-10L. (Kasotakis, et al., 2013)

Table 4 outlines the primary advantages and disadvantages of the two primary crystalloid fluids used in first echelon medic response. Glomerular filtration rate (GFR) is an estimate of how much blood passes through the tiny waste filters called glomeruli in the kidney. These two crystalloids share the same disadvantages, including the fact at least 3x the lost blood volume must be replaced with crystalloid fluid. (Rose & Grande, 1998)

| **Primary Crystalloid Fluids Used by Military Field Medics** | | |
|---|---|---|
| **Solution** | **Advantages** | **Disadvantages** |
| **0.9% NaCl** | Inexpensive<br>Blood Compatible<br>Replenishes extracellular fluid space<br>Increases GFR | Non-physiological $Na^+$ and $Cl^-$ concentrations<br>Contributes to interstitial oedema<br>Large volumes required for replacing blood loss (≥ threefold) |
| **Lactated Ringer's** | Inexpensive<br>Physiologic electrolyte concentrations<br>Replenishes extracellular fluid space<br>Increases GFR | |

**Table 4: Advantages and disadvantages of primary crystalloids used by field medics (Rose & Grande, 1998)**

## The 'Bloody Vicious Cycle' of Trauma

A 'vicious cycle' of major abdominal vascular injury was described by Kashuk *et al.* in 1982 (shown below in Figure 6). Massive haemorrhage causes tissues to lose oxygen and becomes hypoperfused triggering a hypoxic state. Hypoxia worsens any hypothermia caused by both blood loss and significant fluid resuscitation; also hypoxia in trauma patients significantly contributes to acidosis, which is arterial pH under 7.35 (normal is 7.35-7.45). (Kashuk, Moore, Millikan, & Moore, 1982)

Hypothermia occurs when the body's core temperature drops below 35°C; 46% of trauma patients needing invasive abdominal surgery are hypothermic, while 21% of all critically wounded patients are hypothermic. This condition can alter both intrinsic and extrinsic blood coagulation pathways and possibly affect platelet activity. Any transfused fluids can contribute to hypothermia if not warmed to 40°C. (Hsu & Pham, 2011)

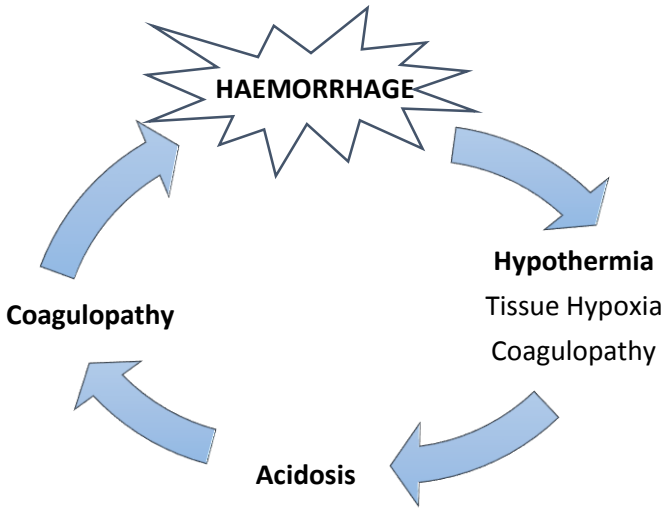


**Figure 6: 'Vicious Cycle' of Major Abdominal Vascular Injury (Kashuk, Moore, Millikan, & Moore, 1982)**

As hypoxia worsens, lactic acid accumulates in the tissues eventually causing the body's pH to drop significantly—a condition termed severe metabolic acidosis. Fluids typically used in excessive resuscitation tend to be unbalanced crystalloid solutions like normal

saline; these solutions have pH values significantly more acidic than normal blood (e.g. saline has a pH of 5.5) lending to metabolic acidosis. Respiratory acidosis can also occur, increasing $CO_2$ levels due to hypoventilation. Coagulopathy is the impairment of the blood's ability to timely and properly clot. Both hypothermia and acidosis further damage coagulation factors; continued coagulopathy can in turn trigger secondary, or delayed, haemorrhage. (Gerecht, 2014)

The term 'massive transfusion' (MT) has multiple definitions, but the primary definition is transfusion of at least 10 red blood cell units in under 24 hours. Amongst patients arriving at civilian trauma centres, generally 1-3% need a MT while 15% of the most acutely injured patients require one. Severely wounded combat victims are likely to need a MT given the weaponry, tactics, and environments involved. In 2007 it was estimated 5% of patients admitted to U.S. combat hospitals in Iraq needed a MT. (Borgman, et al., 2007) This statistic is deceiving because it does not account for the vast number of soldiers KIA, most of whom die from non-compressible haemorrhage. Most combat victims requiring MT need it in the field, long before reaching a trauma centre.

The mortality rate of those admitted combat victims needing MTs is over 30%; such high mortality is due to this 'vicious cycle' also termed the 'lethal triad' of hypothermia, metabolic acidosis, and coagulopathy. Additionally the trauma itself directly induces coagulopathy in nearly 30% of transfusion cases, and this patient subset is referred to as experiencing coagulopathy of trauma. (Borgman, et al., 2007)

## Acute Traumatic Coagulopathy & Haemostatic Resuscitation

In 2003 Brohi *et al.* reported a retrospective study involving 1,088 trauma patients. Approximately 25% of these patients arrived with an acute coagulopathy and were found to be four times more likely to die than other patients with coagulopathy. This early coagulopathy subset of patients has been seen in other studies across more than 20,000 patients. (Brohi, Cohen, & Davenport, 2007)

Hypoperfusion, or shock, is now believed to cause acute traumatic coagulopathy; this is contrary to the former assumption that acidosis, hypothermia, depletion of clotting factors, and blood dilution can directly attribute to all coagulopathy cases. (Brohi, Cohen, & Davenport, 2007) Base deficit (BD) is a clinical measure of metabolic acidosis. It is defined as the amount of base solution needed to bring 1L of acidotic blood to a normal pH of 7.4 (units of mEq/l); the greater the BD, the more acidic the blood. Ranges of 2-5, 6-15, and >15 indicate mild, moderate, and severe hypoperfusion respectively. (Schulman, 2003)

Studies have revealed no patient with a normal BD has prolonged prothrombin or partial thromboplastin times. Alternatively, patients with increasing systemic hypoperfusion exhibit a lengthening of clotting time directly dependent on degree of hypoperfusion. Prevalence of prolonged clotting time is 20% in patients with a BD above 6. (Brohi, Cohen, & Davenport, 2007)

Over one third of patients at the Combat Surgical Hospital or Emergency Department are admitted with acute traumatic coagulopathy, which has an overall mortality of 80%. Haemostatic resuscitation (HR) is the early treatment known to help prevent and treat this coagulopathy. (Bowling & Pennardt, 2010) HR entails both minimising crystalloid-based resuscitation while immediately employing necessary blood products; it also involves prevention of acidosis and hypothermia. The high chloride content of saline and other crystalloid solutions can aggravate hypothermia and acidosis while possibly increasing systemic inflammation which plays a role in coagulopathy of trauma. (Gerecht)

The HR process can involve fresh whole blood (FWB), stored-packed RBCs, fresh-frozen plasma (FFP), platelets, the coagulation end product fibrinogen, or recombinant coagulation factor VIIa. The HR products used in the military today are whole blood and its primary components (RBCs, plasma, platelets). This approach generally calls for transfusion of RBCs, plasma, and platelets in a 1:1:1 ratio, with fresh RBCs being

preferred to pRBCs. Recombinant fibrinogen is currently being evaluated by the US Army as a haemostasis aid, while recombinant factor VIIa is also undergoing studies and looks promising for patients receiving MT for both blunt and penetrating trauma. (McMullin, Holcomb, & Sondeen, 2006)

## Component Therapy

After World War I, the process of blood component fractionation became possible; whole blood and its separate components were banked, and RBCs, FFP, and platelets began being used in regular trauma management protocols. pRBCs and whole blood tend to be administered with crystalloid. Fresh-frozen plasma is good for replacing lost coagulation factors in haemorrhaging patients and is indicated for MT. Platelets are used when thrombocytopoenia (platelet deficiency) is contributing to haemorrhage and platelet counts drop below $50x10^9$/L; administration is indicated in large volume haemorrhage. (Kaplan & Maerz, 2015) Findings of a US army combat support hospital study involving 246 patients indicate a FFP to pRBC ratio of 1:1.4 is independently associated with improved survival, while a 1:1 ratio should be used in massive transfusion for trauma patients with insufficient clotting. (Borgman, et al., 2007)

Although RBCs have a refrigerated storage length of up to 42 days, there is a lack of prospective studies looking at increased storage time in critically wounded and ill patients. Platelets and FFP can only be stored for 48 hours and are generally not available in more forward combat zones; additionally FFP is hard to find and is seldom available at the forward hospitals. (Rose & Grande, 1998) According to Army Ranger data from conflicts in Somalia, one-third of the FFP bags fractured when thawed. Operating surgeons at this time had to use fresh, warm, whole blood and reported being impressed with how it contributed to stopping diffuse coagulopathy. (Mabry, et al., 2000)

Component therapy is a standard method of haemostatic resuscitation, but components are stored with added anticoagulants and must be refrigerated or frozen until use. They must then be thawed and warmed to approximately 40°C before administration to avoid inducing or worsening hypothermia. These restrictions make CT too burdensome for SOF medics and other primary responder medics in militaries around the world. (Bowling & Pennardt, 2010)

Use of CT in cases involving massive transfusion can worsen the 'lethal triad' of trauma. Complications due to CT contribute to the 'lethal triad' and become exaggerated in MT; these include hypothermia, thrombocytopoenia, and hypocalcaemia. (Repine, Perkins, Kauvar, & Blackborne, 2006) Also long-term storage of RBCs (≥ 28 days) is thought to be associated with deep vein thrombosis and MOF if ≥5 RBC units are transfused. (Spinella, Carroll, Staff, Gross, & Mc Quay, 2009)

## Fresh Whole Blood Transfusions

Fresh whole blood is defined as blood collected and stored at 22°C for up to 24 hours; more recent findings have indicated FWB can be stored at 22°C for as long as 72 hours. Shelf life of refrigerated whole blood is 21-35 days depending on the amounts of anticoagulants and preservatives added before storage. (Perkins, Cap, Weiss, Reid, & Bolan, 2008) One whole blood donation consists of 450-500ml blood with haematocrit ≥38%. Haematocrit is packed cell volume (PCV), or the volume percentage of RBCs in blood. (Avery Jr & Avery, 2010)

In 1910 it was acknowledged whole blood could improve platelet counts and moderate bleeding in patients with low platelets. (Perkins, Cap, Weiss, Reid, & Bolan, 2008) Fresh whole blood was incorporated in both British and American hospital practices in WWI after the advent of storage solutions in 1915. Stored whole blood was used significantly in WWII, with approximately 500,000 units stored and shipped to US military hospitals

over one 13-month period. (Spinella, Warm fresh whole blood transfusion for severe hemorrhage: U.S. military and potential civilian applications, 2008)

The advent of blood fractionation heralded an end to whole blood transfusions as a primary general protocol because CT is cost-effective, targeted, efficient and safe. However whole blood is still advised in cases involving cardiac surgery and MT. (Spinella, Warm fresh whole blood transfusion for severe hemorrhage: U.S. military and potential civilian applications, 2008) The other situation calling for fresh whole blood is when RBC component therapy is not available and transfusion is required urgently and without delay to address severe, uncontrollable haemorrhage. This situation, although uncommon in civilian settings, is common in warfare.

FWB is able to counter diluting effects of haemorrhage, manages microvascular bleeding and cytopoenia (reduced RBCs), conserves time in emergent situations, and limits donor exposure when the patient needs multiple components. (Perkins, Cap, Weiss, Reid, & Bolan, 2008) Transfusing older RBCs into severe trauma patients can result in adverse outcomes avoidable with FWB use. Fresh whole blood has high efficacy in treating both shock and coagulopathy, and it does not exacerbate endothelial or immune dysfunction. Old RBCs which undergo a certain amount of lysis have been seen to damage endothelial cells; endothelial damage has also been seen after administration of platelets in component therapy. (Spinella, Whole Blood vs Components for Hemorrhagic Shock, 2013)

The primary risk with FWB transfusion is infectious disease transmission, which is minimised using rapid (15-minute) screening tests (Arai, Petchclai, Khupulsup, Kurimura, & Takeda, 1999). But in cases where screening cannot be done due to either lack of materials or time, the risk of disease is present. Blood must always be typed and cross-matched, meaning the donor blood is tested with patient plasma to check for aggregation of antibodies and antigens. If blood types of both donor and recipient are

not known or cross-matching cannot be performed, there is a significant risk of immune responses leading to an uncontrollable clotting cascade termed an acute haemolytic transfusion reaction.

## Fresh Whole Blood vs Component Therapy

A 2009 retrospective study involving patients with similar traumatic haemorrhage, 100 receiving FWB and 254 receiving CT, revealed FWB is associated with 30-day survival in trauma patients with haemorrhagic shock. This was the first large retrospective study to examine 24-hour and 30-day survival of these two groups. FWB was seen to independently improve 30-day survive, with a comparative 113% increase in 30-day survival. Speculated causes of this observation include FWB has increased plasma and platelet function and concentration, the increased amount of anticoagulants and additives administered to the CT group, and aged RBCs (storage > 14-21 days) were rarely needed in FWB transfusion. (Spinella, Perkins, Grathwohl, & Beekley, Warm Fresh Whole Blood Is Independently Associated With Improved Survival for Patients With Combat-Related Traumatic Injuries, 2009)

In haemorrhagic shock patients, stored whole blood is also associated with lower donor exposures, better resuscitation, and improved haemostasis compared to CT. Also one unit of stored FWB has the haemostatic effect of 8-10 platelet units. Storage of whole blood does have negative consequences of decreased function of platelets and certain coagulation factors. Warm FWB (WFWB) is still recommended for first-line haemorrhagic shock therapy whenever feasible.

WFWB is used within 6 hours of collection because it is not refrigerated; no cold exposure means no impaired platelets. A 1991 study of paediatric (<2 years) open-heart patients compared those receiving post-operative WFWB, FWB used 24-48 hours after donation, and CT. The largest prolongation of coagulation time along with increasing levels of

bleeding were seen in the CT group. FWB and WFWB were seen to exhibit similar haemostatic effects. (Manno, et al., 1991)

Blood fractionation and component therapy allow for more efficient use of blood components. The components are processed, tested, and freeze-dried, then reconstituted before use. Component therapy eliminates what is largely considered an impractical and wasteful practice of using whole blood. However the storage and administration of blood components make it impossible for most field use. (Kauvar, Holcomb, Norris, & Hess, 2006)

While combat support and field hospitals have equipment to freeze and thaw fresh-frozen plasma and platelets, forward surgical units and centres do not. When there is large need for aggressive resuscitation, WFWB can be called for because blood banks generally prove limited in both supply and staff. FWB, warm or otherwise, is the advisable choice in forward combat care or whenever CT supply can be interrupted. (Repine, Perkins, Kauvar, & Blackborne, 2006) In the real-life emergent disaster caused by the September 11 attacks, the Red Cross proved capable of collecting sufficient quantities of WFWB to meet need.

Use of WFWB may be the only efficient resuscitation method for field responders to combat haemorrhage-associated coagulation dysfunction within the first minutes of an injury. Special Operations Forces medics need only carry a collection bag, blood administration set, and blood typing cards in addition to their normal equipment. A comprehensive direct comparison of WFWB and CT is shown below in Table 5.

**SIDE-BY-SIDE COMPARISON OF WFWB VS. CT**

| | Temp (°C) | Hct (% RBCs) | Platelets | Coag. Factor % | Fibrinogen | Anticoag. & Additives |
|---|---|---|---|---|---|---|
| ***WFWB*** | 37 | 38-50% | 150,000-400,000 | 100% | 1500mg | 63ml |
| ***CT*** | -30 to 0 | 29% | 80,000 | 65% (of initial) | 750mg | 205ml |

**Table 5: Comparison of WFWB vs component therapy (Kauvar, Holcomb, Norris, & Hess, 2006)**

Although one unit of WFWB is the approximate volume equivalent of one unit of CT, WFWB does not require warming, has higher RBC and platelet concentrations, contains significantly more coagulation factors, and has double the fibrinogen. Battlefield pRBCs must be stores in what is termed a 'golden hour container' which keeps products cold for 72 hours. Although it is portable, it is battery-powered and must be recharged. (Rice)

Administered anticoagulants can aggravate coagulopathy and the 'lethal triad.' FWB has also been shown in clinical settings to improve the body's clotting abilities and contributes to reversal of dilutional coagulopathy. (Kauvar, Holcomb, Norris, & Hess, 2006)

## Fresh Whole Blood in the Field

British military medics and their US counterparts have a limited first-line arsenal to combat battlefield injury. They carry de-nerving agents for pain, tourniquets to control bleeding when possible, gauze and dry fibrin sealant dressings, and wrap dressings similar to cling film to control haemorrhage. Wraps are intended to compress wounds and promote coagulation or confine bleeding within internal cavities. Most medics also

carry crystalloid fluids such as 0.9% NaCl for fluid resuscitation. Field medics currently have no immediate method of managing or increasing survival odds of non-compressible truncal haemorrhage casualties beyond containing bleeding within a body cavity.

United States SOF medics have been confirmed able to safely perform collection and administration of WFWB in austere settings; this confirmation was given by the non-commissioned officer in charge of the Special Operations Combat Medic Skills Sustainment course in 2009. SOF medics and all first-echelon field medics in combat must be fitted with proper equipment and receive necessary training in WFWB transfusion. This skill sustainment training course has been in effect since 2004, and the primary source of error in the practice sessions were bags not full enough to use properly (15% incidence). (Bowling & Pennardt, 2010)


**Figure 7: US Army (top) and Marine Corps (bottom) combat medic lifesaver bags (Chinook Medical Gear)**

Transfusion reactions and pathogen transmission are the two primary risks of FWB transfusions; blood-typing cards address the first issue by providing blood type results within 10 minutes. In the US a recently FDA-approved card named ABORhCard© developed by Micronics, Inc. has come to market which is credit card-sized and provides results in under one minute. Whole blood cross-match tests have been developed and protocols outlined in military manuals, but type-specific blood which has not been cross-matched has been used often in military circumstances without serious consequences. An important point to remember is only type-specific FWB should be used in a transfusion, as there is no 'universal donor' for FWB. This 'universal donor' belief comes from erroneous references to pRBCs—a blood component—as 'blood.' (Bowling & Pennardt, 2010)

Rapid infectious disease screening tests exist which are small and lightweight—easy for a medic to carry; these tests significantly lessen risk of blood borne disease transmission and began receiving FDA approval in 2006 (Spinella, et al., Risks associated with fresh whole blood and red blood cell transfusions in a combat support hospital, 2007). Studies have shown such tests give no false negatives, despite manufacturing guarantees in the range of 98.2% and 99.4%. (Bowling & Pennardt, 2010) These disease screening tests are not typical components of field blood transfusion kits but typing cards are always included.

**Figure 8: Typical components of a field blood transfusion kit (Bound Tree Medical, 2013)**

The US Navy 'walking blood bank' and buddy transfusion are two ways in which the US military has incorporated use of FWB transfusion into combat care field procedure. Buddy transfusions involve drawing and transfusing blood in the field, compared to drawing in a hospital, then banking, screening, and delivering to front lines. Whole blood banking has limitations defined by refrigeration and limited shelf life, along with the fact supplies are likely to be inadequate in austere conditions. (Hagman, 2012)

The US Navy's 'Walking Blood Bank' is in place primarily in case of a mass casualty situation. No blood is carried on the ships when out to sea or deployed, so this blood bank system is the only way to have blood on-board and available. In the special case of a patient requiring immediate surgery, the patient is marked 'red' and two or more people donate blood. This system requires pre-screening in the unit before deployment—"dog tags" are not relied upon to define matches. Rosters must be maintained to keep track of co-located personnel. Self-contained field blood transfusion kits (FBTK) are used; they contain a bag with the anticoagulant citrate phosphate

dextrose (CPD), tubing, and catheter. When filtration is to be performed, Y-tubing containing a 0.2 micron filter is used to filter fungi and bacteria (image shown below in Figure 9); one end is connected to a bag of normal saline, another to the donor bag. The saline is started first, followed by the donor blood. If the patient has adverse reactions, the infusion is stopped and Benadryl is intravenously administered before re-initiating transfusion. (Rice)

**Figure 9: Image of a filtered blood administration set for US military (Rice)**

The buddy transfusion protocol requires proper training, donor selection protocols, and intraosseous (IO) route access; the IO route provides access to the systemic circulation via the “non-collapsible” bone marrow matrix. IO devices are special needles designed to enter the bone cortex for drug and fluid delivery. Buddy transfusion requires the medic to quickly place a sternal IO into the patient, draw blood from the buddy donor into a bag, and use gravity to draw the blood into the patient through standard tubing. (Hagman, 2012)

**Figure 10: Special Operations Forces field transfusion (Chinook Medical Gear)**

Whole blood banking and buddy transfusions are a necessity in military field operations. The amount of WFWB transfusions in Afghanistan and Iraq has generally increased from 2001 to 2007; in these countries over 6,000 units of WFWB were transfused between 2003 and 2007. Patients received an average of 5.8 units with a maximum of 48 units. Today risk of MT, which responds best to whole blood transfusion, can now be predicted with approximately 80% accuracy in patients suffering penetrating or blunt trauma. (Spinella, Warm fresh whole blood transfusion for severe hemorrhage: U.S. military and potential civilian applications, 2008)

Buddy transfusion systems have major drawbacks in military settings, especially in emergent and extreme conditions. Donors to 'walking blood banks' are allowed to give no more than one unit of blood at a time, and they must receive plasma volume expander after donation. The donor is then put on light duty for a minimum of 72 hours, which means other soldiers must undertake their more intensive responsibilities. (Bowling & Pennardt, 2010) Aircrew members are restricted from flight duty for 72 hours after blood donation and for 24 hours after plasma donation. (Army Regulation 40-8, 2007) During conflict or emergency conditions, losing manpower is detrimental; another evident limitation to buddy transfusions is the ratio of wounded soldiers to available matching personnel.

## Autotransfusion

Autotransfusion, the process in which a person receives their own blood, was first outlined in 1818 to treat postpartum haemorrhage. Almost a century later it was being used in abdominal trauma. In recent decades increasing demand for large amounts of blood and more strict legislation to ensure quality of donated blood have reinvigorated interest in autotransfusion. (Caliste, McArthur, & Sava, 2014) Because the donor and recipient are the same person, autotransfusion may lessen risks associated with allogeneic (coming from a different person) transfusion such as ARDS, pathogen exposure, and pneumonia. (Salhanick, et al., 2011)

Full-thickness hollow viscus injury (HVI) is a complete tear of one or more hollow abdominal organs (e.g. the bowels, but not the liver). Such an injury was once a contraindication for autotransfusion due to concern of blood contamination. A retrospective study was published in 2014 evaluating 179 patients with penetrating and blunt abdominal trauma who underwent intraoperative blood transfusion; the data indicated no evidence of emergent autotransfusion worsening clinical outcomes in patients with HVI. Autotransfused patients did bleed more and exhibit lower initial systolic blood pressures, but these findings are expected because autotransfusion in cases with HVI are likely to be performed in the direst of circumstances and sickest patients. (Caliste, McArthur, & Sava, 2014) The fact autotransfusion data involves some of the sickest and most compromised casualties indicates a lack of adequate and properly-characterised data surrounding autotransfusion in trauma settings.

Many casualties suffering from truncal haemorrhage bleed into their pleural cavities. A 2011 study was performed in which blood was removed from such patients to evaluate it and compare to fresh whole blood. The haematology profile comparing haemothorax blood and FWB is shown below in Table 6. It was discovered 726 ml of haemothorax blood is equivalent to one unit of RBCs. Haemothorax blood has decreased but still sufficient RBCs for autotransfusion.

| *Parameter* | *Pleural blood* | *Venous blood* |
|---|---|---|
| *Haematocrit (%)* | 26.4 | 33.9 |
| *Haemoglobin (g/dL)* | 9.2 | 11.7 |
| *Platelets (K/µL)* | 53.0 | 174.4 |
| *WBC (K/µL)* | 9.8 | 11.0 |

**Table 6: Haematology profiles of pleural and venous blood (Salhanick, et al., 2011)**

Compared to venous blood, haemothorax blood has significantly depleted fibrinogen and is deficient in various coagulation factors. Pleural blood has normal electrolyte concentrations but the concentrations are significantly higher than its venous blood counterpart. These findings indicate haemothorax blood cannot adequately substitute for FWB, cryoprecipitate, or FFP. More research must be done to determine when and how to transfuse haemothorax blood, but this blood could be a better volume expander than crystalloids alone or altogether in the first few minutes of truncal haemorrhage. (Salhanick, et al., 2011)

Delaying aggressive crystalloid fluid resuscitation has been shown to improve the outcome for hypotensive patients with penetrating torso injuries. (Bickell, et al., 1994) On the battlefield casualties with non-compressible haemorrhage are losing blood much faster than can be supplied by a buddy, and the severe amount of blood loss cannot be mediated by only crystalloid volume expanders. Immediate autotransfusion of haemorrhaged blood alone or alongside crystalloid fluids could provide a method of sustaining casualties, allowing them to reach a facility for surgical care.

## Hemosep® Cell Salvage Device

Allogeneic transfusions have possible but uncommon risks such as disease transmission (primarily HIV and Hepatitis C), immune reactions, transfusion-related acute lung injury, and other rare side effects. Although estimated transmission frequency is 1/200,000-2,000,000 for HIV and 1/30,000-1/150,000 for hepatitis C, new viruses such as hepatitis G and human herpes virus 8 are being discovered in donors considered healthy. Hepatitis G is a new virus which could possibly contribute to chronic or acute hepatitis, while human herpes virus 8 is associated with Kaposi's sarcoma. Additionally allogeneic transfusions can be costly; avoiding them has shown to reduce total treatment costs in abdominal and orthopaedic surgery by about $5,000 per patient in the US. (Spahn & Casutt, 2000) In both civilian and military settings, allogeneic transfusions are essential despite drawbacks and potential risks, but on the battlefield availability of necessary donor blood is limited at best.

In high blood loss surgery or situations involving circulatory support machines such as a cardiopulmonary bypass circuit, the blood lost or retained in the reservoir can be processed and transfused back into the patient via cell salvage and haemoconcentration. Cell salvage involves collecting blood from a patient in the operative field then, either directly or after washing, re-delivering the blood to the patient. This process—both with and without washing—is helpful during an operation, as it was found to decrease the proportion of orthopaedic patients who need perioperative allogeneic transfusion; cell salvage has not been shown to be more than marginally effective post-operatively. (Huet, et al., 1999)

Terence Gourlay at Glasgow's University of Strathclyde, in collaboration with British medical technology company Brightwake® Limited, developed a novel haemo-concentration and cell salvage system called Hemosep®. It is licensed to Advancis® Surgical Ltd, and Health Canada first qualified it as a Class II medical device in November 2012. The device is CE marked and has begun being marketed to the healthcare sector

in Canada, Europe, and other regions recognising the CE mark. The Hemosep® system consists of a 500ml capacity blood bag containing a chemical sponge technology along with an orbital shaker to agitate the contents. (Topfer, 2015)

The Hemosep® process begins with a hospital wall vacuum system pulling blood from a surgical site or blood reservoir through the suction tool and into the processing bag. Inside the bag lies a silicone-based superabsorber material surrounded by a control membrane. During cardiopulmonary bypass (CPB) procedures, the patient's blood is diluted to approximately 20% packed cell volume (PCV) to ensure there is an adequate circulating blood volume for the patient and the bypass circuit. Diluted blood enters the bag and the superabsorber soaks up excess plasma to re-concentrate the blood. One gram of superabsorber absorbs up to 240ml/g of fluid; each bag contains 12g of the superabsorber, so it can remove up to 3L of fluid. The control membrane contains 1µm-sized pores to prevent absorption of any cellular species while allowing free flow of plasma; WBCs are the largest of the cell species at 12-15µm diameter, while RBCs are 6-8µm and platelets are smallest at 2-3µm. The elements of the Hemosep® bag are shown below in Figure 11. (Gourlay & Robertson, 2014)

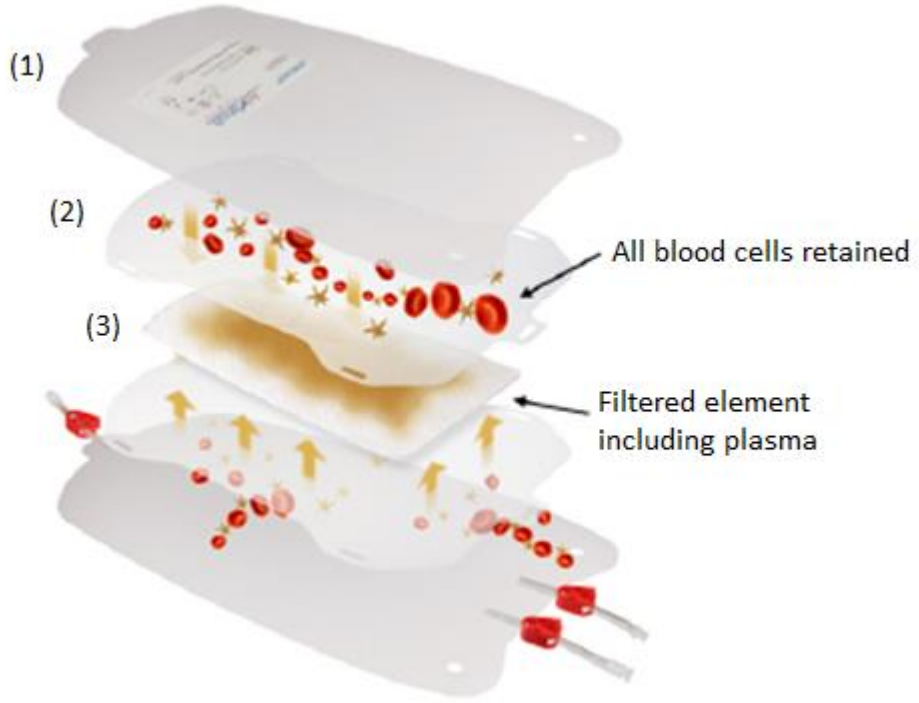


**Figure 11: The Hemosep® bag is the active processing section of the cell-salvage system. It consists of a blood bag (1) containing a suspended filter membrane bag (2) which surrounds a sheet of superabsorber material (3) (Gourlay & Robertson, 2014)**

The bag is placed on an orbital shaker during processing; this speeds up the concentration process by moving blood over the membrane in waves, scouring the surface and preventing cells from settling in the pores. When the appropriate degree of haemoconcentration is accomplished (normal range is ~30-45%), the concentrated blood is released to a transfer bag from which it can be IV-transfused to the patient. Figure 12 displays the complete system involving Hemosep® bag, shaker, pump, and reservoir. All unwanted blood products absorbed by the superabsorbent pad become a gel-like substance held within the membrane, making for simple waste disposal via incineration. (Gourlay & Robertson, 2014)


**Figure 12: Complete Hemosep® system: Hemosep® bag (1), orbital shaker (2), collection bag for transfer to patient (3), Intraoperative pump and reservoir (4), and suction (5). (Gourlay & Robertson, 2014)**

A study published in 2013 evaluated the Hemosep® system's effectiveness in patients undergoing cardiopulmonary bypass. The pooled reservoir blood was removed and salvaged at the end of the operation. The salvaged blood contributed to post-operative blood management strategies, and significantly reduced need for allogeneic transfusion without any incidence of technical failure. (Gunaydin & Gourlay, 2013)

The current incarnation of the Hemosep® system concentrates blood hematocrit from diluted (≥20%) to normal (30-45%) in approximately 40 minutes. Modifications are being made to the membrane which cut concentration time to 15-20 minutes; the new membrane also enables expedited concentration without agitation. These developments make the Hemosep® bag a potential component for use in frontline, in-field military medical response; the necessary additional components are a manually-powered vacuum to move blood through the system and a component to remove both air and major sediment from the blood.

## Field Autotransfusion System

A “salvage-only” intraoperative blood salvage study (IBS) was performed in a UK deployed combat support hospital during one month in 2011. During this period all admissions were identified for IBS and the procedure performed on all adult patients likely to require massive transfusion. The employed salvage system involved washing of the blood to remove plasma-phase contaminants. Although cell salvage was shown to be meaningless in managing blast injury to extremities, clinically meaningful volumes of blood were proven salvageable from other wounds—especially gunshot wounds and cavity injuries. (Bhangu, Nepogodiev, Doughty, & Bowley, 2013)

The Hemosep® cell salvage system is simple, streamlined, portable, and easy to use; these traits indicate it could be taken into the field once its dependence on power is eliminated. Currently the civilian HemoSep® system requires a heavy electrically-powered orbital shaker for agitation; however new membrane technology permits rapid haemoconcentration without agitation. This membrane improvement is a considerable advancement toward making HemoSep® suitable for field use. Further considerations to making Hemosep® field-deployable inspired the concept of employing a manual hand-crank pump to remove the need for typical hospital wall-suction and eliminate dependence on all electrical power. The project aim became the development of a modified field technology for cell salvage and autotransfusion which would be fully manual and portable for practical military deployment.

The British military emphasised their primary immediate goal in the field for non-compressible haemorrhage casualties was to expeditiously retransfuse the haemorrhaged blood. New modifications to the Hemosep® membrane make it practical in the field both time-wise and labour-wise, but the field transfusion system must perform basic autotransfusion at its core. Figure 13 outlines the components of the complete field autotransfusion system.

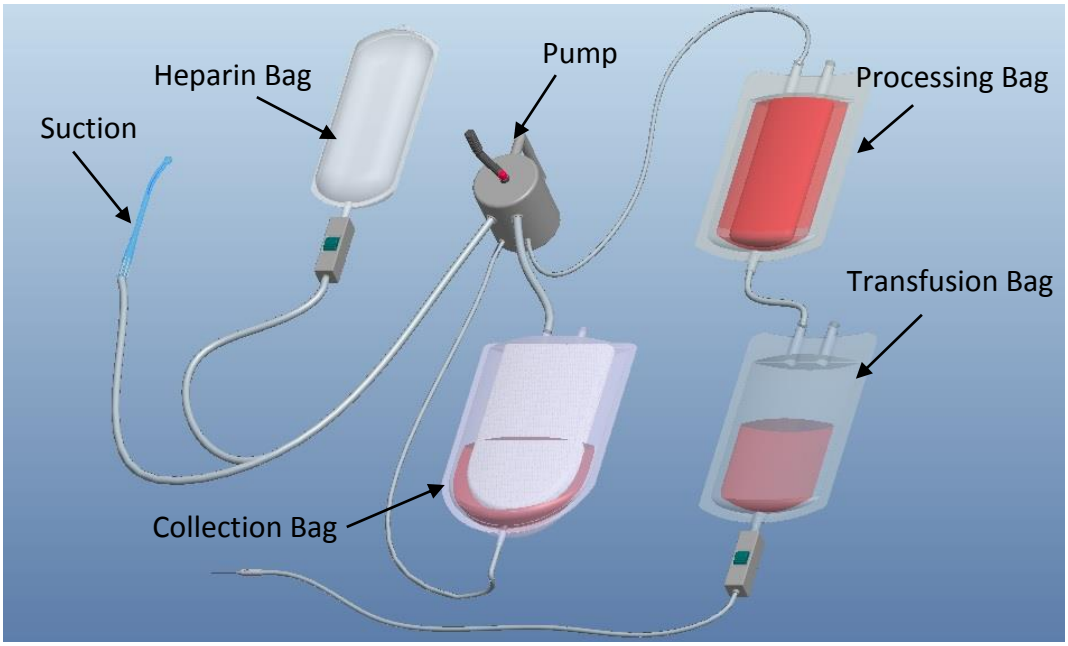


**Figure 13: Components of complete field autotransfusion system (Gourlay & Robertson, 2014)**

The components of this system include a suction device to take up blood from the wound site, anticoagulant-infused crystalloid fluid, pump, collection bag, processing bag, and transfusion bag. Anticoagulant is not needed for any chest wounds as shed blood from the chest is missing key coagulation factors and will not clot; consequently it primarily functions to boost oxygen carrying capacity of the patient's blood. Anticoagulants can be valuable for blood shed from other wound sites and for blood intended to be held instead of immediately autotransfused.

The collection bag will receive blood from the wound; as is the nature of blood shed from a wound site, the fluid will be a turbulent blood-air mixture. All air and major contaminants must be removed before retransfusion; the collection bag must perform these tasks efficiently without causing significant haemolysis. The processing bag, in this case the Hemosep® bag, is unessential if autotransfusion is urgent to ensure patient stabilisation but can be included if desired. The blood is finally deposited into a transfusion bag and then retransfused.

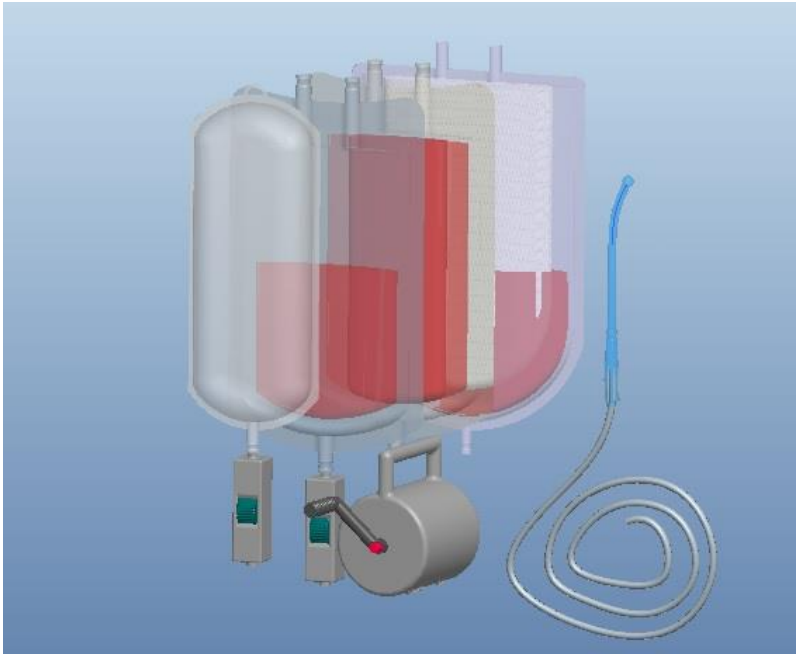

**Figure 14: Schematic of compacted autotransfusion device (Gourlay & Robertson, 2014)**

All components of this autotransfusion system are bags except for the pump mechanism and suction nozzle. Most of the system can be made compact by laying the bags on top of one another; the bags and nozzle can be stored in a small kit (which must be designed), so the only component of notable size or weight is the pump.

## Novel Peristaltic Pump

Military field settings require devices to consume little to no electrical power. The approach developed by Terence Gourlay and his team at University of Strathclyde in Glasgow is to design a novel vacuum generation system consisting of a peristaltic pump mechanism containing one axle and two independent sets of roller pumps. The pump system must be capable of constantly pulling blood from the wound site while moving the blood into the collection bag or Hemosep® bag and returning blood to the patient only when desired. (Gourlay & Robertson, 2014)

The novel peristaltic field pump is being designed to generate a high flow for wound site extraction (~20L/min) and a low flow (~500ml/min) for return. The high flow roller mechanism is capable of operating independently or simultaneously with the low flow mechanism; the low flow system can be activated/deactivated by turning a switch to engage/disengage the gear teeth between the two roller pumps. Manual operation is accomplished by turning a hand crank on the leading end of the pump system while holding the pump body or a torsion handle with the other hand. The basic components and design are outlined below in Figure 15. Future redesigns to the handle will also allow an electric screwdriver to crank the pump. (Gourlay & Robertson, 2014)

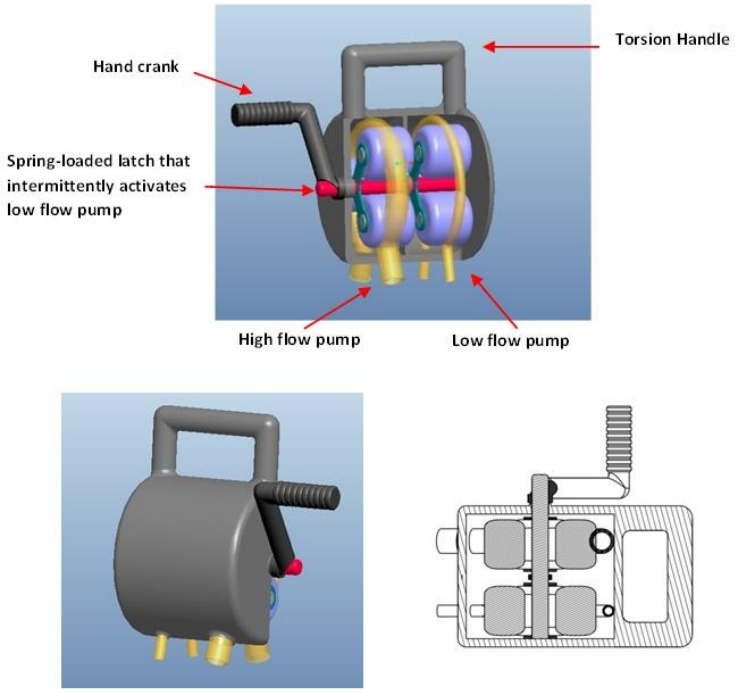


**Figure 15: Components of manual peristaltic pump (top), outer casing (bottom left), and cross-sectional view (bottom right) (Gourlay & Robertson, 2014)**

The pump cylinder is separated into three interlocking sections; the first section contains the gears used to increase output speed using a 1:4 gear ratio. The second section houses the high flow roller mechanism while the third contains the low flow rollers and latch mechanism allowing its activation/deactivation. Figure 16 shows the 3D computer-

aided drafting (CAD) design for the first prototype printed entirely in clear polymer ABS (acrylonitrile/butadiene/styrene); as a proof of concept prototype, the rollers, gears and spring-loaded latch mechanisms functioned successfully. The fragility of the ABS material did not permit testing with the tubing. All tubing has 2mm wall-thickness, and inner tube diameters for the high and low flow pumps are 12.5mm and 5mm respectively. (Gourlay & Robertson, 2014)

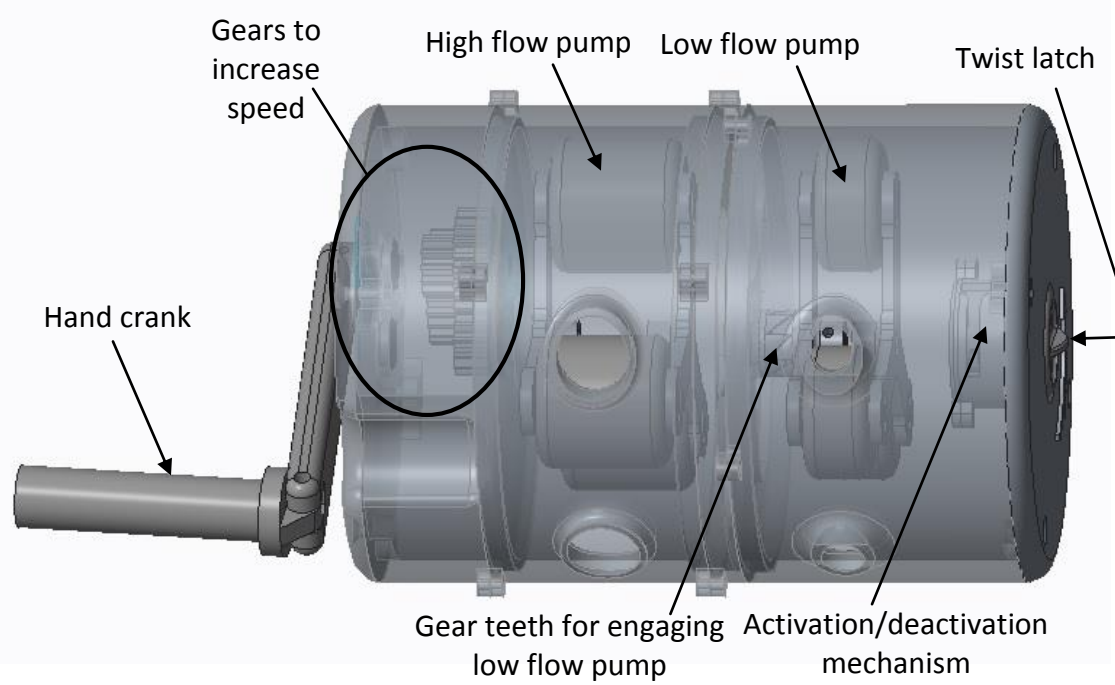


**Figure 16: First printed iteration of manual peristaltic pump**

Later iterations have decreased the pump's profile. Gears, rollers, and other interior pieces are now stainless steel. All outer casing was printed in a lightweight material consisting of a graphite and carbon fibre mixture built in 0.1mm layers; successful testing with tubing attached showed this material warped under tension (3D Alchemy, 2012). A third iteration is underway with outer casing and handle printed in aluminium. This peristaltic system is designed to generate a maximum high and low flow pump rate of 14.8L/min and 0.59L/min respectively when the handle is turned at 120 rpm, but no wet lab testing with fluids have yet been performed.

## The Collection Bag: Defoaming & Filtering

Blood extracted from a haemorrhaging wound especially in the field will contain undesirable substances such as particulate debris, tissue fragments, and other foreign material. Debris can include any field contaminants or biological substances such as cell fragments, platelet clots, damaged leucocytes, clotted cells, or fibrin. A majority of these impurities need to be removed before returning blood to the patient. Although "washing" is a typical method for removing contamination, it involves multiple steps and usually centrifugation; these processes are slow and impossible to perform on the battlefield with limited supplies and time. (US Patent No. US6517732 B1, 2003)

Air is frequently drawn from the environment when suctioning blood from a bleeding wound, and the air can damage blood components. Typical blood drawing from wound sites results in an intensive mixing of blood and air within the cannula and tubes; to obtain effective drawing-off of blood, hospitals use high suction (40-60 L/min) wall vacuums which cause additional damage to blood components. More recent systems have been designed to remove air from the blood while attempting to limit any damage to blood components; however these systems are bulky and power-consumptive. (US Patent No. US6517732 B1, 2003)

Given the damaging potential of air, the air should be removed as soon after suction as possible and extraction done again immediately before re-entrance to the body. Microaggregate blood filters with pore size ranging from 25-40µm are attached in-line between the transfusion bag and patient; these filters prevent air infusion which can cause a deadly air embolism. The filter in these devices is a polyester screen media with high filtering capacity; one product example is the Haemonetics® SQ40 filter which has a large open area, utilises a pleated screen design, and removes particulates larger than 40µm (Figure 17).

**Figure 17: Example of an in-line microaggregate transfusion filter (Haemonetics, 2013)**

Arterial in-line filters are used to remove gas emboli in extracorporeal circuits and could possibly be used in a field transfusion system. These filters employ a hydrophilic membrane technology which filters air along with micro-contaminants such as bacteria and fungi. Polyethersulfone (PES) is a typical in-line filtration membrane achieving high flow rates with very low protein binding. (Pall Medical, 2009)

**Figure 18: Examples of 0.2µm in-line PES air filters: Pall™ AEF (Pall Medical, 2011) and Acropak 20 (Pall Medical, 2009)**

The collection bag is the first downstream component in the field autotransfusion system which can house technology for air removal (defoaming) and contaminant filtration. These tasks are to be performed by a novel device developed by Brightwake® Limited (Nottingham, UK) consisting of a polyester sock and inner layer of polyester foam. The

sock is composed of thinly woven strands of polyester which filter out particulates approximately ≥50-70µm in diameter.

An inner polyester defoaming sponge is placed within the sock; this sponge is sprayed with silicone antifoam agent A or B to limit the surface tension of the foam; lowering surface tension is necessary to ensure foam breakdown into usable blood. The primary difference between these two agents is B contains emulsifiers while A does not. Antifoam agent A is composed of hydrophobic silica dispersed in a silicone oil, while agent B is a water-based emulsion. Emulsifiers are added to ensure the quick and thorough spreading of the silicone through the foam medium. (Höfer, et al., 2003)


**Figure 19: Photos of Brightwake® sock (left), sock in high-flow suction canister (right)**

## Thesis Aims

The final component of the collection bag subsystem is a device to

(1) hold the foam and filter sock,

(2) slow the incoming flow,

(3) disperse the flow across the inner surface of the defoaming/filtering sock, and

(4) accomplish directed fluid flow without inducing significant haemolysis.

The blood-air mixture coming from the high flow manual pump will be very turbulent upon entering the bag, and this novel intermediary device needs to make the flow more laminar and spread fluid across the surface of the defoamer and sock without causing haemolysis. A certain fluid volume must flow over a certain amount of surface area for the defoamer to efficiently remove air from the blood.

The goal of this thesis is to design a bag-mountable intermediary device to control blood flow without inducing haemolysis, thereby creating a compact and portable defoaming and filtration field apparatus. Figure 20 below is an illustration of the general position, size, and shape of the intermediary device.

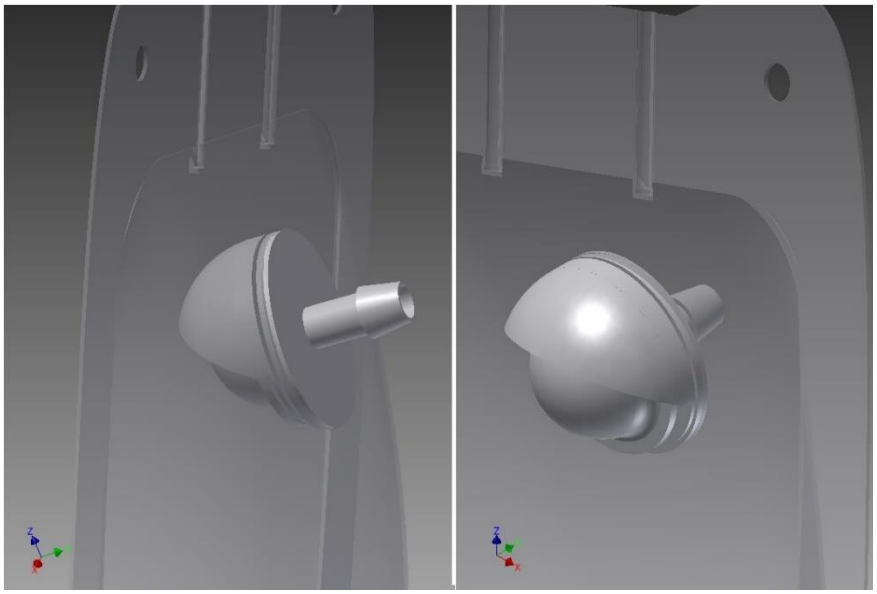

**Figure 20: Device through which blood flows into collection bag**

## Initial Concept Design

The design of this intermediary device for blood defoaming and filtration follows the steps of an iterative design process; these steps are concept development, computer modelling, and laboratory testing (outlined below in Figure 21). Once device requirements are established, concepts are defined and a design determined. The device design is then modelled using a variety of computer programs including those for 3D CAD drawing and simulation; simulation programs such as ANSYS® perform multiple tasks including finite element analysis (FEA) and computational fluid dynamics (CFD). No amount of computer modelling can replace the practical value of hands-on laboratory testing, which is the next step in the design process. After both the modelling and lab testing phases, the device is evaluated for performance; if performance needs improvement, the concept is modified and re-evaluated until attaining a final working prototype.

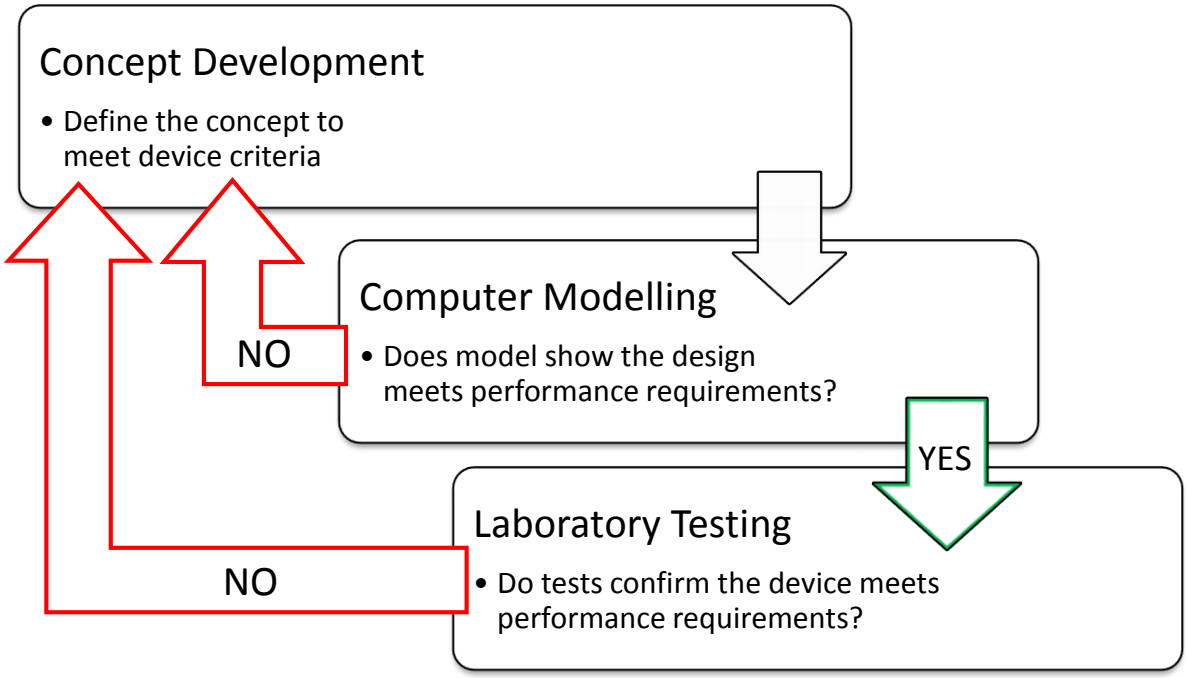


**Figure 21: The Design Process adopted within this project**

The first factor affecting device design is the position of the fluid flow device--incoming blood must enter the bag through the top or side. Cutting the top of the bag and dropping the device and its attached components through the centre consumes all usable interior space, leaving no room for addition of future components. The collection bag will be a modified version of the Hemosep® outer shell because it is already in production, is the appropriate size and shape, and can be inexpensively altered. Removing the top section of the bag would involve more extensive remodelling of the Hemosep® shell.

Attaching the blood flow device to the upper side of the bag lowers input flow resistance by allowing blood to flow horizontally into the vertically-hanging bag located above the patient. Side attachment also requires minor modification to the Hemosep shell and does not consume the depth of the bag allowing for future alterations or additions to the interior space. Placement on the upper side of the bag was chosen for the aforementioned reasons.

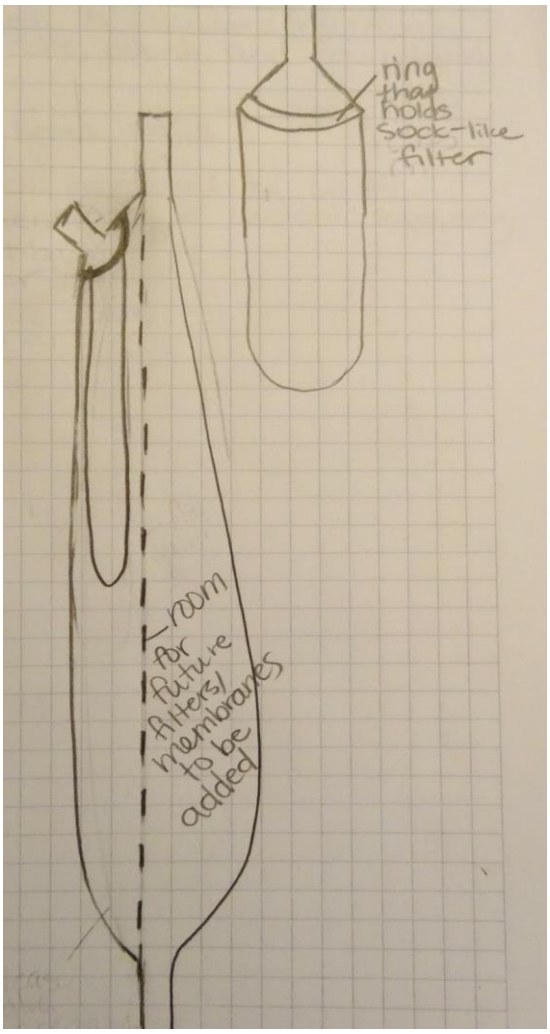


**Figure 22: First sketches of vertical defoaming and filtration bag system**

After determining position, device design became dictated by the task of directing turbulent horizontal fluid flow across the inner surface of a vertically-hanging sock. The input fluid must be slowed, smoothed, and spread out across the surface of the attached sock and foam. Slowing and smoothing the flow requires a mechanism which significantly turns the streamline to decrease velocity without shearing the blood while also radiating the blood in all directions across the circumference of the attached foam and sock. Figure 23 below displays the inspiration for the eventual concept design of the collection bag device.

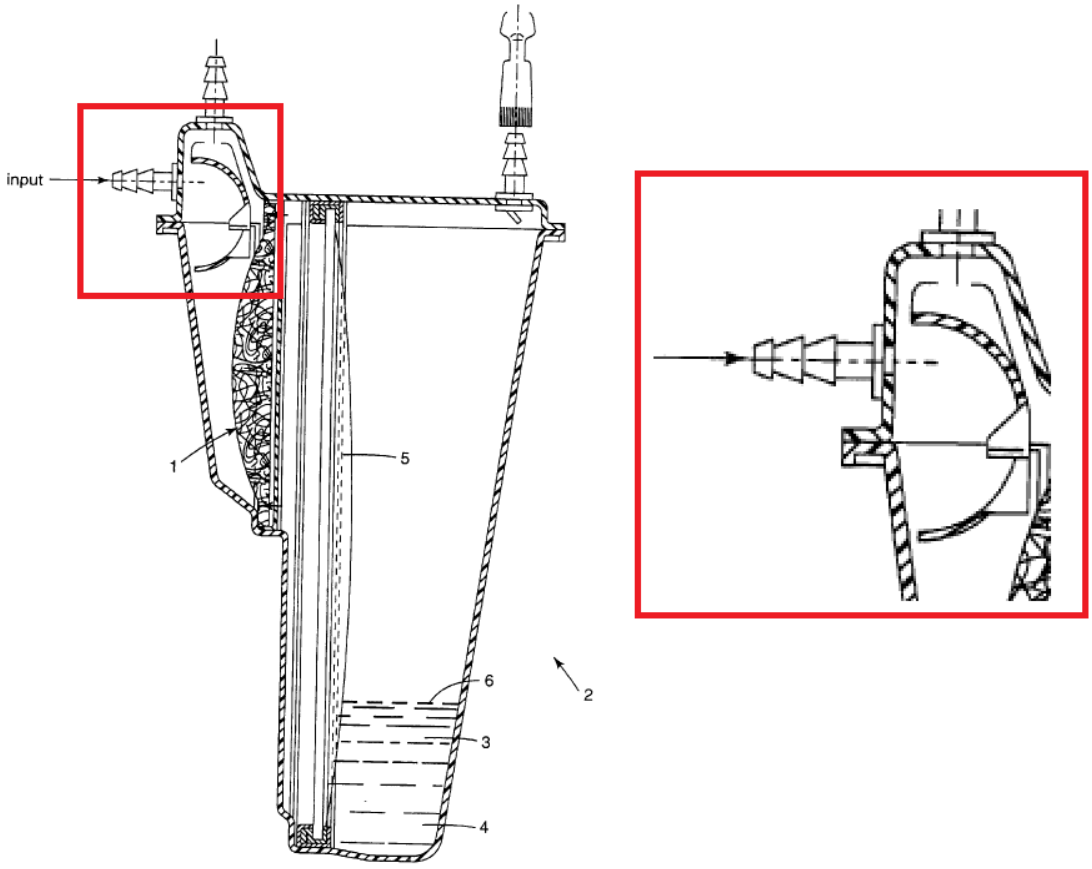


**Figure 23: Example of a defoamer/filter device with horizontal blood input (left); fluid inlet for the device (right) (United States Patent No. US 6,482,360 B2, 2002)**

This patent, for a novel antifoaming agent (component 1 in Figure 23), displays a container with horizontal fluid input. To decrease turbulence and speed within minimal shear, the streamline is turned 180° in a circular path, then the flow is thinned when exiting through a narrow outlet before dropping into the compartment containing the defoaming sponge. Similar fluid control mechanisms are employed in other blood processing devices with horizontal inflow. Designs such as these inspired the concept of using a spherically-shaped mechanism for the collection bag device.


**Figure 24: Example of a typical mushroom-type aerator sparger (Korea International Trade Association, 2015)**

The spherical component for the blood flow device is a sparger; to 'sparge' means to spray or sprinkle. Typical mechanical spargers as shown above contain pores which introduce gases into the fluid, but the sparger in this biomedical device contains no holes. Horizontal blood flow hits the vertically-situated sparger; the sparger turns the fluid streamlines approximately 180° and directs flow radially outward. Any surface perpendicular to flow exerts direct force on the blood, while any surface parallel to flow exerts a shearing force; a constantly and steadily changing sparger slope minimizes these shearing forces, so the sparger requires an approximately hemispherical shape.

The sock and inner foam layer must fall downward through the collection bag, so the next design requirement was to introduce a component which positions the sock around the vertical sparger; the component must allow blood to flow along the sock's inner surface while preventing the sock from resting on the sparger. Attaching a spherical 'hood' to the rim of the sparger prevents blood from flowing down the outer sparger surface; placing a second hood over the first forces the upward blood flow to run between the hoods while providing a surface across which the sock can rest. A uniform space between all surfaces of the two sparger components was designated for blood flow. Sketches of this initial design are shown in Figure 25.

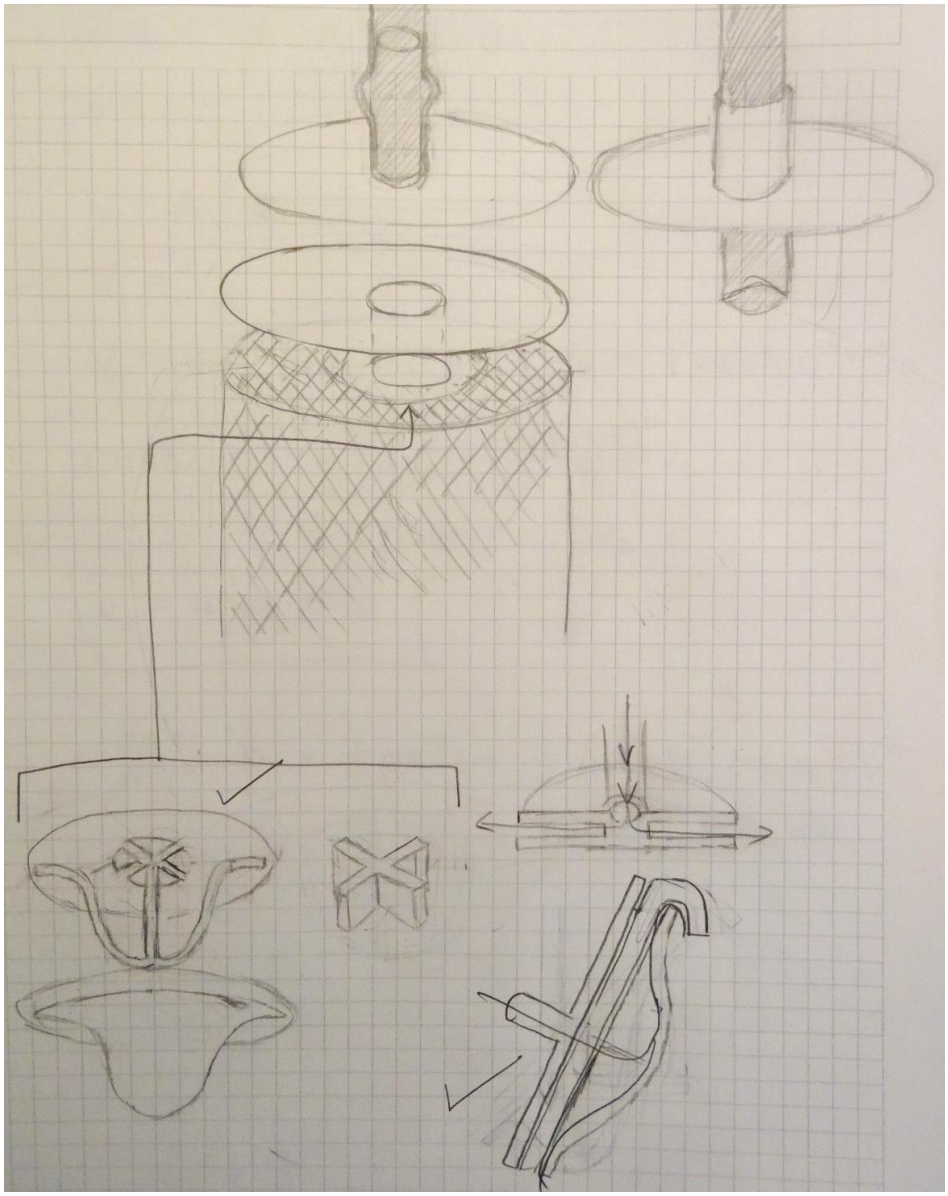

**Figure 25: Initial design sketches of sparger, hoods, and connector**

The two sparger components were initially connected with a single post running through the centre of the flow; the post attached to the outer hood component via a simple 'X'-construct. This setup allowed the complete sparger mechanism to be printed as one unit and prevented any objects from obstructing radial flow across the sparger. The sparger component was later separated into two pieces which were assembled post-printing, and the initial concept sketches for these designs are shown in Figure 26.

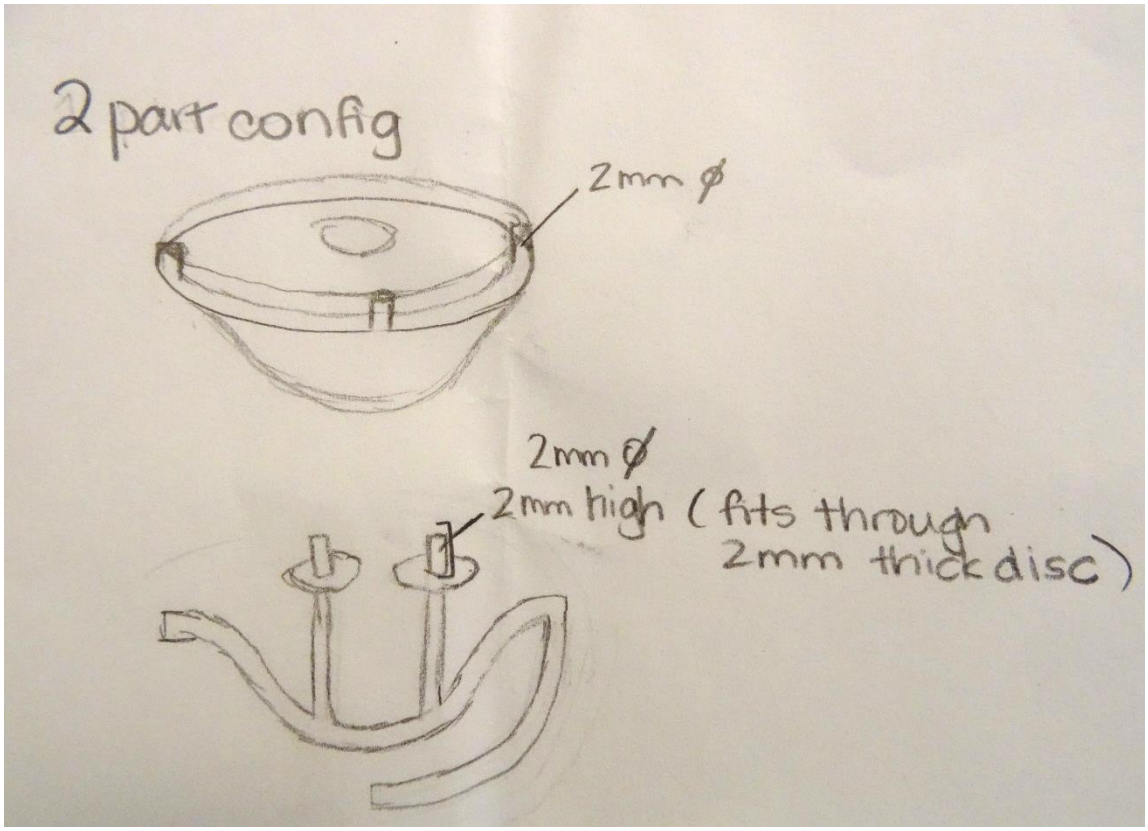


**Figure 26: Revised sparger sketches breaking component into two parts**

The final pieces of the novel blood flow device are a basic circular disc and a tube connector. The top of the sock was to be glued between the disc and the outer surface of the sparger component; this complete defoaming and filtration unit would then be placed inside the collection bag. The flow holes were given 8mm diameter in all three device discs. The exterior of the bag required a simple slip-on tube connector with a wedged insert to grip the inside of the tube; an example of such a connector is shown below (Figure 27).

**Figure 27: Example of slip-on tube connecter with wedge insert to grip blood tube**

The primary pieces of this novel device are displayed below in a 3D CAD image (Figure 28). In summary the individual components of the intermediary blood flow device are:

1. Blood dispersal component with:
    a. Inner sparger with attached hood
    b. Outer hood attached to a simple disc
2. Simple disc to grip the open edge of the sock
3. Slip-on tube connector for outside of collection bag

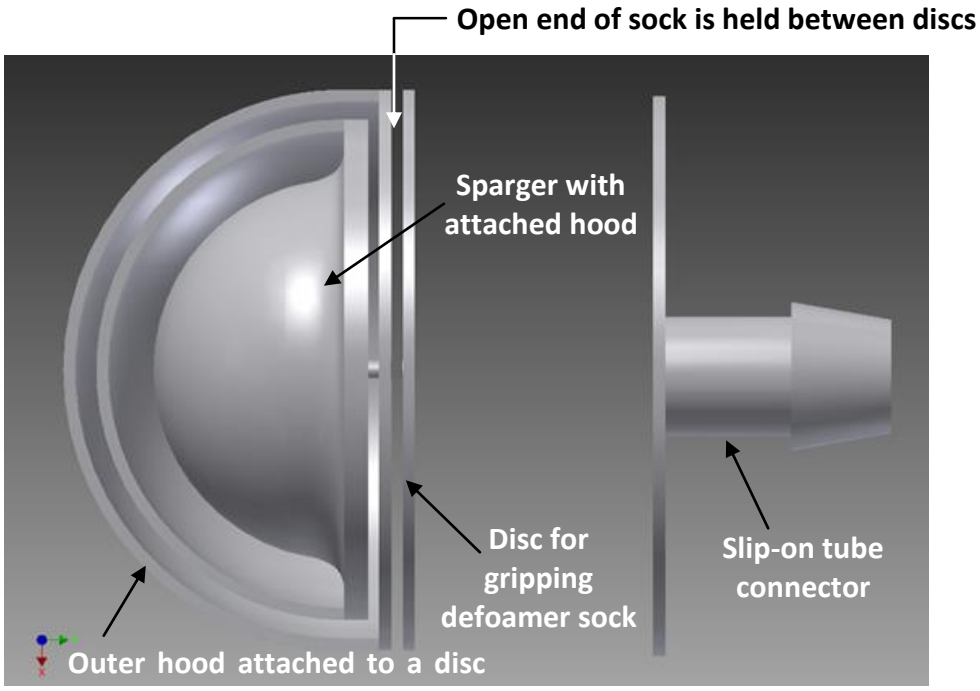


**Figure 28: 3D CAD drawing of components of blood flow device**

## Materials & Methods

The design process involved computer programs for building and analysis, 3D printers for component production, and 'wet lab' testing for fluid flow and haemolysis. Computer modelling entailed use of 3D CAD software and fluid simulation software; printing was done by two different printers over the course of the project. The laboratory testing consisted primarily of visualising water flow through the spargers, but haemolysis testing was able to be performed on multiple prototypes before thesis submission.

## Autodesk® Inventor® 3D CAD Drawing

Inventor® is a 3D CAD modelling program developed by US-based software company Autodesk®. The program is capable of creating 3D prototypes for visualisation along with static and dynamic simulations through use of FEA. The specific Inventor file formats used in this project are those for parts (IPT) and assemblies (IAM); assemblies are files containing multiple parts combined and oriented with user-applied constraints. Files are exported as standard STL file types for printing purposes; all prototypes for this project are sketched and built using Inventor®. An example of the steps for prototype construction is illustrated in Figure 29.

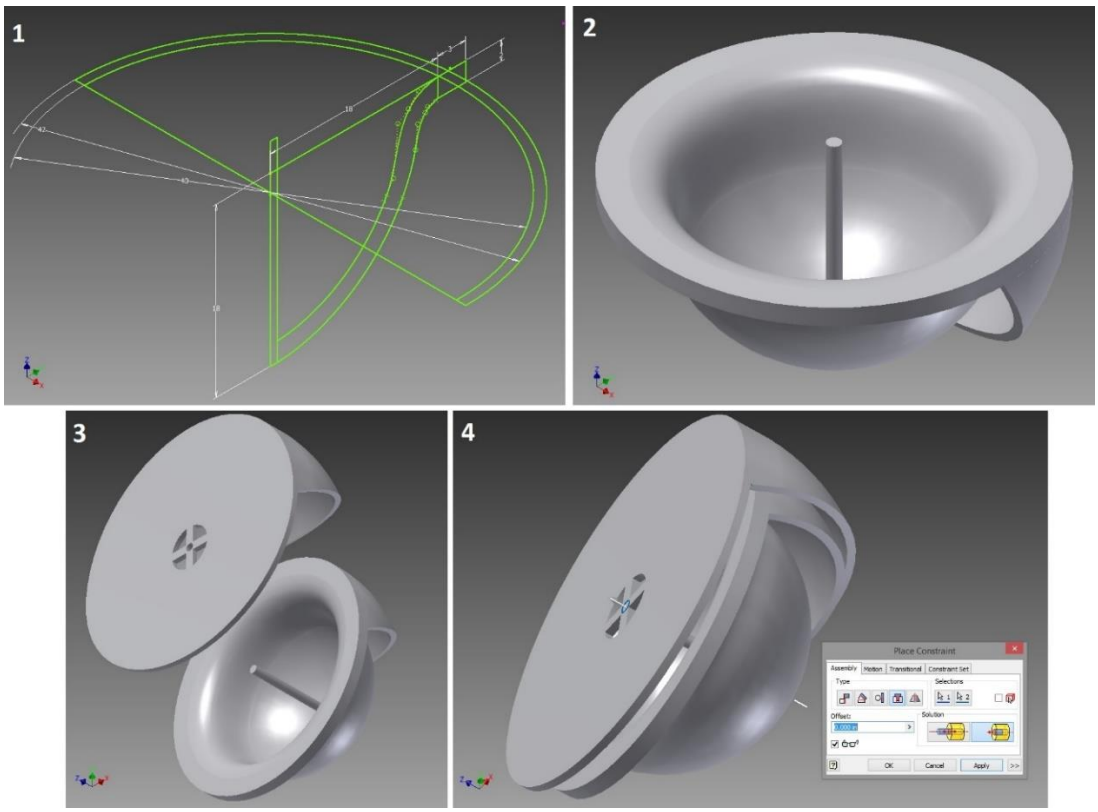


**Figure 29: Example of Autodesk® Inventor® CAD construction steps. Part files (top) consists of dimensioned sketches (1) extruded and rotated to form parts (2); Assembly files (bottom) consist of placing components into the file (3) and constraining them in place (4)**

## ANSYS® Fluent® Fluid Modelling

Fluent® is a CFD software program manufactured by US-headquartered engineering software company ANSYS®. This CFD software is capable of modelling fluid flow and similar phenomena such as heat transfer. The real-world applications of this software are troubleshooting of existing systems and visualisation of actual behaviour before or during prototype production.

ANSYS® Workbench® is the framework used to tie together the complete simulation process of all ANSYS® engineering programs including Fluent®. CAD drawings are imported into Workbench® from various modelling programs such as Inventor®; next the

model is 'meshed,' then system parameters such as fluid properties and inlet/outlet are specified. Meshing is a pre-processing step in which the surface domain of an object is broken into simpler subdomains called 'elements'. Elements can be a variety of shapes such as triangles, tetrahedrons, or polygons; the directions of the elements can be regular or unstructured, and their sizes and shapes can be consistent or varying. Tetrahedral meshing was used in this thesis work.

The inlet parameter of the fluid model is a constant velocity of 4.94 m/s; this value is calculated using a volumetric flow rate balancing equation (Figure 30). An incoming manual pump maximum velocity of 14.9 L/min converts to $2.483 \times 10^{-4}$ $m^3/s$; this velocity and the output surface area of the collection bag tube are used to find the speed of fluid flowing into the bag. The blood density value input into the model is 1060 $kg/m^3$ (Cutnell & Johnson, 1998), and viscosity is 0.04 poise (P) which converts to 0.004 kg/m·s.

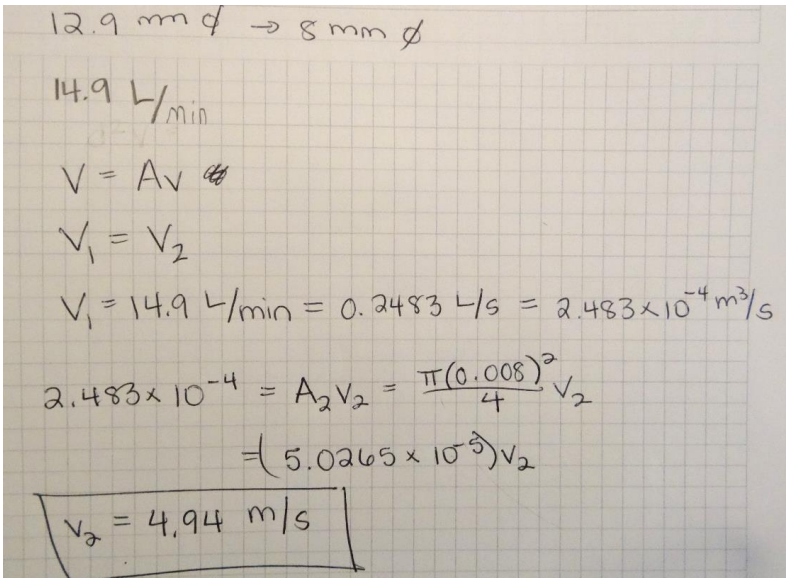


**Figure 30: Photo of volumetric flow rate balancing math to solve for inlet velocity**

After completing the setup process, a flow simulation can be run through the meshed and defined system to visualise fluid movement. Fluent® analysis was performed on prototype iteration #1 (see Figure 48) within this project, but fluid modelling will be performed again on the final working prototype(s) beyond thesis completion.

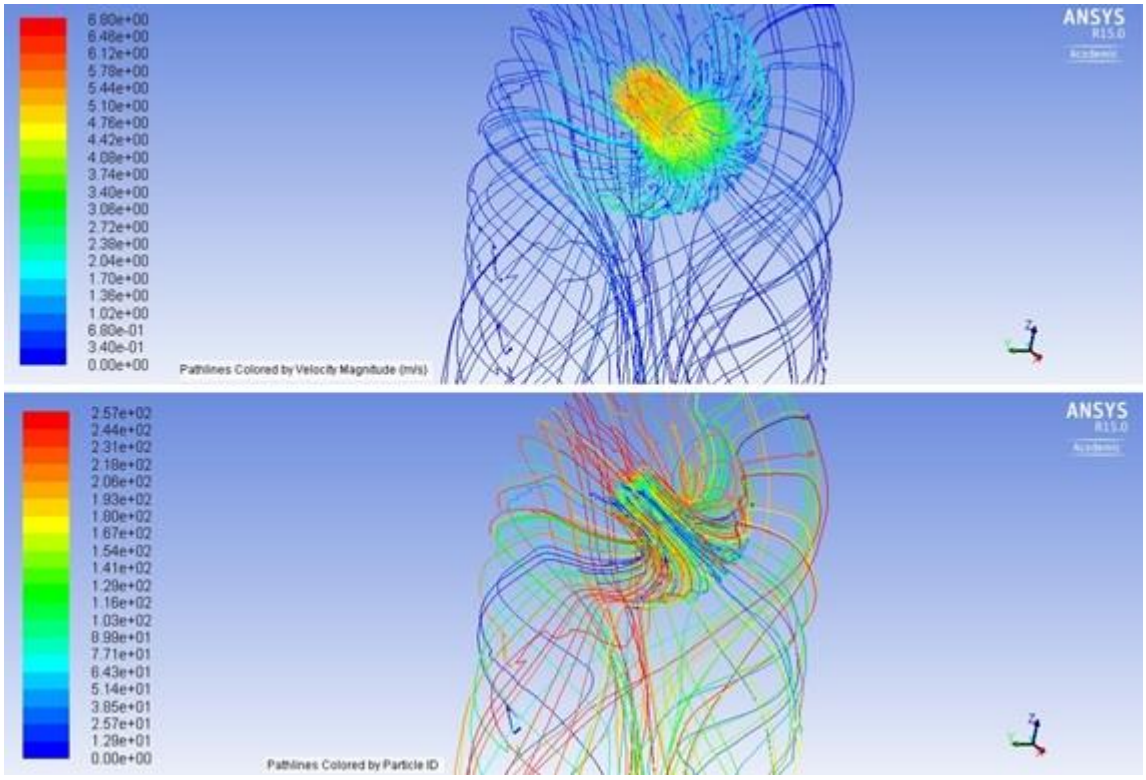


**Figure 31: Example of ANSYS® Fluent® pathline images tracking velocity (top) and particles (bottom)**

## 3D Printing: Machines & Materials

The printer used to print iterations #1 and #2 ((see Figures 48 and 59) in this project is the Stratasys® EDEN350 in conjunction with Object Studio® software; it belongs to the Design, Manufacture & Engineering Management (DMEM) department at University of Strathclyde. This printer utilises PolyJet® technology, a printing process involving jets to deposit liquid photopolymer which is UV-cured in thin layers. The support material used in the EDEN350 printer is a soluble gel-like substance removed using high-pressure water spray. (University of Strathclyde, n.d.)

The largest model this printer can produce is 340x349x200 mm with resolution of up to 1600 dpi. The EDEN350 has an accuracy of 20-85µm and a precision (layer thickness) of ≥16 microns; the printer's precision is limited by the material used, and the precision

used for the prototypes is unknown. The material used for the components is rigid opaque ABS polymer, the properties of which will be discussed later. (University of Strathclyde, n.d.)


**Figure 32: Image of Stratasys EDEN350 printer belonging to DMEM at University of Strathclyde (University of Strathclyde, n.d.)**

The Biomedical Engineering department at University of Strathclyde procured an EnvisionTEC® Perfactory® Desktop XL printer (Figure 32) in conjunction with Magics® software; the system became available for use midway through the project period and was used to print iterations #3 and beyond (see Figures 66, 76, and 81). The printer employs Direct Light Projection technology to produce fine details in printed objects, and there are no limits to geometric complexity. It has a constant build speed of 3-7mm per hour depending on material.

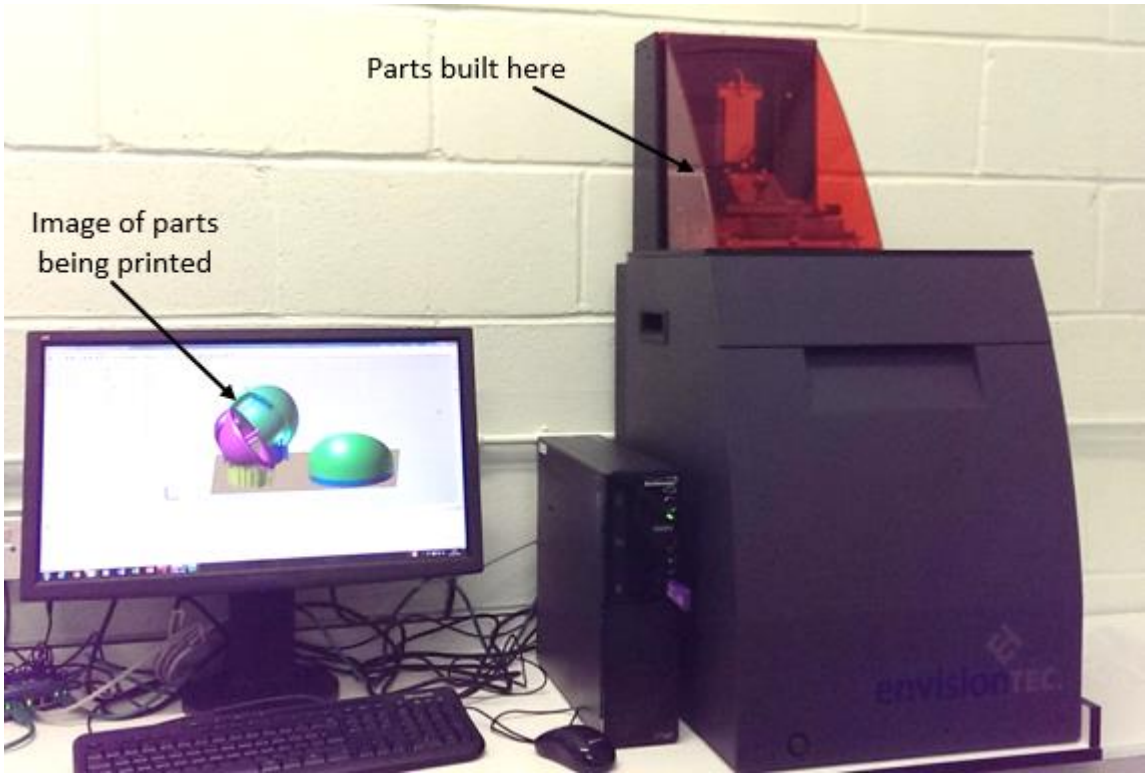


**Figure 33: Photo of complete EnvisionTEC® setup for 3D printing**

The printed parts can be allowed to cure overnight or be cured in a post-curing chamber (Figure 34). This system has two photoflash lamps emitting intense UV radiation between 300-700nm. The object is placed in the unit, treated, then turned 180° and cured again. This post-curing machine enables the printed component to be fully hardened within minutes.


**Figure 34: Photo of EnvisionTEC® Post-Curing UV machine**

The printable space for the EnvisionTEC° Desktop XL printer is 100x75x100mm, with a resolution of 25-150µm (25-50µm for the material used in this project); components for this blood device are printed at a precision of 50µm (EnvisionTEC). The support structures produced are rigid rod-shaped structures in a user-defined arrangement. Upon completion the supports are severed and sanded, then the component surface is smoothed using fine, wet sandpaper. Parts are printed using HTM140 material, a methacrylic-/acrylic- resin manufactured by EnvisionTEC®, which has material properties superior to ABS. Table 7 compares the material properties of ABS and HTM140 (EnvisionTEC) (Test Standard Labs, 2014).

| MATERIAL PROPERTIES OF PRINTING MATERIALS | | |
|---|---|---|
| PROPERTY | **ABS (acrylonitrile/butadiene /styrene)** | **HTM140 (methacrylic-/acrylic-resin)** |
| **TENSILE STRENGTH** | 44 MPa | 56 MPa |
| **FLEXURAL YIELD STRENGTH** | 68.9 MPa | 115 MPa |
| **FLEXURAL MODULUS** | 2.2 GPa | 3.35 GPa |
| **ELONGATION AT BREAK** | 24.3% | 3.5% |

**Table 7: Material properties comparison: ABS vs HTM140**

**Figure 35: Photos of prototypes being printed in EnvionTEC® printer**

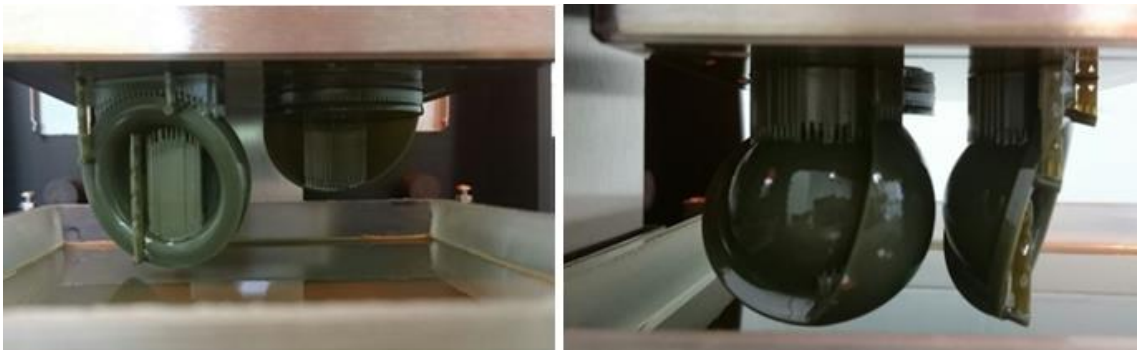

**Figure 36: Photos of prototypes in EnvisionTEC® machine immediately after completion**

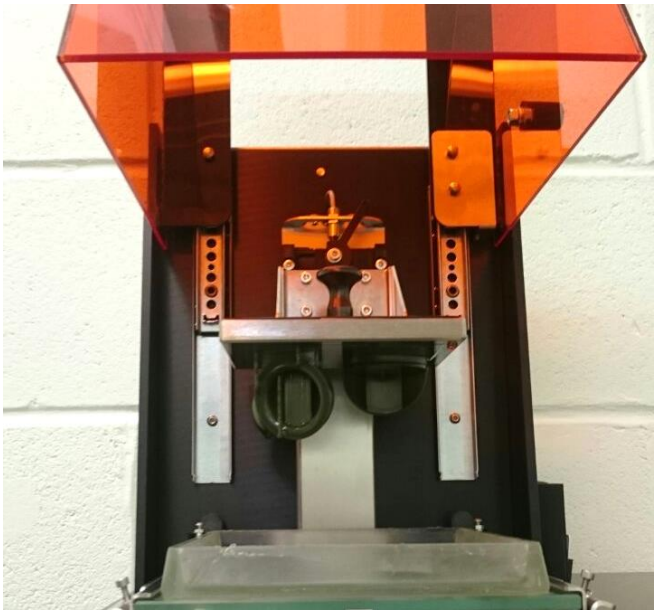

**Figure 37: Photo of prototypes in EnvisionTEC® machine before removal**

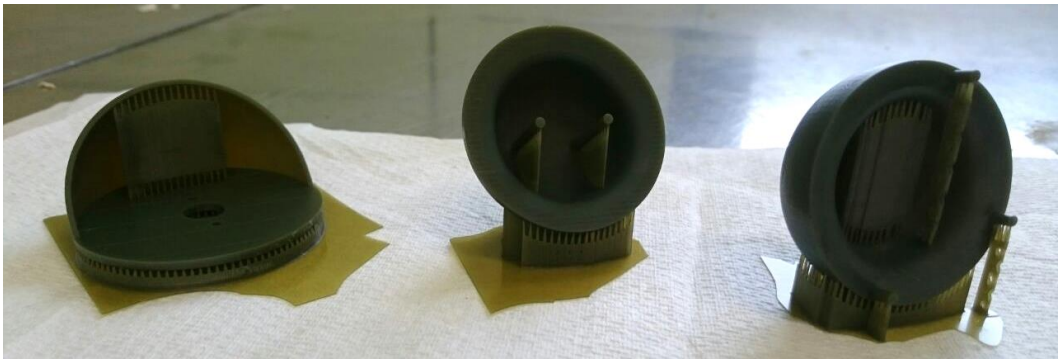

**Figure 38: Photo of prototypes shortly after removal from EnvisionTEC® machine**

## Laboratory Experiments

The data obtained from practical laboratory flow experiments enabled visualisation of fluid flow. Water was chosen because it has low density and viscosity (a worse-case scenario compared to blood) and is readily available; if water flow can be properly directed, blood flow should be controlled as well. Blood is a biological fluid, and shearing forces generated within the device may lyse red blood cells; the blood flow tests were valuable in elucidating the effects of the spargers on RBCs.

### Water Testing

The experimental setup (Figure 39) for testing water flow through the sparger prototypes consisted of:

- two fluid reservoirs
- metal rod stand with attached clamp
- PVC tubing (9.6mm ID, 2.4mm wall thickness)
- peristaltic pump (max rate of 3.9 L/min)
- tap water (~1.2L)

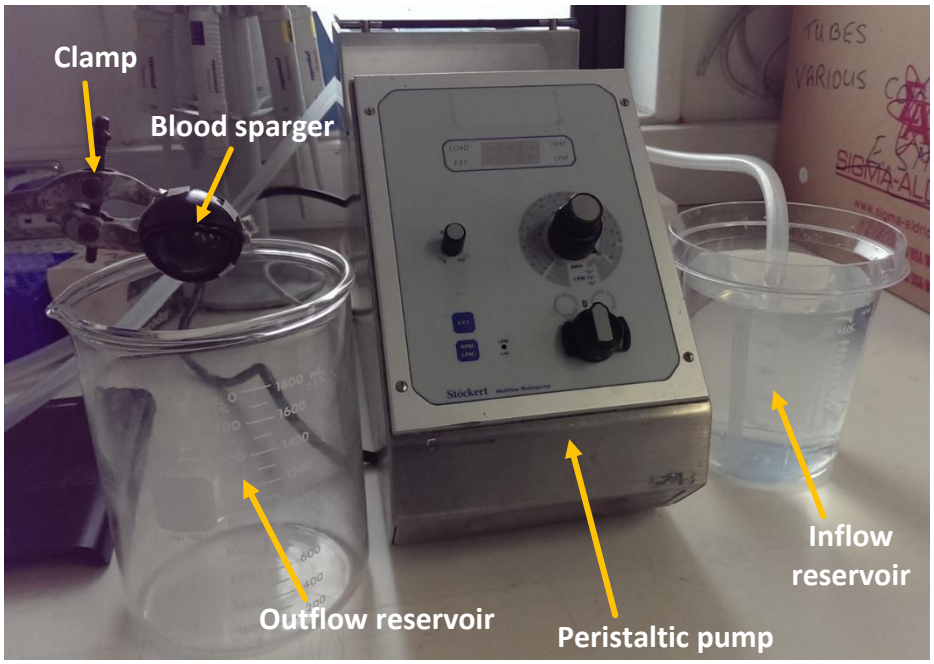


**Figure 39: Photo of experimental setup for water testing**

Tubing with 9.6mm inner diameter and 2.4mm wall thickness was threaded through the roller pump (Stoeckert Shiley multiflow roller pump, 10H series, model 10-10-00); one end of the tube was attached to the slip-on tube connector and the other end placed in the inflow reservoir containing approximately 1.2L water. Placing both tubes in the same container permitted continuous flow, but the pulsatile flow caused the single-reservoir setup to shake significantly which obstructed spray visualisation.

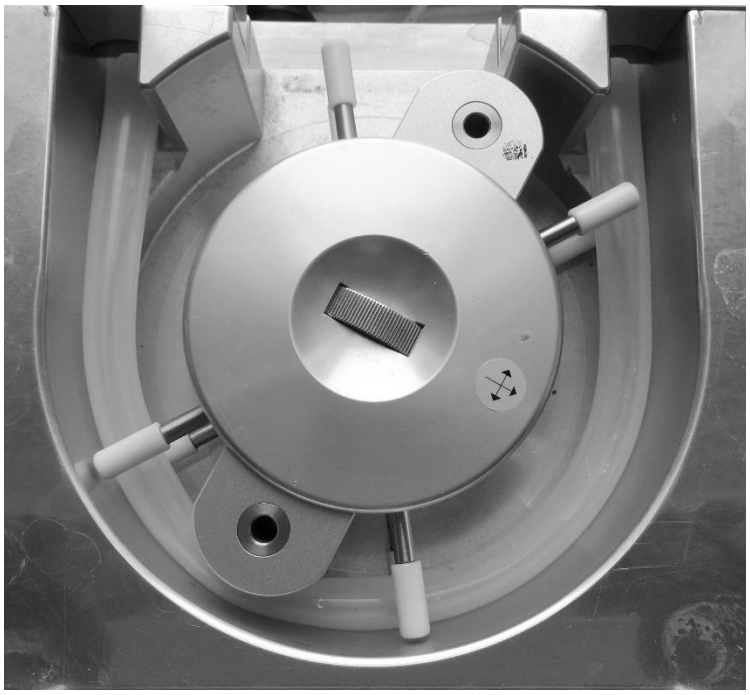

**Figure 40: Photo of roller pump with tubing**

The pump was run at a maximum volumetric flow rate of 3.9 L/min which, although lower than the projected 14.8L/min maximum manual pump rate was the highest achievable rate of any peristaltic pump in the laboratory. At maximum speed the water takes approximately 20-30 seconds to transfer between reservoirs; both the time and speed were sufficient to visualise general flow dynamics and determine flow changes between iterations. Each available prototype was tested a minimum of six times to ensure repeatability of results.

## Haemolysis Testing

The experimental setup for haemolysis testing was very similar to water testing; the two differences in this new setup were (1) fresh bovine blood was used instead of water and (2) both tubes were placed in the same reservoir to allow continuous flow (Figure 41). Additionally saline was pumped through the tubing before each trial to remove all blood traces, and the reservoir and connector were thoroughly cleaned and dried between runs. Fresh blood, all from the same specimen, was run continuously for 5 minutes in each trial.


**Figure 41: Photo of experimental setup for haemolysis testing**

The blood testing procedure for each run was:

1. Place 500ml blood into reservoir, put both tube ends into blood
2. Run pump at maximum speed for 5 minutes
3. Stop pump, take sample of blood
4. Empty reservoir, pump saline through tube until no blood remains
5. Clean reservoir and connector

Blood samples from each trial were then placed in 1ml Eppendorf® tubes and spun in a centrifuge for 10 minutes at 3,000 rpm (Figure 42). A pipette was used to remove 200µl of the upper plasma layer from each of the four blood samples; the samples were placed in a 96-well plate reader (Labsystems® Multiskan Ascent®) and read at 540nm wavelength (Figure 43).


**Figure 42: Photo of samples in centrifuge for haemolysis testing**


**Figure 43: Photo of 96-well plate reader for haemolysis testing**

In this sparger device RBC rupture is primarily due to shearing forces. Destroyed RBCs are less dense than intact RBCs, and the haemoglobin gives the supernatant a visible red tint after centrifugation; the darker the upper layer, the greater the degree of haemolysis (Figure 44). Although haemolysis can be seen visually, a spectrophotometer was used to quantify the amount of haemolysis (Cyprotex, 2015).

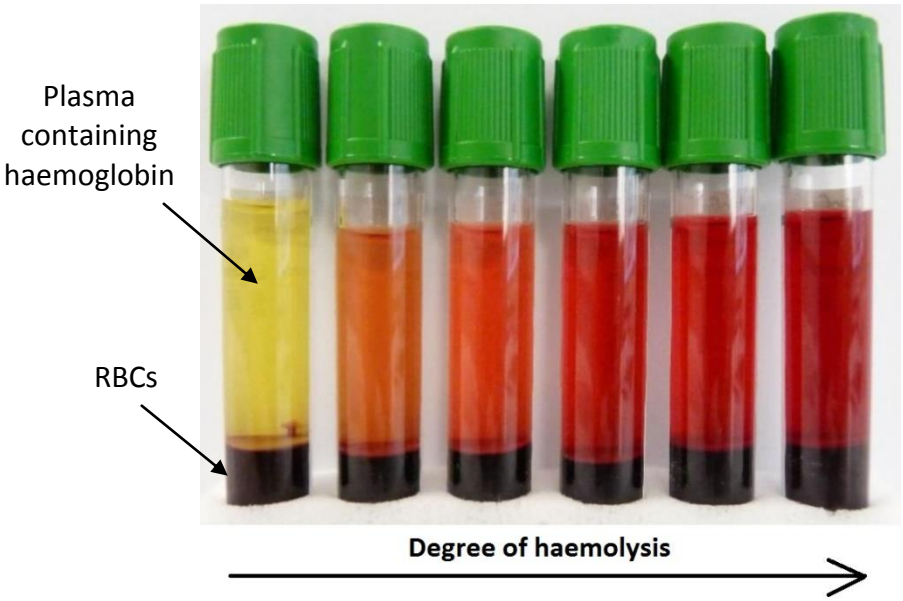


**Figure 44: Example of haemolysis evidenced by haemoglobin staining**

# Computer Modelling & Laboratory Testing

Beyond concept design, the other two steps of this project's iterative design process were computer modelling and laboratory testing. Each iteration was drawn in Inventor® and the STL part files sent to be printed. Successfully printed prototypes were tested in the laboratory using water, and both spray profiles and flow velocity were visualised through photos and videos. The final step of laboratory testing took place at the end of the cyclical iterative process—analysis of blood, the system's biological component, to mimic the intended application and test for haemolysis due to shear forces. Additionally the first iteration was modelled using Fluent® to capture general flow dynamics of the sparger design.

## Iteration #1

The first design iteration involved construction of all device components based on a set of free-handed sketches. The overall size of the complete device was determined by the size of the curved sparger surface; the surface needed to be deep enough and close to spherical in shape to re-route the fluid 180° as gradually and steadily as possible, avoiding unnecessary shearing or velocity increase.

### CAD Drawings

Two tube connectors were designed to fit into the medical grade PVC tubing with 9.6mm diameter. One connector prototype was made slightly longer at 25mm height with a marginally narrower wedge of maximum diameter 12mm (Figure 45, left); the second prototype was shorter at 20.5mm with a wider wedge of maximum diameter 12.5mm (Figure 45, right). Multiple tubes were available with varying elasticity and hardness, so the two connector diameters were 3D printed to provide a sampling range and ensure compatibility; the two heights were chosen to test whether tube grip was affected by inserted connector length. Diameter of the connector disc, along with diameter of all other discs in the device, was set at 47mm.

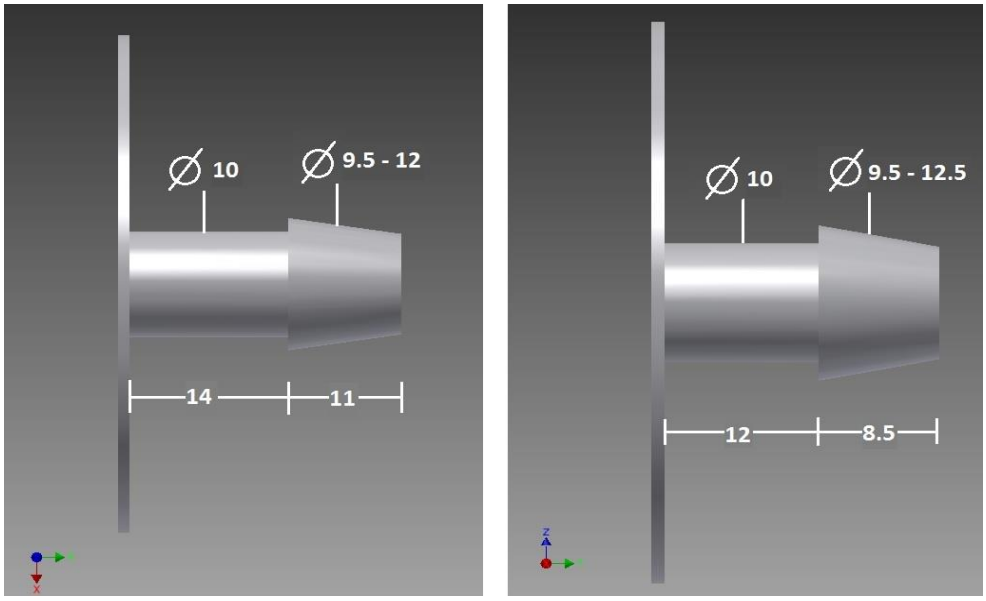


**Figure 45: CAD images of slip-on tube connector prototypes**

The disc for compressing the sock had an inner diameter of 8mm and outer diameter of 47mm (Figure 46). The first iteration of the disc was made 1mm thick because its purpose was to be glued to the sparger and hold the sock to the device.

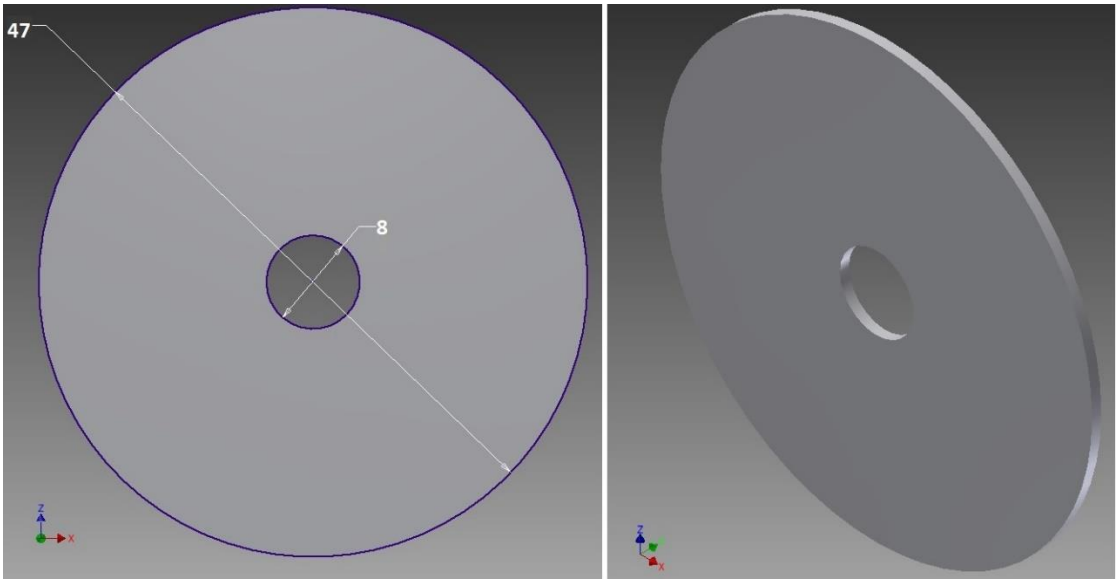


**Figure 46: CAD images of disc (iteration #1)**

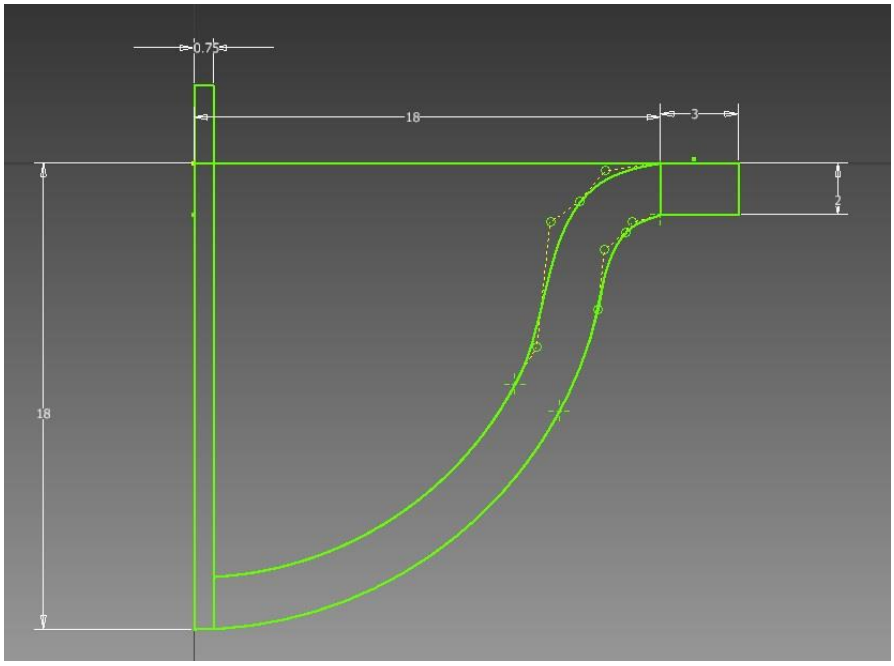


**Figure 47: CAD image of sketch rotated to create sparger construct**

The final diameter of the sparger—43.5mm—was defined by the need for acceptable depth. If too shallow, shearing along the sparger surface would be extensive and the air-blood mixture would flow at an unacceptably high velocity; conversely the sparger needed to be shallow enough for bag placement and not too wide for the sock. Diameter of the outer piece was then determined by sparger size because it had to maintain a 2mm separation from the sparger's lip and hood.

The curved sparger construct (Figure 48, bottom) was 2mm thick with an almost spherical shape and a 3mm lip along the circumference. The pole through the centre was 1.5mm diameter, as this was the thinnest rod printable according to the 3D printer specifications. The uniform space between the outer and inner sparger components was set at 2mm; this distance was chosen because it was not exceptionally narrow—it should thin flow without dramatically increasing fluid velocity or damaging blood components. The outer hooded disc and both hoods were 1mm thick, while the 'X'-construct was 2.5mm thick for holding the post and spherical insert in place. Two hood sizes were tested, 90° and 60°, to evaluate their effects on flow speed and spray profile.

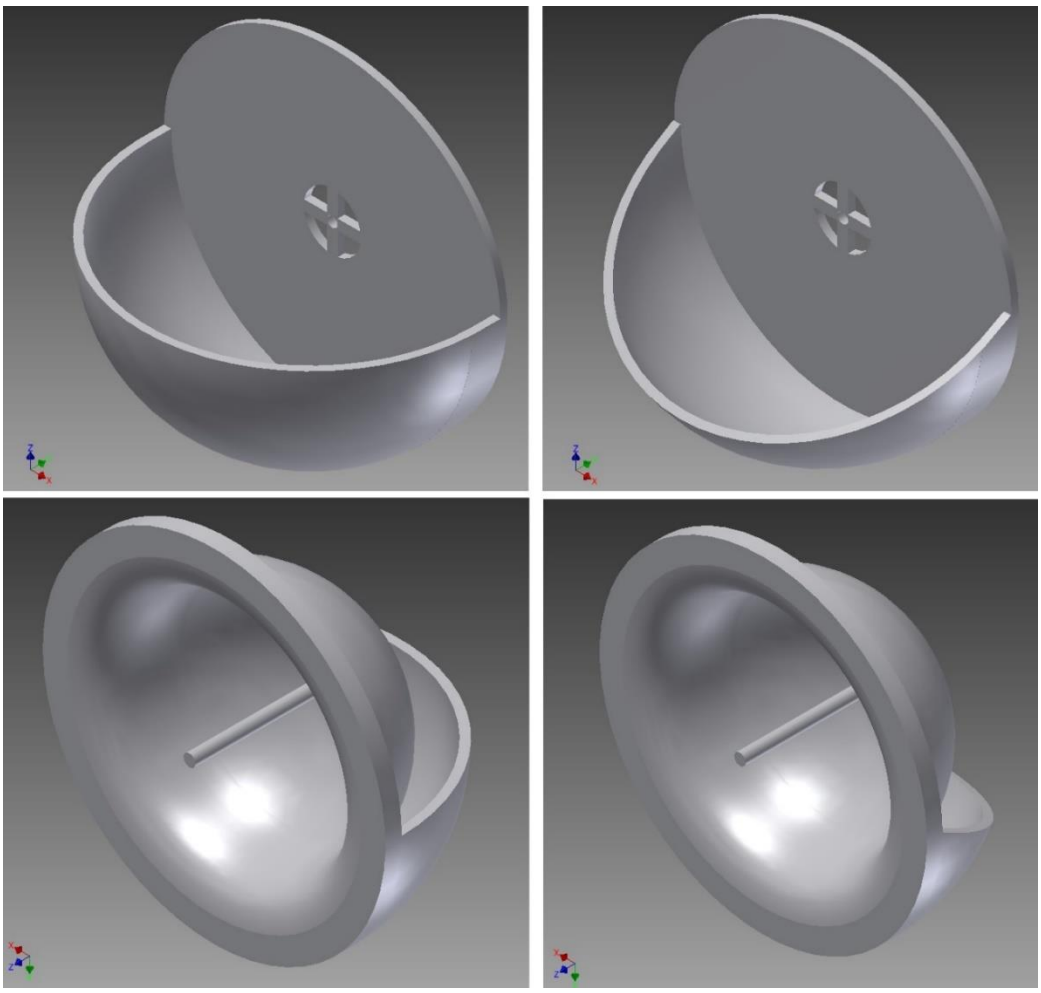

**Figure 48: CAD images of 90° (left) and 60° (right) hoods (iteration #1)**

These pieces were assembled into one file before being sent to the DMEM 3D printer; the entire sparger construct—both the inner and outer pieces—were printed as one part. Multiple views of the two assembled structures are displayed in Figures 49 and 50.

**Figure 49: CAD Images of 60° sparger assembly (iteration #1)**

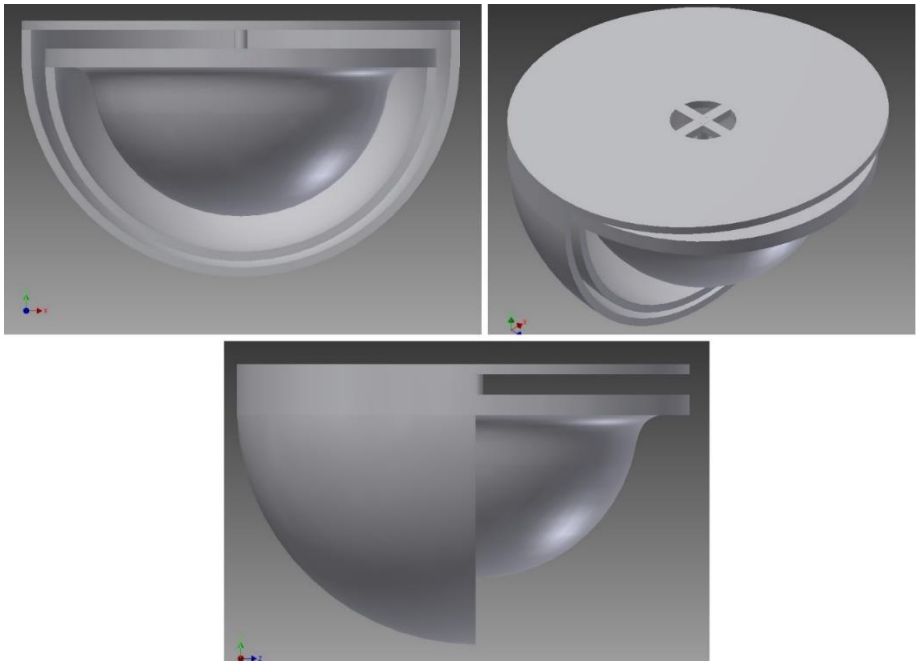

**Figure 50: CAD Images of 90° sparger assembly (iteration #1)**

The 3D model imported into ANSYS® Workbench® was an inverse model of the flow device itself; the solid structure denotes fluid flow space (space around the sparger and in the sock), while any areas consumed by the flow device are 'hollowed out'. The fluid model constructed and used to simulate flow for iteration #1 is depicted below (Figure 51). The long half-cylinder structure represents the sock.

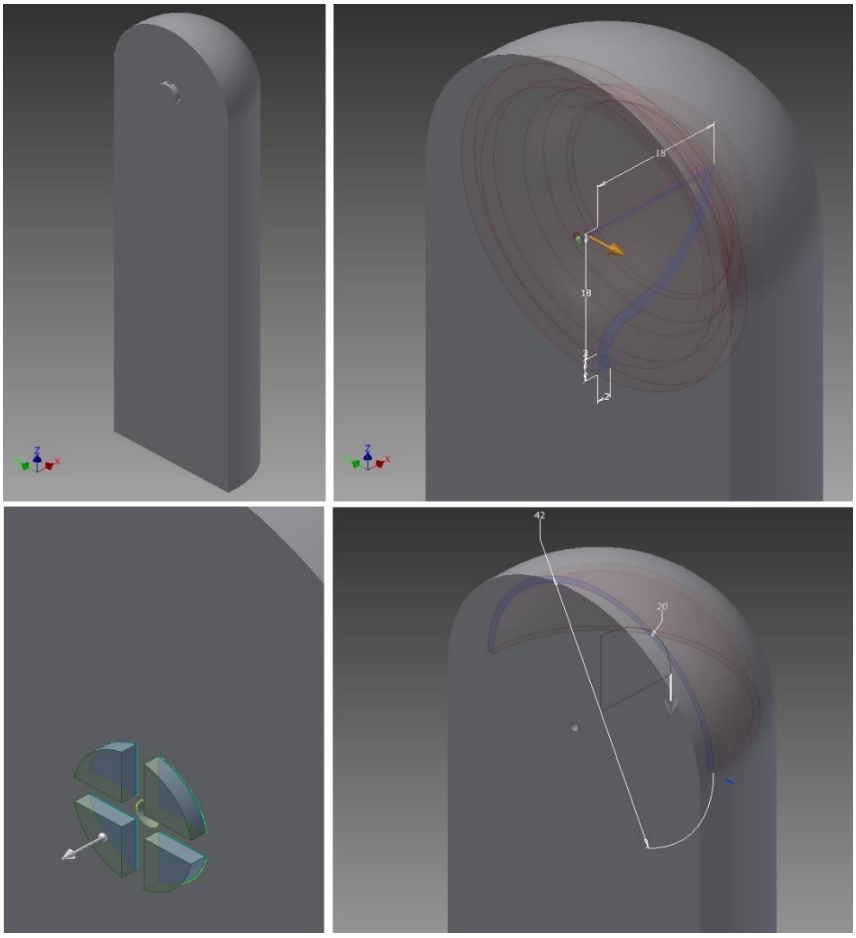

**Figure 51: Inverse CAD model representing fluid space**

The flow simulations yielded generally expected results, with flow velocity significantly decreased before exiting the sparger. No fluid appeared to run down the sparger's outer surface; a small amount of fluid fell back into the basin—adding to flow turbulence—but most fluid pathlines extended radially outward as anticipated (Figures 52 and 53).

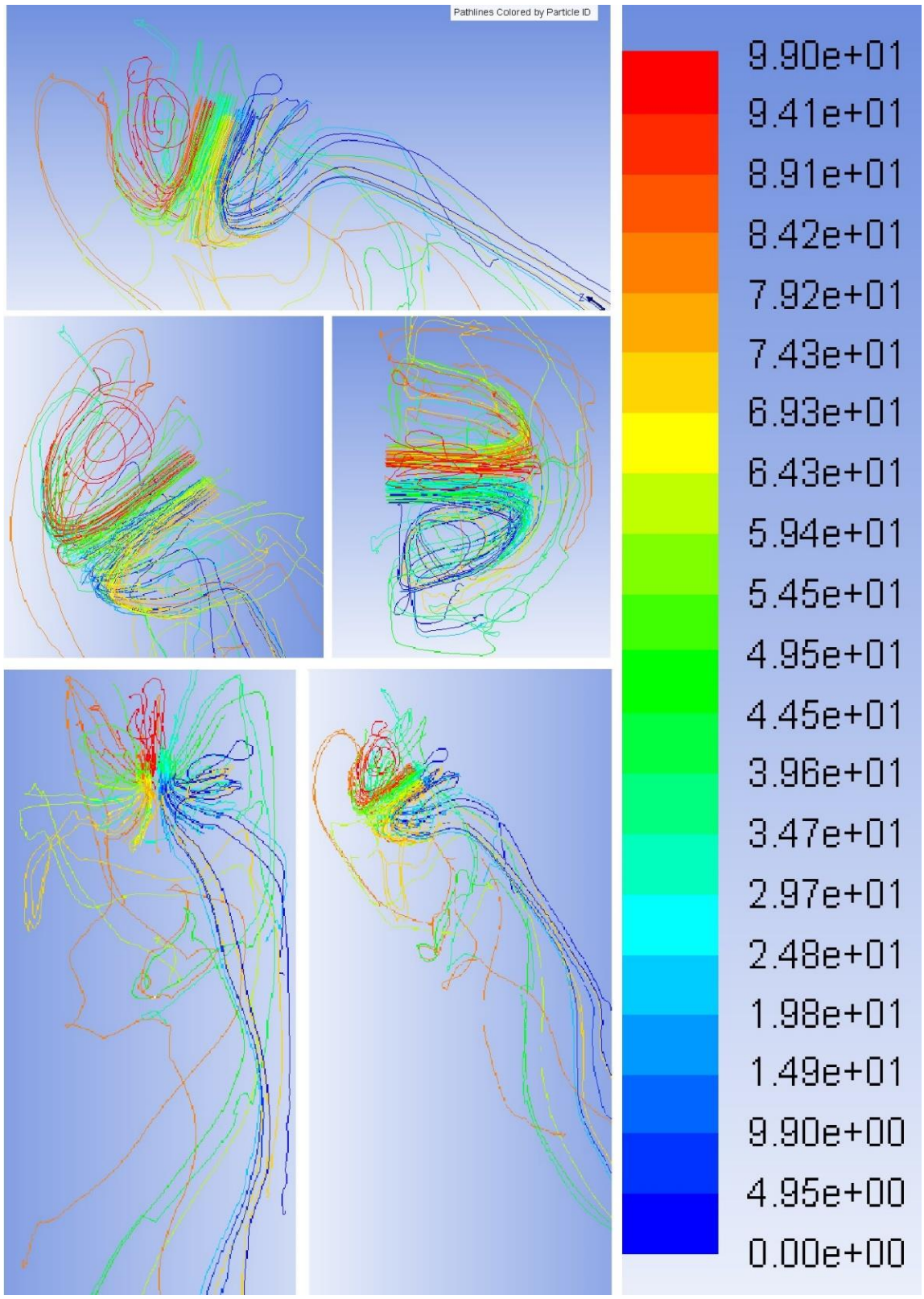


**Figure 52: Flow simulation images tracking particle pathlines by identity**

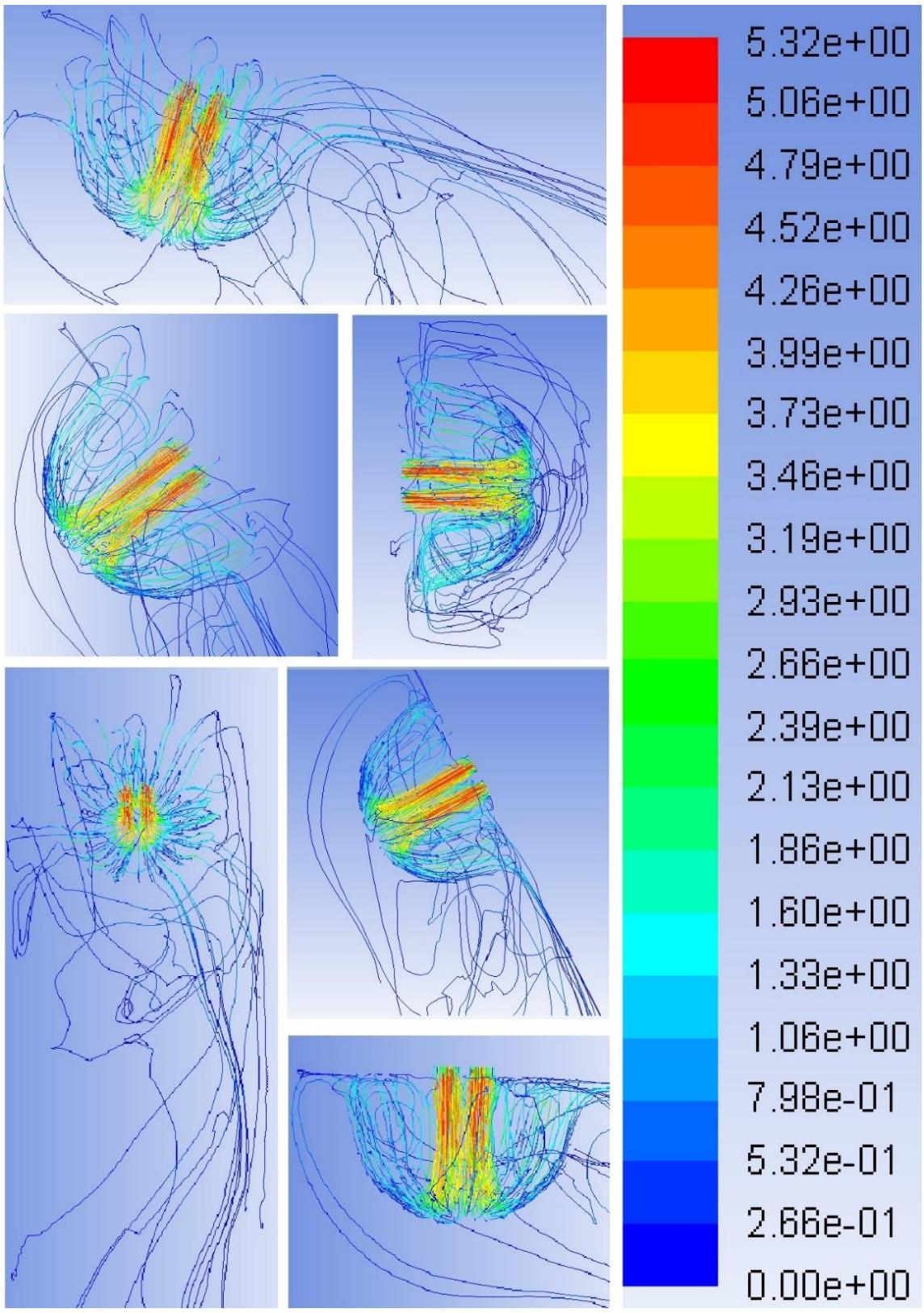


**Figure 53: Flow simulation images tracking particle pathlines by velocity**

Flow data was then used to visualise the primary radial flow directions along the sparger; this was accomplished by tracking 1,000 particles released at the inlet—a single release, not continuous flow (Figure 54). This simulation revealed most pathlines radiate vertically or horizontally. The laboratory water testing done in later iterations proved this phenomenon to be accurate.

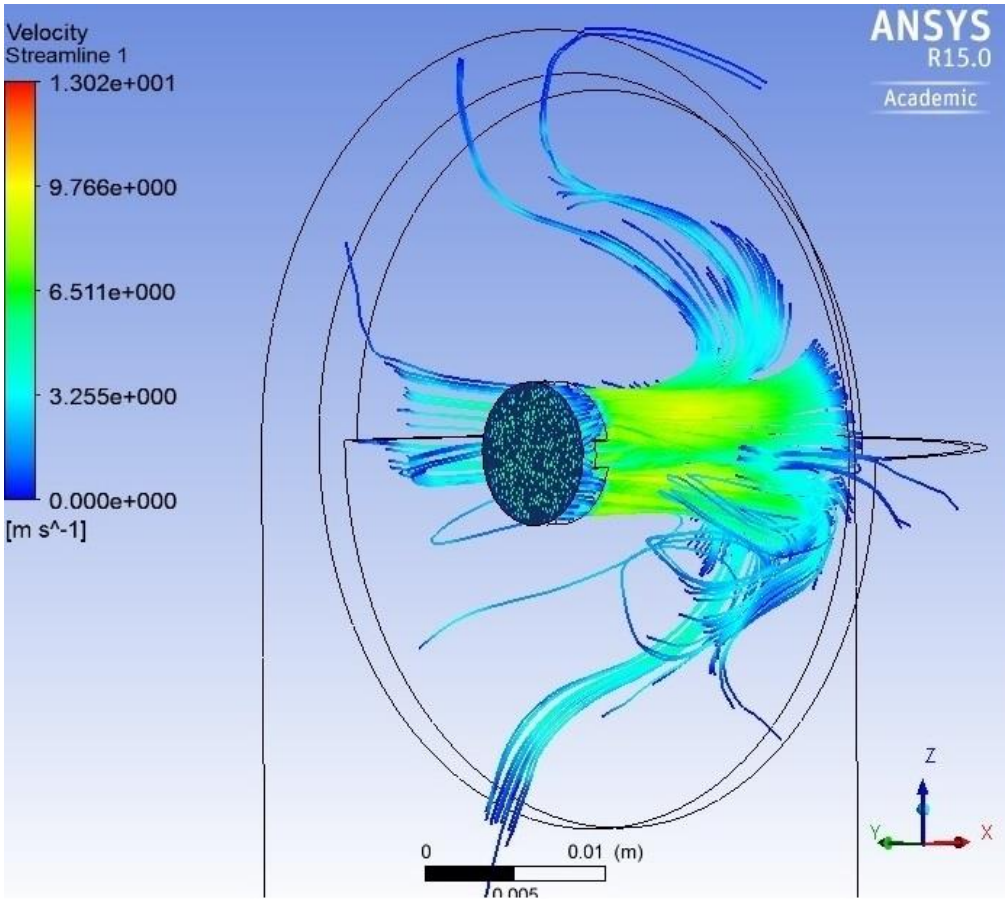


**Figure 54: Flow simulation image demonstrating four primary directions of fluid flow**

A filleted post design was also fluid modelled; the simulation revealed a slight fillet around the post base eliminated most fluid fall-back (Figure 55). However the centre rod prototype was never printed or tested with a fillet.

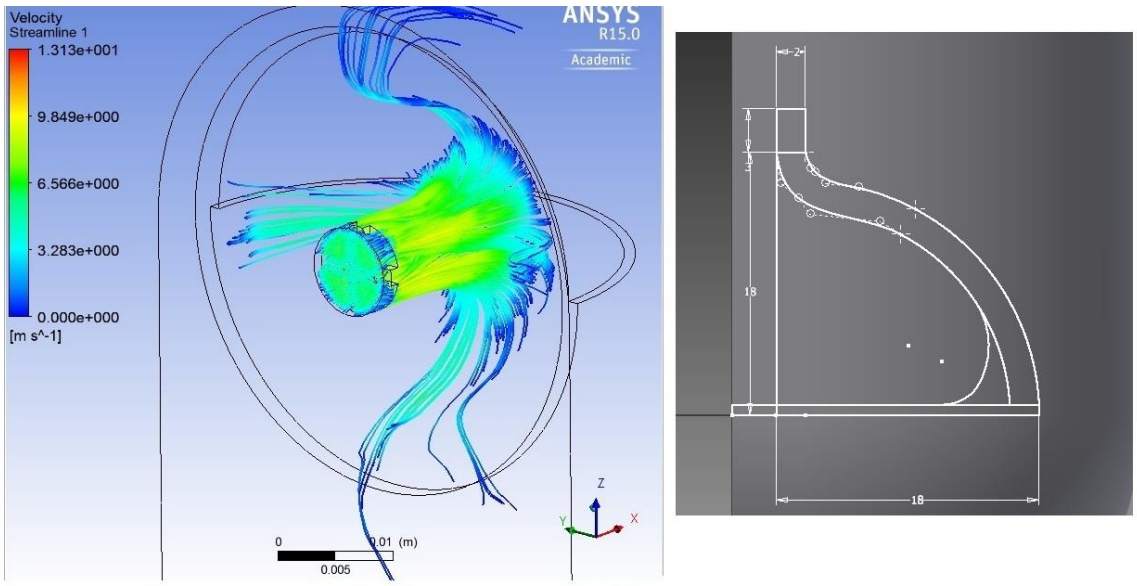


**Figure 55: Flow simulation image demonstrating effect of filleted centre post**

Fluent simulations are not very accurate due to the input fluid properties and the fact the model is considered a rigid structure. Density and viscosity are the two fluid properties used to define blood in the Fluent® simulations. Blood suctioned from haemorrhaging wound sites will be a turbulent blood-air mixture, but this type of fluid cannot be represented in Fluent®. Additionally blood must be treated as a Newtonian fluid within this and most modelling programs because the software is not developed to model biological materials. In reality blood is a non-Newtonian fluid because RBCs naturally aggregate, meaning viscosity is a function of shearing rate; the faster the blood moves the thinner it becomes and vice versa. (Blood Flow Online, 2015) Additionally a solid structure provides inadequate representation of flow through a malleable sock, but it does assist in visualising flow across the rigid sparger.

## 3D Printing

The Stratasys® printer was unable to reliably and accurately print iteration #1 prototypes. The 1mm discs proved too thin, arriving broken or warped; however the slip-on connectors printed successfully and are pictured in Figure 56.

**Figure 56: Photo of connector prototypes**

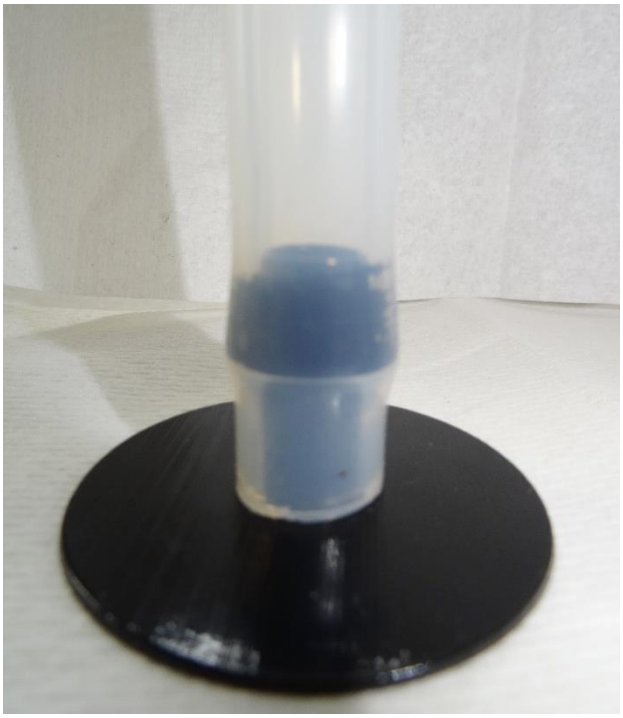

**Figure 57: Photo of slip-on connector with tubing**

The narrower and longer connector fit securely into a 9.6mm inner diameter PVC tube without need for lubricant, and the parts could not be separated after attachment (Figure 57). The length of the connector did not appear to increase security, so future iterations could be made lower profile (~2mm shorter) without risking leakage or

separation. However the present connector worked well, so these printed pieces were used for the duration of project testing.

The poor resolution of this printer, the complexity of the design, and fragility of the material meant the sparger component failed to print; during support removal, the posts were either destroyed by the water spray or broken upon handling. All of the spargers arrived in two pieces and could not be salvaged (Figure 56). The ability to remove support material became a primary focus for subsequent iterative designs.

**Figure 57: Photos of printed sparger pieces missing connecting post (iteration #1)**

## Iteration #2

Due to 3D printer limitations, the second design iteration separated the complex component into two pieces which were connected after printing. A single centre post did not allow for this component separation, so the structure was removed. The new two-part component needed to be stable, and the flow along the sparger surface needed to be as unobstructed as possible.

The first and most minor design alteration for the second iteration was increased thickness and strength of all disc structures within the device; the new thickness was set at 2mm (Figure 58).

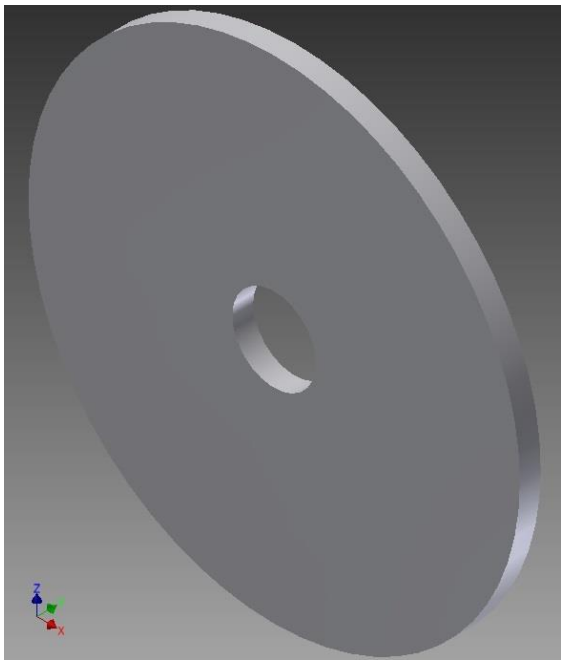

**Figure 58: CAD image of revised disc (iteration #2)**

Major design changes had to be applied to the sparger component; the structure needed to be separated into two parts and assembled after printing. Posts remained necessary to maintain a 2mm separation of inner and outer part surfaces. Certain configurations were considered including the placement of multiple posts inside the sparger around the fluid inlet, as well as placement of posts around the exterior of the sparger along the flat lip. Both arrangements were drawn and printed for testing (Figure 59).

Two vertical posts with 1mm fillets were chosen instead of four evenly-spaced posts to limit the number of radial flow disruptions. Vertical alignment was selected because although flow volumes on the sides should remain similar, more fluid will flow down due to gravity. The large downward flow volume was anticipated to cause seesawing of

horizontal posts and tilt the sparger upward, ultimately obstructing flow between the hoods (Figure 59, right).

The second configuration—placement of three posts along the outside—ensured the sparger basin surface remained unaffected; a fourth post at the most distal point of the hood was unnecessary for stability, and presence of the outer hood prevents a person from securely pressing the top post into place (Figure 59, left). All posts were given a 2mm diameter for additional strength, and a disc stop was placed on each post to ensure proper insertion distance. Holes were placed in the discs to allow insertion of the posts. Two versions (60° and 90° hood) of the 3-post and 2-post designs were sent to print.

**Figure 59: CAD images of 3-post (left) and 2-post sparger pieces (right) (iteration #2)**

## 3D Printing

The new discs printed well and were thick enough to resist any bending; as such no more improvements were required. The final disc is shown in Figure 60.

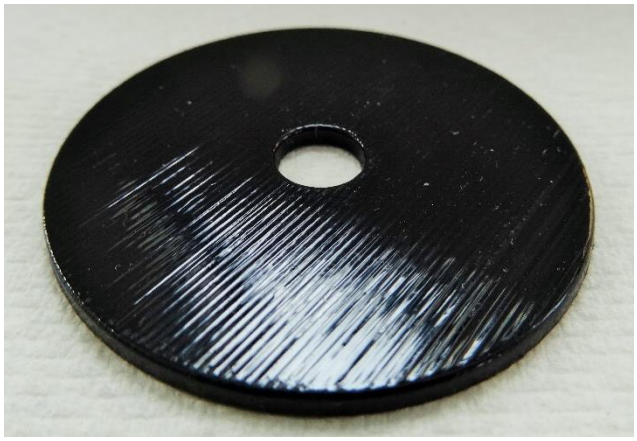

**Figure 60: Photo of printed discs (iteration #2)**

Printing of the sparger pieces highlighted the brittleness of the ABS material; multiple pieces arrived broken. Only two of the four prototypes was capable of assembly and testing: the 3-post sparger with 60° hood and 2-post sparger with 90° hood (Figure 61).

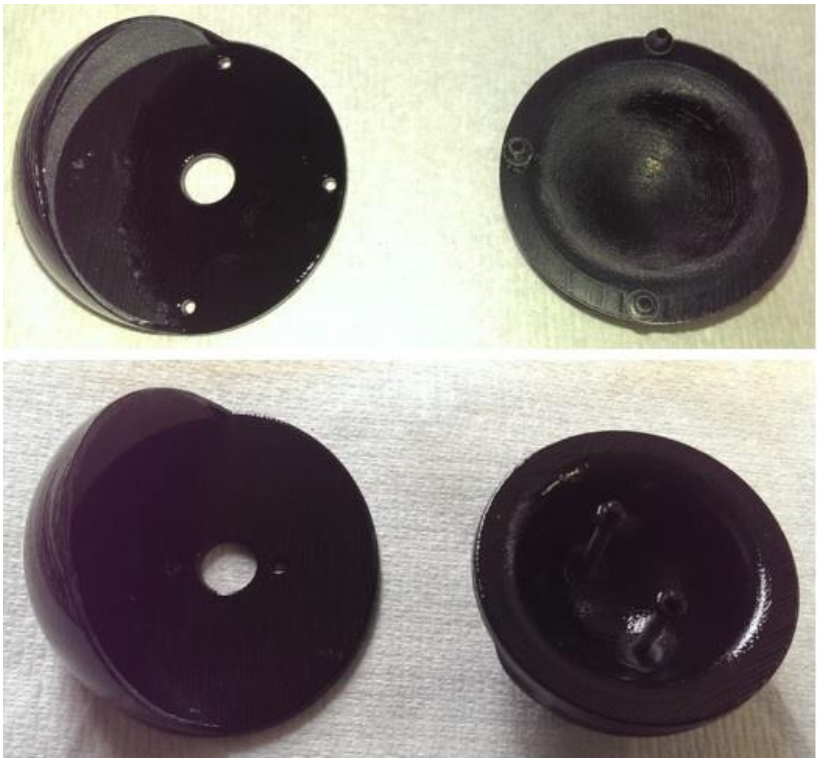

**Figure 61: Photos of 2-post (top) and 3-post (bottom) sparger pieces (iteration #2)**

The pieces fit together well and did not require glue; the side profiles of the two usable prototypes are shown in Figure 62.

**Figure 62: Side profile photos of tested spargers (iteration #2)**

## Laboratory Water Testing

The first prototype to be attached to the tube connector and tested with water was the two-post sparger configuration with 90° hood. The spray from the sparger was quite violent and varied significantly. The water spray extended outside the reservoir and the container had to be held up to catch the fluid; regardless of containment attempts, water was still pooled on the counter after each trial run. Also the 90° hood appeared to cause the water to bend upward almost 90° around the bottom edge of the hood—one of the reasons why the water sprayed beyond the containment reservoir. Evidence of the spray profile is seen Figure 63.

**Figure 63: Photo of front spray profile with 2-post 90° hood sparger (iteration #2)**

Although not visable in photos or video, a seesawing effect did occur in the vertical 2-post sparger; movement was evidenced by warping upon inspection the following morning. After drying overnight the sparger was permanently tilted; the posts also snapped before a photo was taken (Figure 64).

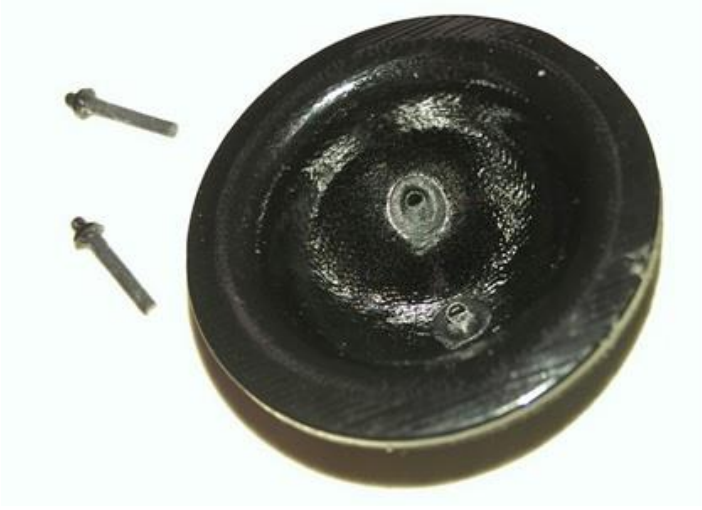

**Figure 64: Photo of breakage occurring in printed prototypes (iteration #2)**

The 60° 3-post sparger was water tested and found to have a smaller angle of spray, with all water falling into the reservoir (Figure 65, right); also the flow was slower, steadier, and more controlled than in the previous prototype. The greatest fluid volume flowed downward through the sparger as expected, but volume through the hood increased with flow rate. There was a significant amount of fluid running down the outside of the sparger, but this is expected when volumetric flow rate and velocity are low.

**Figure 65: Photos of spray profiles with 60° hood sparger (iteration #2)**

## Iteration #3

The trial run with the 3-post prototype from iteration #2 yielded positive results; therefore this iteration was reprinted using the new EnvisionTEC® printer. Additionally a 4-post prototype was designed to determine whether the 2-post prototype results were due solely to sparger movement or because of posts located within the sparger basin.

## CAD Drawings

The 3-post design from iteration #3 was given one minor alteration in the next design cycle; a small 0.5mm raised lip was added to the bottom half of the sparger to examine whether gap narrowing would even spread of the downward flow. The 2-post design was supplemented with this same lip along with two horizontal posts to prevent any sparger movement. The four posts were all filleted at their base—these fillets further disrupted the inner sparger surface but strengthened the posts. The 90° hood design was not pursued further due to its unacceptable spray profile. The 4mm diameter post stops were removed from all posts because the 2mm disc thickness could be used to control insertion depth. Iteration #3 CAD illustrations below show the two new prototypes (Figure 66).

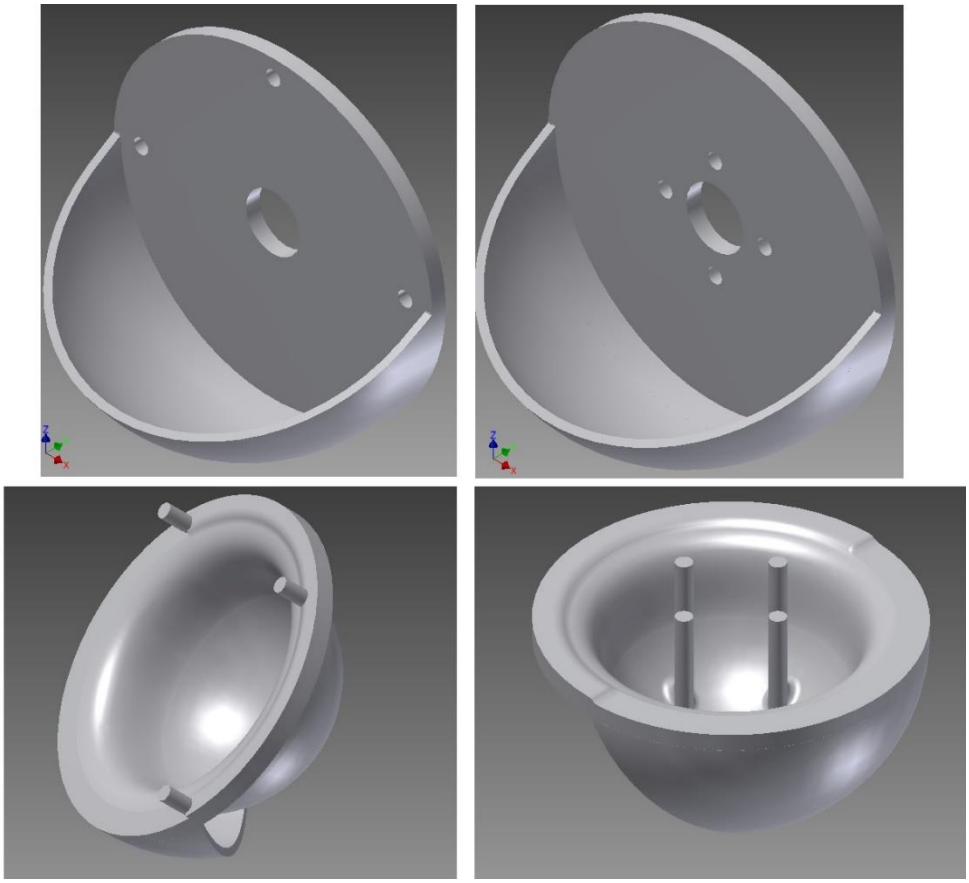

**Figure 66: CAD images of sparger components with raised lip: 3 posts (left) and 4 posts (right) (iteration #3)**

After these designs were printed and tested, the sparger curvature was altered slightly to incorporate the lip (Figure 66) but they were never printed.

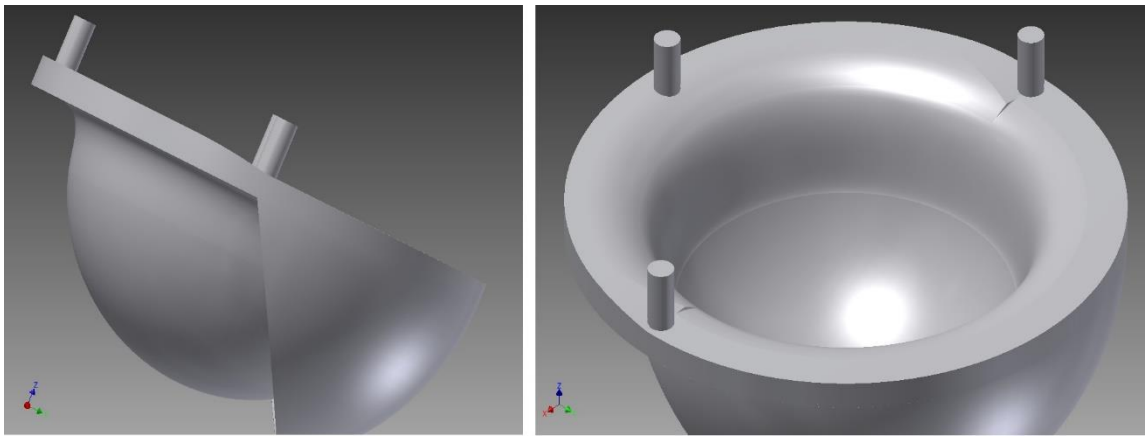

**Figure 67: CAD images of revised lip**

## 3D Printing

The EnvisionTEC® printer provided stronger prototypes; precision was noticeably improved over the DMEM printer, and the holes were easily sanded for a tight fit. Surfaces were very smooth with no residue, but the material was less slippery than the ABS material used for previous iterations. Figure 68 depicts the first printing with EnvisionTEC®, but the thick, crisscrossed support structures could not be satisfactorily removed.

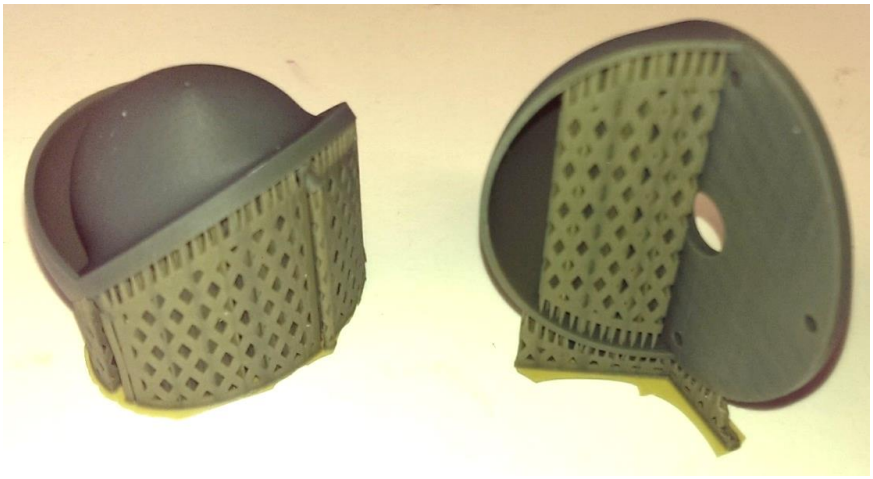

**Figure 68: Photo of first EnvisionTEC® printing, with crisscrossed supports (iteration #3)**

The pieces were printed again following support structure alterations, and the thin vertical supports were easily removed (Figure 68). Wet sanding enabled necessary smoothing of the finished pieces (Figure 70).

**Figure 69: Photos of re-printed prototypes with vertical supports (iteration #3)**

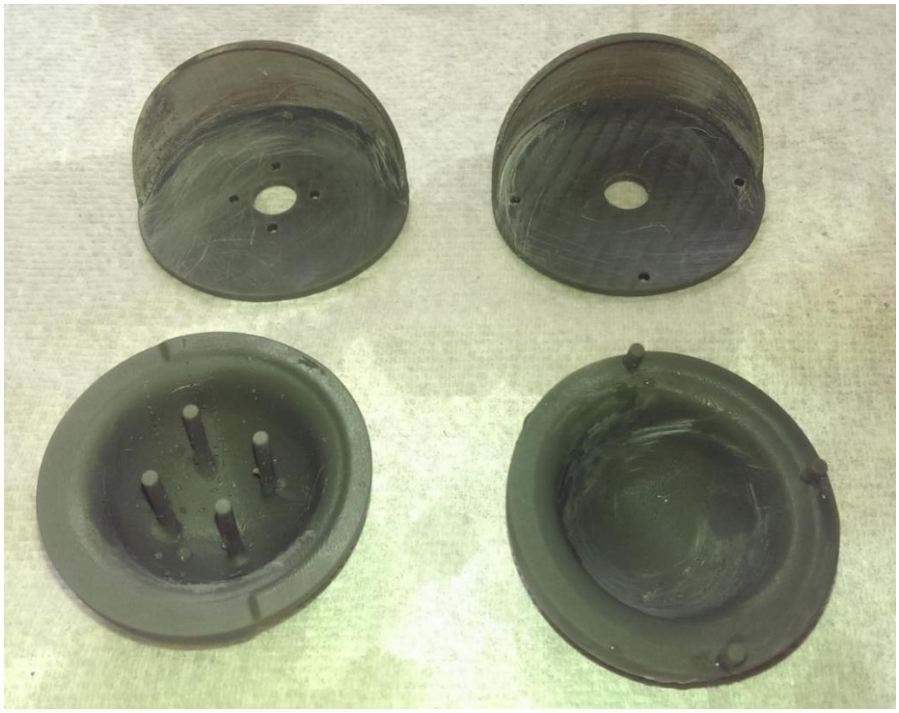

**Figure 70: Photo of 4-post (left) and 3-post (right) printed prototypes (iteration #3)**

The side profile views of both spargers reveal the 2mm spacing for blood flow; the posts inserted into the holes smoothly and the stops proved unnecessary to ensure the 2mm spacing (Figure 71). The posts and holes were coated with a primer (Loctite® 770 polyolefin primer) then a drop of epoxy glue (Loctite® 4061) placed in each hole before insertion to ensure permanence of connection. The same gluing procedure was done for all future iteration assemblies.

**Figure 71: Photos of assembled 3-post (left) and 4-post (right) spargers (iteration #3)**

The 3-post water sparger displayed fairly consistent flow with maximum spray profile seen in the bottom photo of Figure 72. Water flowed up between the hoods similarly to the previous 3-post iteration (Figure 73). Decreasing the outlet space along the bottom half of the rim only served to unbalance the device, causing slight shaking and increasing flow velocity. The prototype still performed adequately, but flow velocity and instability caused by the raised lip determined this additional construct to be counterproductive.

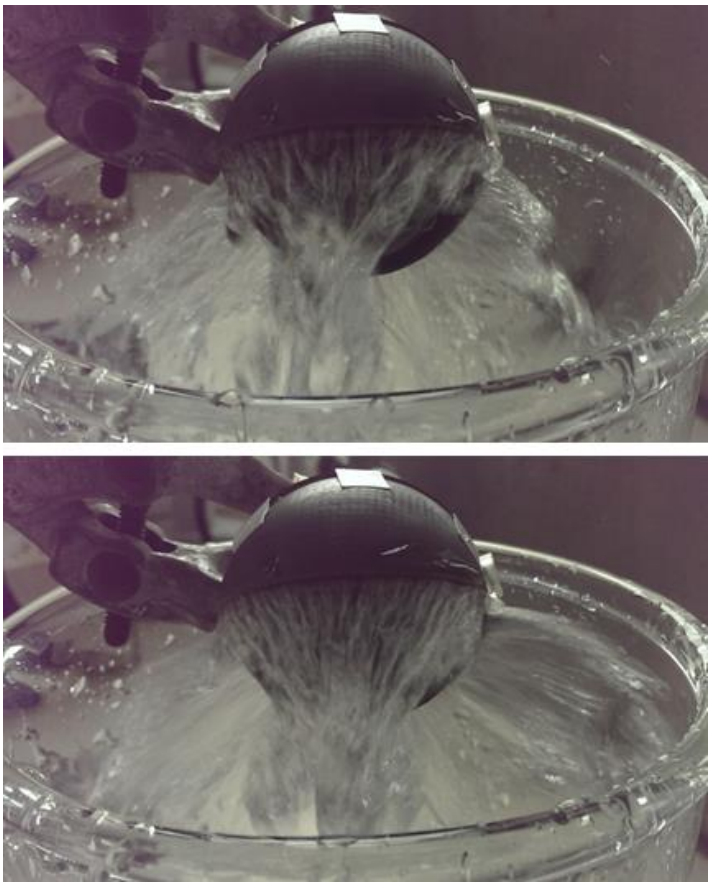

**Figure 72: Photos of front profile spray of 3-post sparger (iteration #3)**

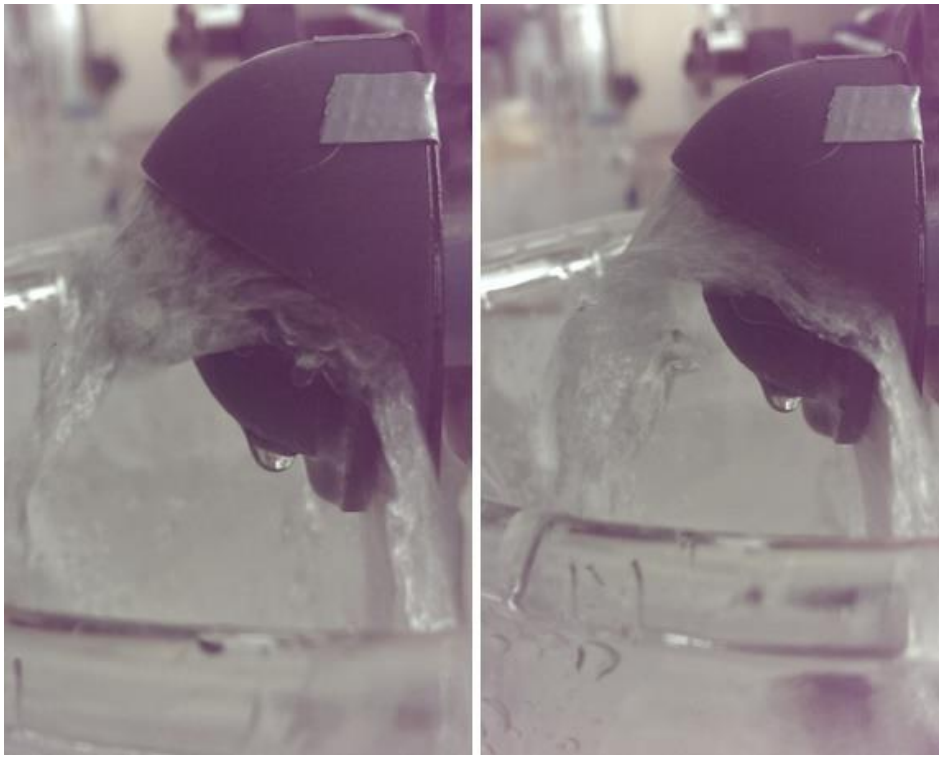

**Figure 73: Photos of side profile spray of 3-post sparger (iteration #3)**

The 4-post sparger was much more stable than its similarly designed 2-post iteration, and no more sparger movement occurred. Despite removing the seesaw effect, the spray still displayed great variation and produced significant splatter on the surrounding counter. The raised bottom lip likely added to the spray variation and flow velocity as it did in the 3-post prototype. The front and side profile photos of the flow capture this variation (Figures 74 and 75).

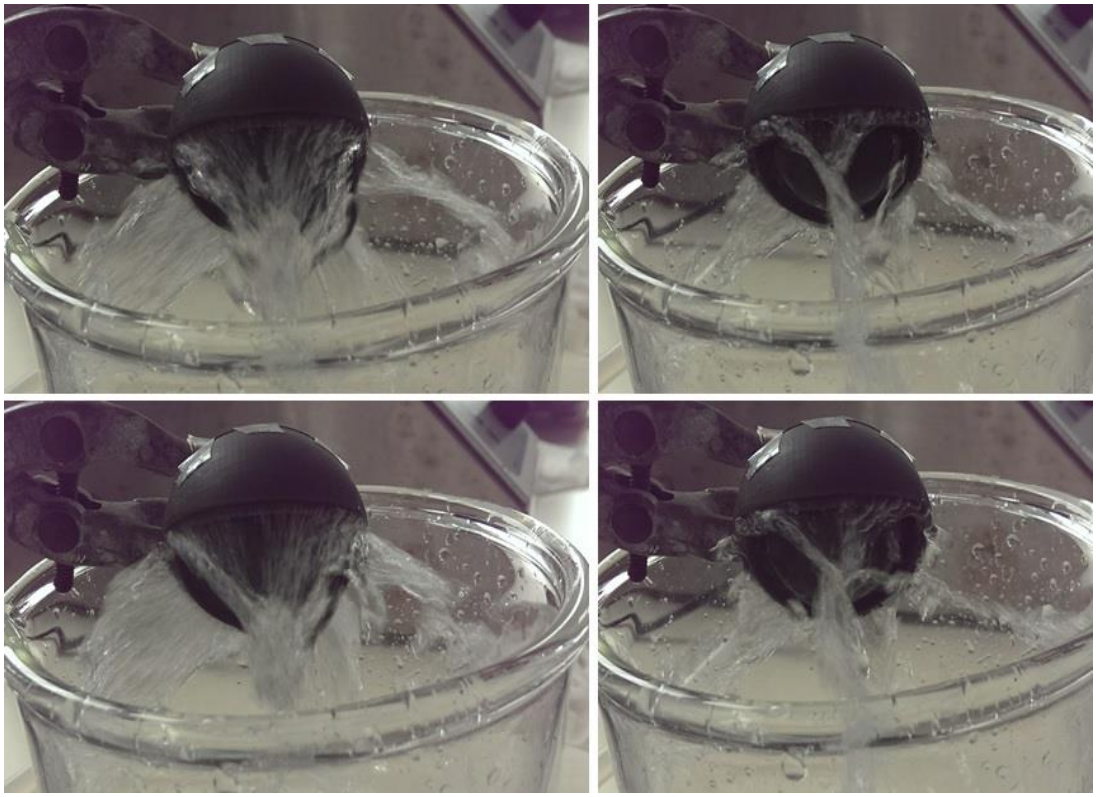

**Figure 74: Photos of variation in front profile spray of 4-post sparger (iteration #3)**

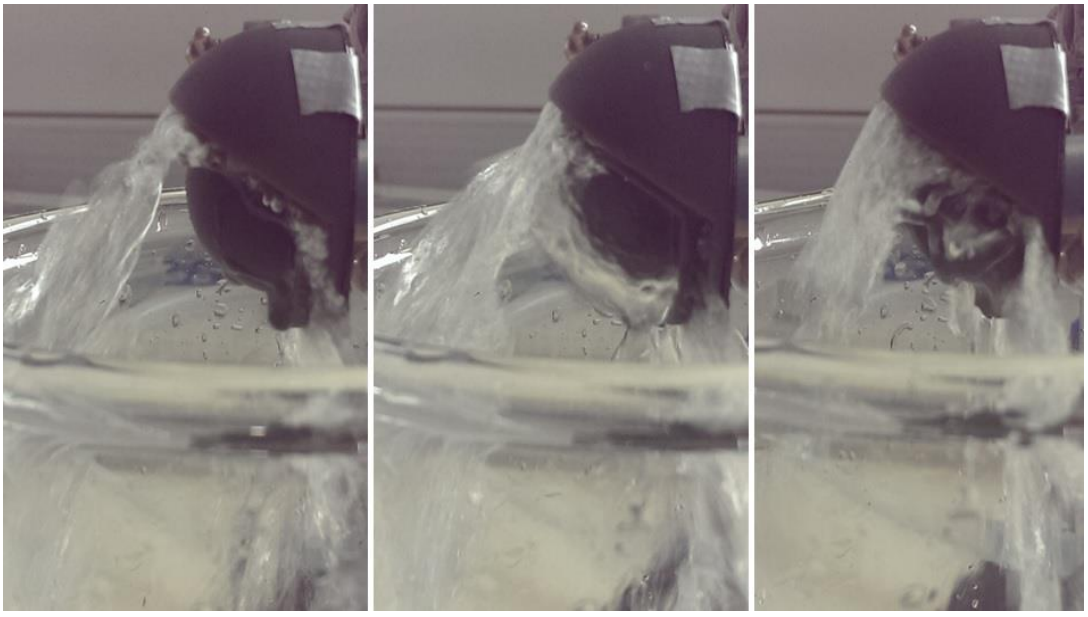

**Figure 75: Photos of variation in side profile spray of 4-post sparger (iteration #3)**

## Iteration #4

The device design underwent a significant change in the fourth iteration; the flow needed to be more uniform, with more flow across the upper half of the sparger and through the hoods. One way to accomplish this was to limit the flow area of the fluid once it hit the basin of the sparger; this was done by eliminating most of the open space within the sparger and forcing more fluid to move upward against gravity.

### CAD Drawings

The iteration #3 three-post sparger proved successful as in the similar iteration #2 despite the raised lip modification which was subsequently removed; however the spread was not even and velocity could still be decreased. To even the flow, an insert was built onto the inside surface of the disc; the insert complements the shape of the sparger while maintaining a 2mm gap for fluid flow (Figure 75). The rationale for this was to allow the fluid to perpendicularly strike the sparger's centre then be forced out in all directions at a depth of 2mm. This limited flow space should direct a larger fluid volume up between the hoods. The curved sparger piece was not altered in this iteration.

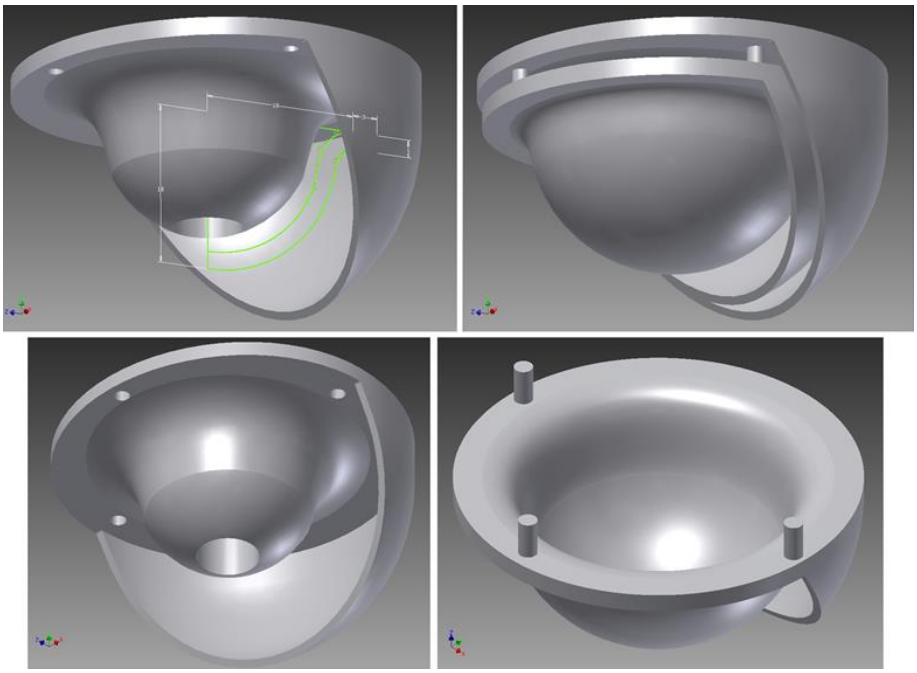

**Figure 76: CAD images of inner and outer sparger components (iteration #4)**

The pieces for iteration #4 printed with the same support structures as in the previous iteration, with very little supports being placed under the outer hood structure or within the sparger. This was to ensure the surfaces in contact with fluid had minimal support structures and thus had a smooth finish.

**Figure 77: Photos of hooded sparger insert with supports (iteration #4)**

The outer sparger surface was not wet sanded as it was not a flow surface of interest, but it was later sanded before blood testing. The new insert within the sparger is visible when looking at the side profile (Figure 78). Holes in the disc were enlarged slightly with a hand file before assembly to allow for a tight fit.

**Figure 78: Photo showing side profile of complete sparger (iteration #4)**

Water testing of iteration #4 yielded significantly different flow results; flow was slower, more even, and had a very limited spray range. Most water flowed directly downward with no side spray; in fact the flow rate was close to half the rate of any previous iteration (Figure 79).

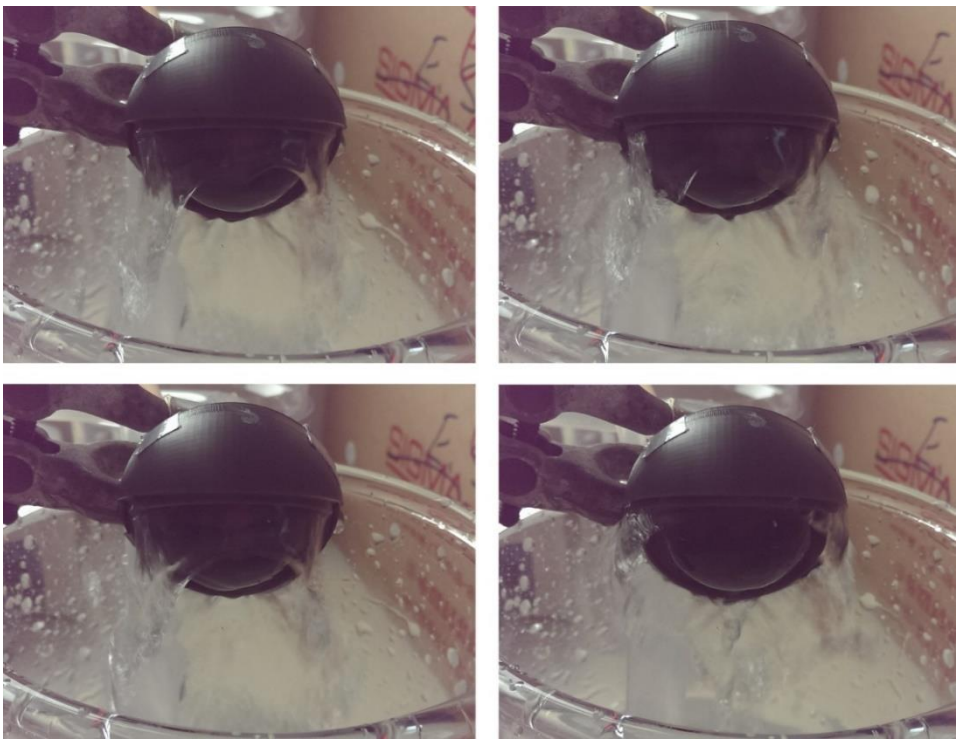

**Figure 79: Photos of sparger front profile spray (iteration #4)**

The only notable drawback to the low velocity was all fluid exiting through the hoods subsequently dropped down and flowed across the outer sparger surface (Figure 80). The device needed to be altered to direct this portion of the flow outward away from the sparger. Despite this issue, iteration #4 proved a significant success in directing and controlling flow.

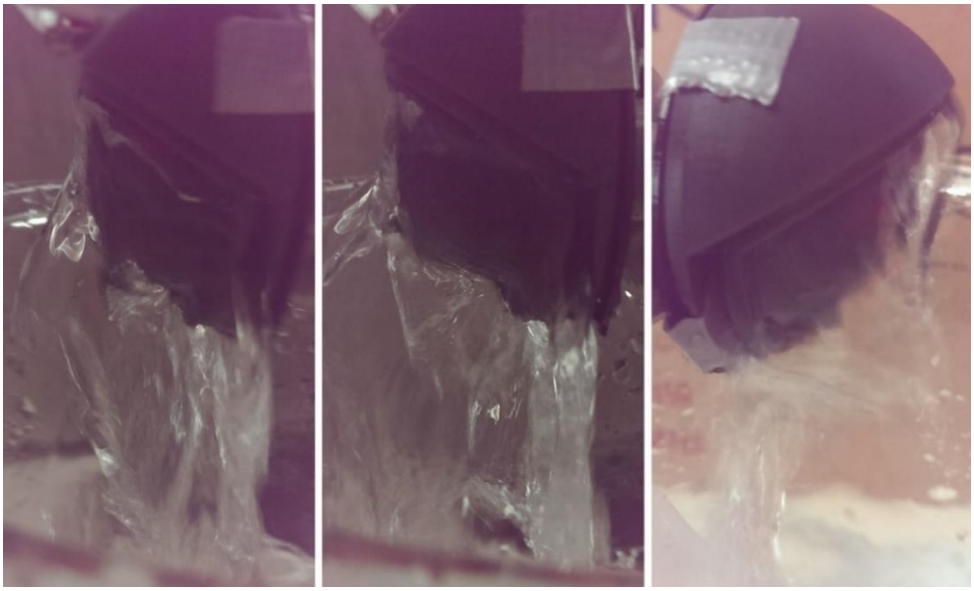

**Figure 80: Photos of sparger side profile spray (iteration #4)**

## Iteration #5

All fluid exiting between the hoods was running down the outside surface of the sparger in iteration #4, but the flow speed of the design was optimal. Fluid must be made to flow across the inside surface of the defoamer and sock instead of running down the sparger and dripping into the bottom of the sock; to direct flow outward, iteration #5 involved modifying the inner hood.

### CAD Drawings

The iteration #4 prototype significantly reduced spray profile, flow distribution, and velocity compared to previous iterations. The primary issue was flow down the outside of the sparger due to low velocity. The simplest modification to address this problem was to control flow profile by extending the inner hood to cover more of the sparger. The inner hood was rotated to 90° then extended downward 8mm while the outer hood remained unaltered. The sock would likely drape over the inner hood given this configuration, which was acceptable because the fluid should flow across the sock's inner surface. Figure 81 displays the inner hood extension while Figure 82 depicts the complete sparger assembly.

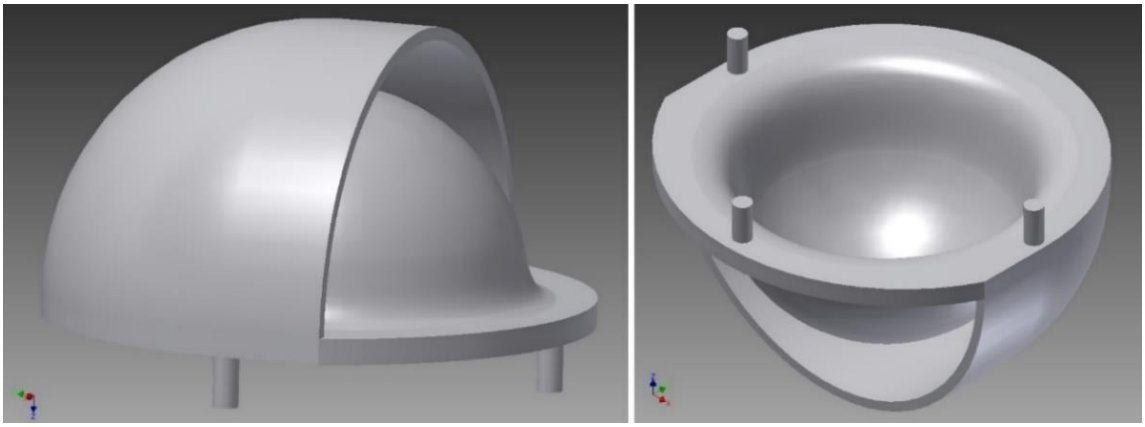

**Figure 81: CAD images of modified inner sparger component (iteration #5)**

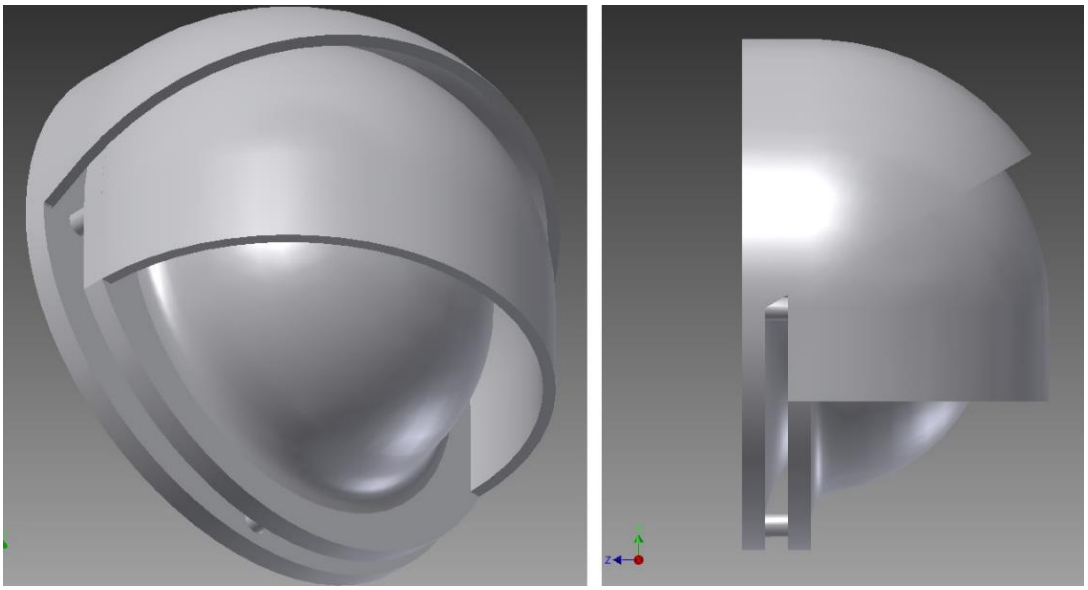

**Figure 82: CAD images of sparger (iteration #5)**

## 3D Printing

The iteration #5 sparger pieces were printed using the same support structure configuration as the previous iterations, with limited supports in contact with primary fluid flow surfaces. (Figure 83). All fluid contact surfaces were wet sanded and the final products are displayed in Figure 84.

**Figure 83: Photos of sparger pieces with supports (iteration #5)**

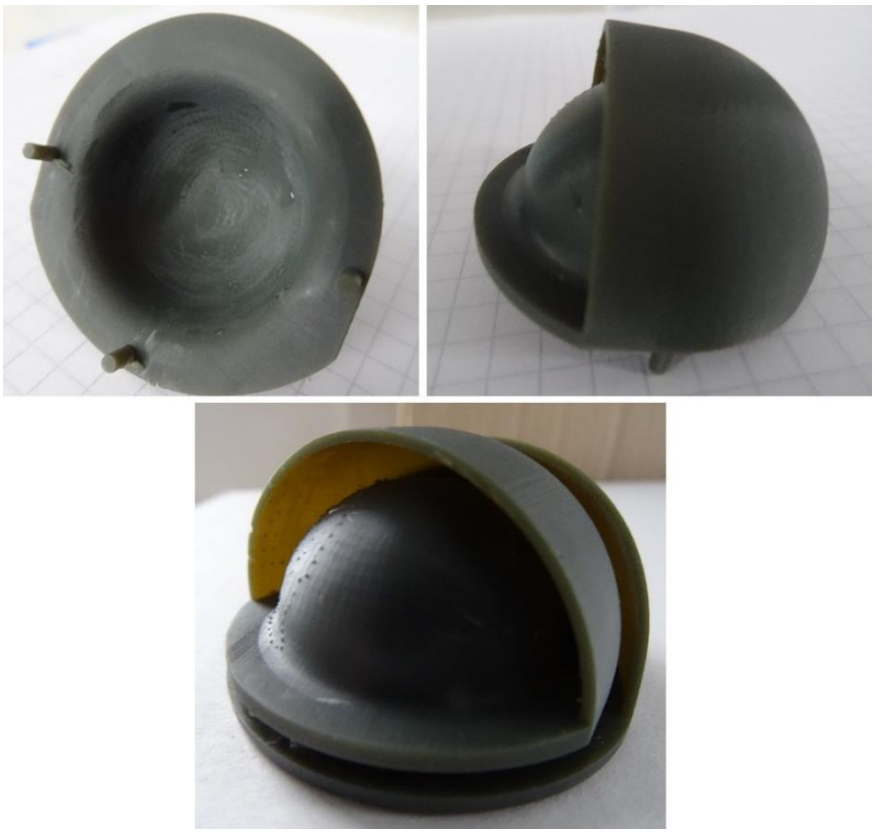

**Figure 84: Photos of finished sparger pieces and assembly (iteration #5)**

## Laboratory Water Testing

The inner hood extension proved successful in directing flow; flow speed was the same as in iteration #4, but now the water ran outwardly across where the defoamer would be placed in the completed device (Figures 85 and 86). Iteration #5 was a successful prototype using simple water flow experiments; at this point certain iterations were

tested with blood to assess their potential real-life application. Moving forward, the remaining area of flow improvement lies in optimising upward flow out of the sparger, such as possibly altering hood spacing or decreasing slope of the sparger or hood. To encourage more even flow across the hood.

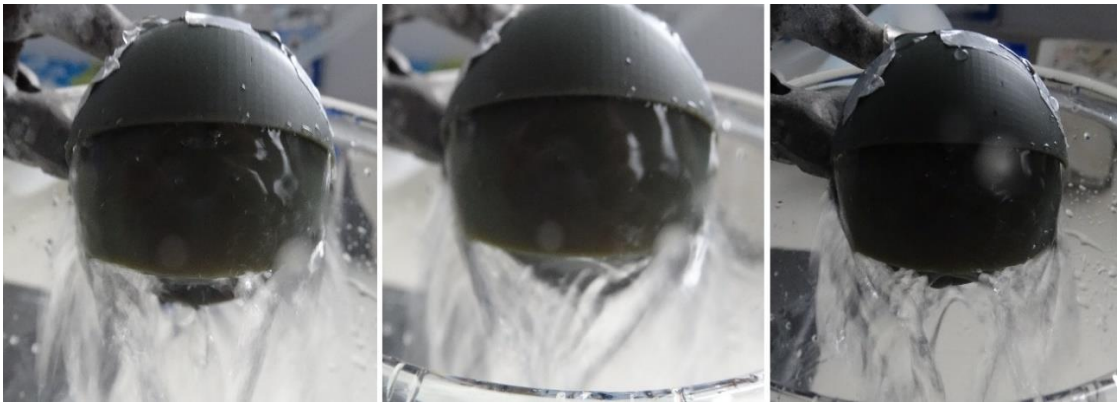

**Figure 85: Photos of front profile spray (iteration #5)**

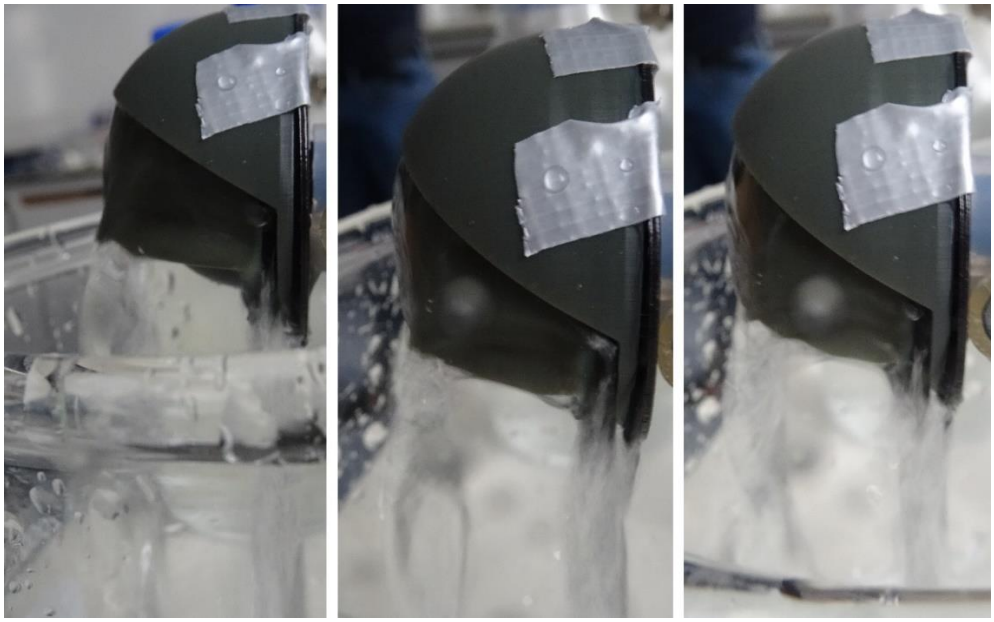

**Figure 86: Photos of side profile spray (iteration #5)**

## Haemolysis Testing

After analysing fluid flow with water, the next step was to test a set of prototypes using blood; blood is a biological fluid containing living cells affected during flow through the device. Although a variety of blood tests exist, RBC lysis evaluation was one of the only viable tests because the current device material is not biocompatible—it will react with blood components and cause problems such as platelet aggregation. The blood flow trials were performed only once due to limited time. More trials will be performed beyond thesis submission.

Four trials were run for haemolysis comparison:

1. Control: no device attached
2. Iteration #3: four posts
3. Iteration #4
4. Iteration #5

A baseline value (control) was established by running blood through the open tube connecter without any sparger. The two-post sparger (iteration #2) was reprinted using the EnvisionTEC® printer and had been selected for testing because it generated the most turbulent and varying flow, but the posts snapped at the last minute. The 4-post configuration of iteration #3 was used because two of the posts in the 3-post model broke while taping the device to the connector. Iteration #4 was chosen because it produced the best flows; iteration #5 had just been printed and was thus tested alongside the other two prototypes to compare with #4.

### Control (No Attachments)

Flow through the baseline configuration with no sparger attachment displayed an expected narrow pulsatile flow ejected from the tube and into the reservoir. The noteworthy characteristic of the impelled blood was its velocity, which was greater than the blood flow through any of the spargers (Figure 87).

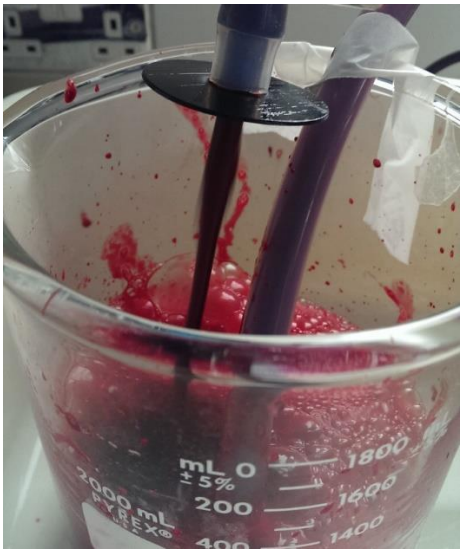


**Figure 87: Photo of blood flow through connector (control)**

The control trial generated a very large volume of foam (Figure 88)—the most of all the trial runs—due to significant air-blood mixing caused by high velocity flow hitting a flat surface (the container wall or the fluid surface).


**Figure 88: Photo of blood foam developed after 5 minutes (control)**

## Iteration #3: 4-post configuration

The blood flow through the 4-post sparger produced the greatest volume and range of blood spatter; however spatter and turbulence were significantly less than with water in this and all models due to the greater density and viscosity of blood. The density of the blood meant gravity exerted a greater force, and as a result blood flowed down the outside of the sparger instead of arching outward (Figure 89). Blood flow did not appear to become obstructed at any point during the 5-minute run.

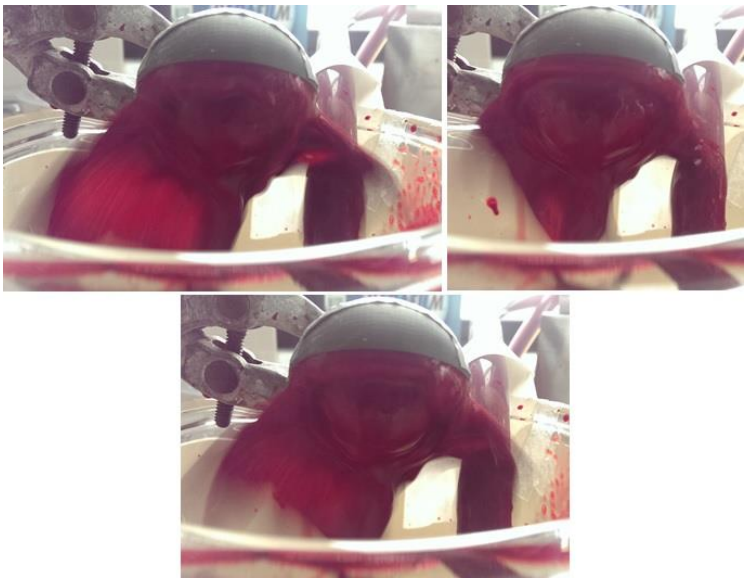

**Figure 89: Photos of blood flow through sparger (iteration #3, 4 posts)**

This iteration generated more foam than the optimal design, iteration #4, due to (1) the open space between the disc and sparger, (2) the 4 posts disrupting flow along the sparger surface, and/or (3) the higher flow velocity compared to iterations #4 and #5.


**Figure 90: Photo of blood foam developed after 5 minutes (iteration #3, 4 posts)**

## Iteration #4

The blood flow through iteration #4 was slow and controlled with blood running over the outside of the sparger, as had been observed previously in water tests (Figure 91). No blood spattered beyond the reservoir area, and the system was stable with very little movement despite the pulsatile flow. No major platelet aggregation was visible during the run, with fluid flowing continuously across the entire sparger circumference.

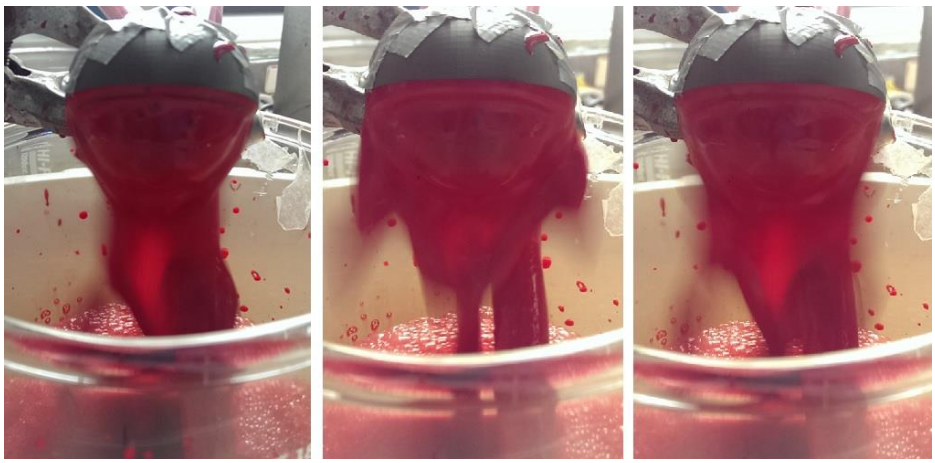

**Figure 91: Photos of blood flow through sparger (iteration #4)**

Foam level was lowest in this iteration likely due to low flow velocity. The collection bag inflow device should produce limited air-blood mixing, and this prototype significantly reduced air incorporation compared to an open flow (Figure 92, compare with Figure 88).


**Figure 92: Photo of blood foam developed after 5 minutes (iteration #4)**

## Iteration #5

Blood flow through the iteration #5 sparger produced a slightly wider spray angle than iteration #4 which may be due to the length of the inner hood or the relationship between the angles of the two hoods. Modifying the inner hood extension, altering hood angles, or moving the axis of inner hood rotation could adjust the angle of spray if necessary. An unforeseen effect of hood extension was complete blockage of flow between the hoods (within 30 seconds) possibly due to rapid platelet aggregation; consequently all flow was forced out the sides or downward, which increases shearing forces and could also contribute to the wider flow angle.

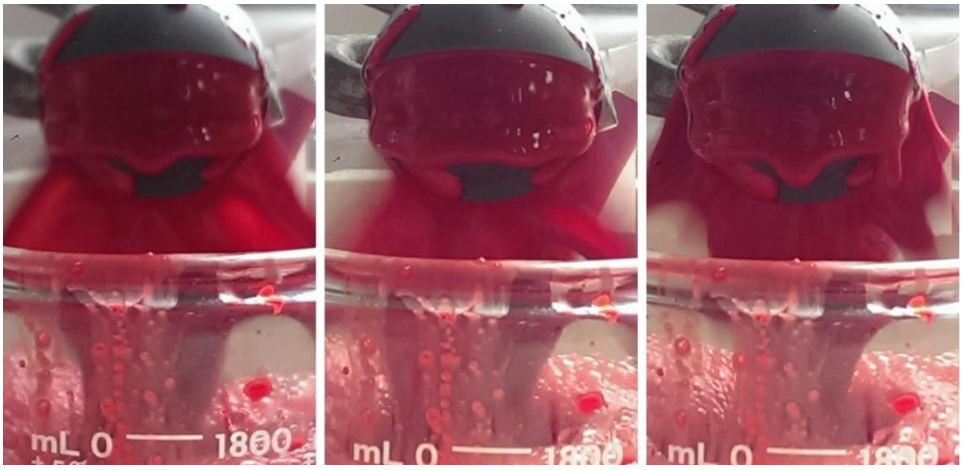


**Figure 93: Photos of blood flow through sparger (iteration #5)**

The iteration #5 sparger produced the largest amount of foam of the three sparger trials, second only to the control (Figure 92). The reason for this result was flow blockage between the hoods forcing the blood to exit through an outlet of decreased surface area. Foam production would likely be similar to iteration #4 if blockage had not occurred.


**Figure 94: Photo of blood foam developed after 5 minutes (iteration #5)**

Samples taken from each test run were placed in 20ml screw-top containers (Figure 95). A 1ml portion was removed and used for haemolysis testing, while the remainder was stored in the lab refrigerator alongside a container of un-pumped blood; the un-touched sample was not tested in this experiment but will be tested at a later time to evaluate pump-induced haemolysis.


**Figure 95: Photo of blood samples collected for testing**

Figure 96 shows the density-separated samples and haemoglobin staining. Centrifugation revealed very darkly stained plasma in iteration #3, indicating a large amount of haemolysis. Haemolysis is likely primarily due to flow turbulence within the sparger's open space; this hypothesis should be tested by evaluating the 3-post open iteration to determine whether inner posts significantly contribute to haemolysis. Plasma staining in iterations #4 and #5 was very similar to the control, signifying these prototypes did not cause haemolysis themselves and are worth pursuing beyond this thesis.

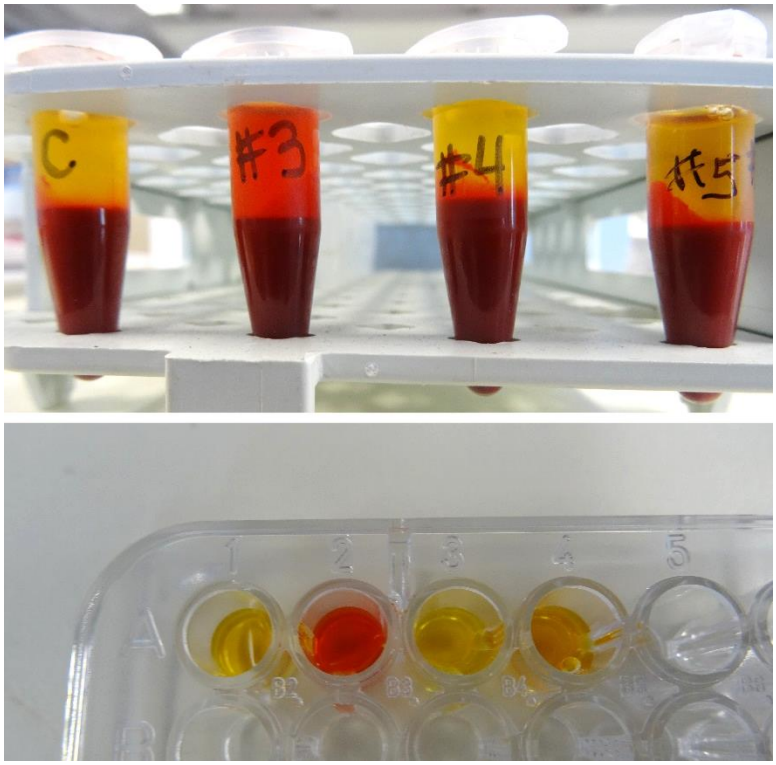


**Figure 96: Photos of plasma staining after centrifugation (from left to right: control, iteration #3, #4, #5)**

The spectrophotometer readings support the visual results and also show iteration #3 produced approximately 6x greater haemolysis than the control run (Table 8). Iteration #4 appeared to reduce haemolysis (by ~14%) compared to baseline, and iteration #5—although causing slightly more haemolysis than the control—may prove to reduce haemolysis with 360° unimpeded flow.

**SPECTROPHOTOMETER READINGS AT 540NM**

| **SAMPLE** | Control (no device) | Iteration #3 (4 posts) | Iteration #4 | Iteration #5 |
|---|---|---|---|---|
| **READING** | 0.212 | 1.377 | 0.182 | 0.280 |

**Table 8: Spectrophotometer readings for blood samples**

Time did not permit conversion of the spectrophotometer readings to % haemolysis values; this involves titration (performing a dilution series) of concentrated haemoglobin to create a standard curve. The haemoglobin source must be of known concentration to quantify the haemoglobin percentages throughout the series and in test samples. This concentrate must to be ordered or produced and a standard curve created; the procedure could not be performed within the thesis timeframe, but it is a next step in the testing process.

# Discussion

Design iteration #4 proved a functional success and will be pursued beyond this thesis. This project involved five complete design iterations in pursuit of a functional bag-mountable sparger device capable of (1) holding the defoaming material and filtration sock, (2) slowing the velocity of incoming flow, (3) dispersing horizontal flow across the inner surface of a vertically-hanging sock, and (4) directing this flow without inducing haemolysis. The presently designed device should be able to grip the defoamer and sock, however neither defoamer nor sock was attached or fluid tested with any device iteration. The sparger device does manipulate flow without damaging RBCs, and it has proven capable of slowing and radially dispersing fluid flow. However an issue remains with directing the upward flow outward away from the sparger and toward the defoamer surface.

The primary structures of the blood flow device were selected for specific functional reasons. A sparger mechanism was chosen because of its radial fluid spread, while a hemispherical shape was employed to minimize shearing and decrease velocity by turning the streamlines ~180°. Hooded attachments were used to arc flow and hold the sock away from the outer sparger surface.

## Summary of Design Process & Findings

The first iteration was not printable due to both hooded pieces being printed as a unit; inner support structures could not be removed without destroying the connecting post. However fluid simulation did show that the sparger shape and design would slow incoming flow. The second iteration separated the part into two components which were connected after printing. Three posts along the sparger's outer rim proved non-disruptive to flow and provided the most stable method of connecting the two pieces. Water testing of iterations #2 and #3 showed the devices worked but needed

improvement because flow was unacceptably fast and unevenly distributed; iteration #3 also induced significant haemolysis.

Iteration #4, which allowed incoming fluid only 2mm of depth across the sparger, dramatically decreased outflow velocity and also did not cause haemolysis. Iteration #5 was a variation on #4, with an inner hood extension meant to prevent upward flow from running down the outside of the sparger. This modification successfully prevented such an occurrence, but flow between the hoods became blocked within seconds; flow cessation is possibly due to platelet aggregation caused by the non-biocompatible device material. Methods of extending the flow outward away from the sparger must be further explored.

## Prototype for Continued Development

Sparger iteration #4 will continue to be pursued and undergo further development as the flow control device for the field-deployable autotransfusion system (Figure 97). The device will need modifications to shape the flow path, but the sparger does not damage blood and outputs a slow, laminar flow in all directions.

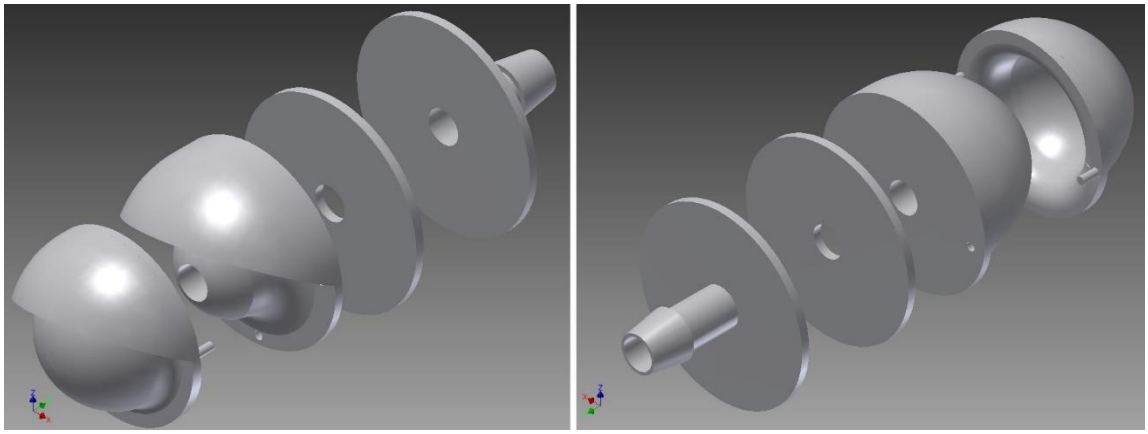

**Figure 97: Images of complete setup involving sparger iteration #4**

Modifications to the structure which could assist in shaping flow include adjusting the hood angles, downward extension of the inner hood, or changing distance between the

hoods; decreasing hood spacing would increase the velocity of the corresponding flow and propel fluid farther. The sock with the defoaming insert has not been handled yet, so size could prove an issue; the device can be scaled down if it overstretches or deforms the defoamer and sock.

## Additional Testing & Future Directions

More experiments are still required to complete the haemolysis testing portion of the current project segment; a standard curve must be created to convert spectrophotometer data to % haemolysis, and the haemolysis experiment must be performed at least two more times to confirm repeatability of results. Also the haemolytic potential of the 3-post iteration #3 sparger must be analysed to confirm the hypothesis that open space within the sparger is the primary cause of haemolysis.

Additional tests to perform with the iteration #4 sparger and its successors include running new fluid simulations using alternative CAD models which do not contain flow within a cylindrical 'sock-like' vessel; instead the sparger device can be extruded out of a large cube simulating free space. The extended hood of iteration #5 will be coated with a biocompatible film and the prototype retested to better evaluate its potential and to determine if platelet aggregation was the cause of flow cessation. Also a blood-air mixture will be generated and run through the sparger; the device must be able to perform well with significant volumes of air in the blood because it mimics blood suctioned from wounds. To assess flow distribution across the sock, a dye-colored saline mixture will be pumped through the device and attached sock. Eventually the system's ability to defoam and filter blood will be tested by attaching the defoamer and sock to the sparger and circulating a blood-air mixture.

When the manual pump is ready for fluid testing, the device will be attached and both water and blood tests performed to evaluate performance and haemolysis. The final testing phases will involve placing the complete device into (and onto) the blood bag to

evaluate the complete system. Furthermore whenever the sparger components are printed in a durable, biocompatible material, blood parameters beyond haemolysis can be measured and device durability tests performed.

## Alternate Designs

Design alterations more complex than minor adjustments to the hoods or flow depths may ultimately be required for this sparger device; if necessary, changes are likely to involve shaping the sock and defoamer. Constructs could be built onto the hooded disc or a thin and compressible 'skeleton' put in place to better shape the sock. The high-flow container shown earlier (Figure 19) holds the sock open and in place using a thin plastic strip hung within the sock; a similar structure could be used within the collection bag system.

The sparger mechanism could still be employed if blood were to enter the top of the bag; a CAD drawing of one possible iteration of a horizontal sparger is shown in Figure 98.

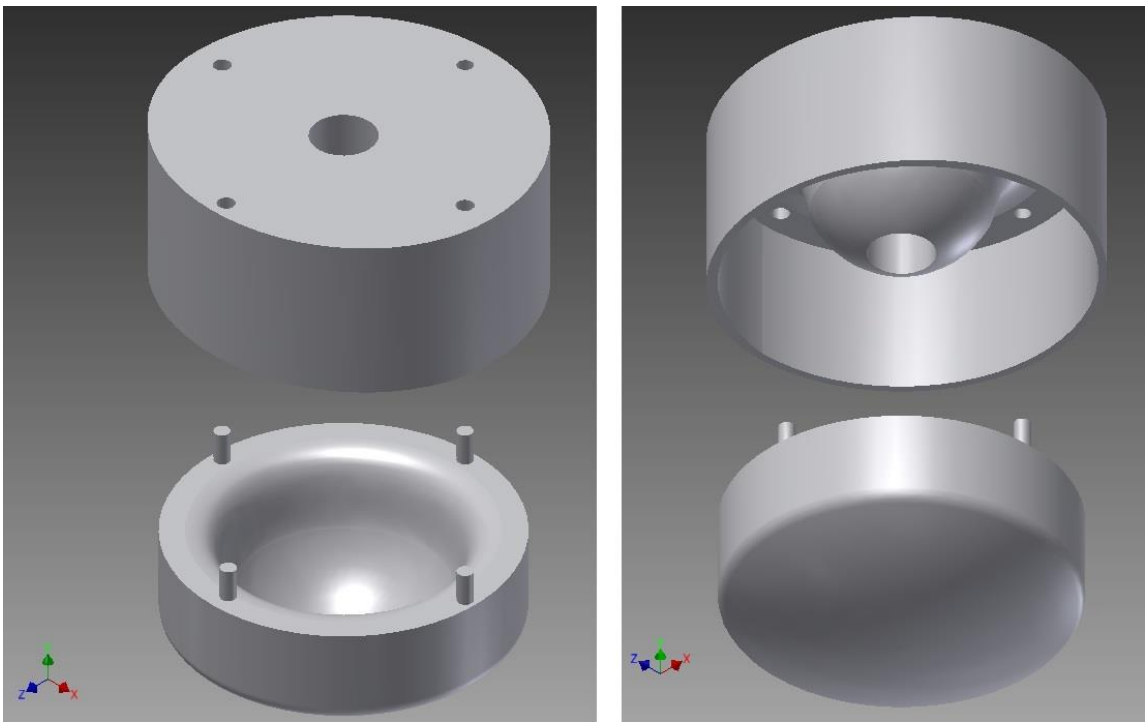

**Figure 98: CAD image of alternate blood flow device #1**

Another alternate design for flow through the top or side of the bag is a simple setup with a cone-shaped insert which produces a ring-shaped flow (Figure 99).

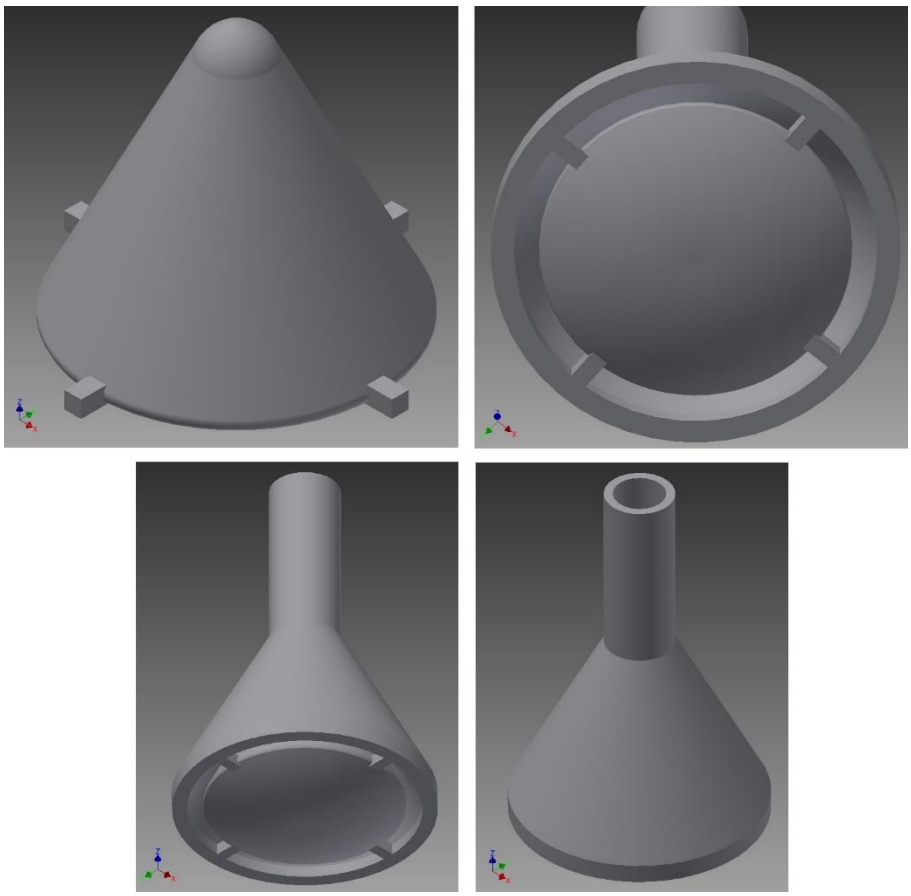

**Figure 99: CAD images of alternate blood flow device #2**

These alternative prototypes are not being pursued, but they are viable possibilities if future obstacles arise rendering the side-mounted sparger prototype unusable. Currently the iteration #4 sparger proves a promising blood flow device, and its development will continue beyond this project remit.

# References


3D Alchemy. (2012). *3d-alchemy.co.uk*. Retrieved from Materials for 3D Printing: http://www.3d-alchemy.co.uk/list-of-materials-for-3d-printing.html

American College of Surgeons. (2015). *ATLS: Advanced Trauma Life Support.* Retrieved from facs.org: https://www.facs.org/quality-programs/trauma/atls

Arai, H., Petchclai, B., Khupulsup, K., Kurimura, T., & Takeda, K. (1999). Evaluation of a Rapid Immunochromatographic Test for Detection of Antibodies to Human Immunodeficiency Virus. *J Clin Microbiol*, 367-370.

Army Regulation 40-8. (2007). *Temporary Flying Restrictions Due to Exogenous Factors Affecting Aircrew Efficiency.* Regulation manual.

Avery Jr, D. M., & Avery, K. T. (2010). Blood Component Therapy. *American Journal of Clinical Medicine*, 57-59.

Bhangu, A., Nepogodiev, D., Doughty, H., & Bowley, D. M. (2013). Intraoperative cell salvage in a combat support hospital: a prospective proof of concept study. *Transfusion*, 805-810.

Bickell, W. H., Wall Jr, M., Pepe, P. E., Martin, R. R., Ginger, V. F., Allen, M. K., & Mattox, K. L. (1994). Immediate versus delayed fluid resuscitation for hypotensive patients with penetrating torso injuries. *The New England Journal of Medicine*, 1105-1109.

Blood Flow Online. (2015). *Blood Viscosity Defined*. Retrieved from bloodflowonline.com: http://www.bloodflowonline.com/learn-about-blood-viscosity/blood-viscosity-basics

Borgman, M. A., Spinella, P. C., Perkins, J. G., Grathwohl, K. W., Repine, T., Beekley, A. C., . . . Holcomb, J. B. (2007). The Ratio of Blood Products Transfused Affects Mortality in Patients Receiving Massive Transfusions at a Combat Support Hospital. *The Journal of Trauma Injury, Infection ,and Critical Care*, 805-813.

Bound Tree Medical. (2013). *BTM Field Blood Transfusion Kit.* Retrieved from boundtree.com.

Bowling, S. F., & Pennardt, C. (2010). The Use of Fresh Whole Blood Transfusions by the SOF Medic for Hemostatic Resuscitation in th Austere Environment. *J Spec Oper Med, 10*(3), 25-35.

Brockoff, A., & Plechinger, H. (2003, Feb 11). *US Patent No. US6517732 B1.*

Brohi, K., Cohen, M. J., & Davenport, R. A. (2007). Acute coagulopathy of trauma: mechanism, identification and effect. *Curr Opin Crit Care*, 680-685.

Caliste, X. A., McArthur, K. A., & Sava, J. A. (2014). Autotransfusion in emergent operative trauma resuscitation. *Eur J Trauma Emerg Surg*, 541-545.

Champion, H. R., Bellamy, R. F., Roberts, C. P., & Leppaniemi, A. (2003). A Profile of Combat Injury. *The Journal of Trauma Injury, Infection, and Critical Care*, S13-S19.

Chinook Medical Gear. (n.d.). *chinookmed.com.* Retrieved from Tactical Medical Kits (TMK).

Cutnell, J. D., & Johnson, K. (1998). *Physics* (4th ed.). Carbondale, IL, United States: Southern Illinois University.

Cyprotex. (2015). *In vitro Toxicology: In vitro Hemolysis.* Retrieved from cyprotex.com: http://www.cyprotex.com/product_sheets/Cyprotex_Hemolysis_Product_Sheet.pdf

Eastridge, B. J., Mabry, R. L., Seguin, P., Cantrell, J., Tops, T., Uribe, P., . . . Blackbourne, L. H. (2012). Death on the battlefield (2001-2011): Implications for the future of combat casualty care. *J Trauma Acute Care Surg*, S431-S437.

EnvisionTEC. (n.d.). *Perfactory Desktop XL.* Retrieved from envisiontec.com: http://envisiontec.com/envisiontec/wp-content/uploads/MK-MCS-DesktopXL-V01-FN-EN.pdf

EnvisionTEC. (n.d.). *Perfactory Material: HTM140 High Temperature Mold Material.* Retrieved from envisiontec.com: http://envisiontec.com/envisiontec/wp-content/uploads/MK-MTS-HTM140Industrial-V01-FN-EN.pdf

Friedman, R. S. (2002). *United States Patent No. US 6,482,360 B2.*

Gan, T. J. (2011). Colloid or Crystalloid: Any Differences in Outcome? *IARS 2011 Review Course Lectures*, 7-12.

Gerecht, R. (2014). Trauma's Lethal Triad of Hypothermia, Acidosis & Coagulopathy Create a Deadly Cycle for Trauma Patients . *Journal of Emergency Medical Services*.

Gourlay, T., & Robertson, C. (2014, Dec 16). Development of a portable blood salvage and auto-transfusion technology to enhance survivability of personnel requiring major medical interventions. *Center of Defense Enterprise: Enduring Challenge*. Defense Science and Technology Laboratory, Centre for Defence.

Gunaydin, S., & Gourlay, T. (2013). Novel Ultrafiltration Technique for Blood Conservation in Cardiac Operations. *Ann Thorac Surg*, 2148-51.

Haemonetics. (2013). *SQ40 Microaggregate Blood Transfusion Filter*. Retrieved from wbt.haemonetics.com: http://wbt.haemonetics.com/en/Products/Filtration-and-Transfusion/Microaggregate-Blood-Tx-Filter

Hagman. (2012). *Pre-Hospital Buddy Transfusion.* Retrieved from rdcr.org.

Höfer, R., Jost, F., Schwuger, M. J., Scharf, R., Geke, J., Kresse, J., . . . Erwied, W. (2003). Foams and Foam Control. In B. Elvers, *Ullmann's Encyclopedia of Industrial Chemistry.* Weinheim: Wiley-VCH.

Holcomb, J. B., McMullin, N. R., Pearse, L., Caruso, J., Wade, C. E., Oetjen-Gerdes, L., . . . Butler, F. K. (June 2007). Causes of Death in U.S. Special Operations Forces in the Global War on Terrorism 2001-2004. *Annals of Surgery*, 986-991.

Hsu, J. M., & Pham, T. N. (2011). Damage control in the injured patient. *Int J Crit Illn Inj Sci.*, 66-72.

Huet, C., Salmi, L. R., Fergusson, D., Koopman-van Gemert, A. W., Rubens, F., & Laupacis, A. (1999). A Meta-Analysis of the Effectiveness of Cell Salvage to Minimize Perioperative Allogeneic Blood Transfusion in Cardiac and Orthopedic Surgery. *Anesth Analg*, 861-869.

Kaplan, L. J., & Maerz, L. L. (2015, Jan 27). *Transfusion and Autotransfusion.* Retrieved from emedicine.medscape.com.

Kashuk, J. L., Moore, E. E., Millikan, J. S., & Moore, J. B. (1982). Major Abdominal Vascular Trauma--A Unified Approach. *The Journal of Trauma*, 672-679.

Kasotakis, G., Sideris, A., Yang, Y., de Moya, M., Alam, H., King, D. R., . . . Velmahos, G. (2013). Aggressive early crystalloid resuscitation adversely affects outcomes in adult blunt trauma patients: An analysis of the Glue Grant database. *Journal of Trauma and Acute Care Surgery*, 1215-1222.

Kauvar, D. S., Holcomb, J. B., Norris, G. C., & Hess, J. R. (2006). Fresh Whole Blood Transfusion: A Controversial Military Practice. *Journal of Trauma Injury, Infection, and Critical Care*, 181-184.

Kelly, J. F., Ritenour, A. E., McLaughlin, D. F., Bagg, K. A., Apodaca, A. N., Mallak, C. T., . . . Holcomb, C. J. (2008). Injury Severity and Causes of Death From Operation Iraqi Freedom and Operation Enduring Freedom: 2003-2004 Versus 2006. *The Journal of Trauma Injury, Infection, and Critical Care*, S21-S27.

Korea International Trade Association. (2015). *BEOT Sparger*. Retrieved from tradeKorea.com: http://www.tradekorea.com/products/productDetail.do?productno=417754

Lawton, G., Granville-Chapman, J., & J, P. P. (2009). Novel Haemostatic Dressings. *JR Army Med Corps*, 309-314.

Mabry, R. L., Holcomb, J. B., Baker, A. M., Cloonan, C. C., Uhorchak, J. M., Perkins, D. E., . . . Hagmann, J. H. (2000). United States Army Rangers in Somalia: An Analysis of Combat Casualties on an Urban Battlefield. *The Journal of Trauma Injury, Infection, and Critical Care*, 515-529.

Manno, C. S., Hedberg, K. W., Kim, H. C., Bunin, G. R., Nicolson, S., Jobes, D., . . . Norwood, W. I. (1991). Comparison of the Hemostatic Effects of Fresh Whole Blood, Stored Whole Blood, and Components After Open Heart Surgery in Children. *Blood*, 930-936.

McMullin, N. R., Holcomb, J. B., & Sondeen, J. (2006). Hemostatic Resuscitation. *Yearbook of Intensive Care and Emergency Medicine*, 265-278.

Pall Medical. (2009). *Supor EKV Membrane Fiilters*. Retrieved from pall.com: http://www.pall.com/pdfs/Laboratory/91927-Supor_EKV.pdf

Pall Medical. (2009). *Supor EKV Membrane Filters.* Retrieved from pall.com: http://www.pall.com/pdfs/Laboratory/91927-Supor_EKV.pdf

Pall Medical. (2011). *Supor AEF 0.2 um Intravenous Filter.* Retrieved from pall.com: http://www.pall.com/pdfs/Medical/11-6916_SuporAEF_Filter_SS_HR.pdf

Pall Medical. (2011). *Supor AEF 0.2 um Intravenous Filter*. Retrieved from pall.com: http://www.pall.com/pdfs/Medical/11-6916_SuporAEF_Filter_SS_HR.pdf

Palmer, C. (2007). Major Trauma and the Injury Severity Score -- Where Should We Set the Bar? *Annu Proc Assoc Adv Automot Med*, 13-29.

Perkins, J. G., Cap, A. P., Weiss, B. M., Reid, ,. J., & Bolan, C. E. (2008). Massive transfusion and nonsurgical hemostatic agents. *Crit Care Med*, S325-S339.

Phillips, E. M., & Davis, G. L. (2014, Dec 8). *Volume Resuscitation.* Retrieved from emedicine.medscape.com.

Repine, T. B., Perkins, J. G., Kauvar, D. S., & Blackborne, L. (2006). The Use of Fresh Whole Blood in Massive Transfusion. *The Journal of Trauma Injury, Infection, and Critical Care*, S59-S69.

Rice, J. R. (n.d.). *Battlefield Blood Transfusion.* Powerpoint.

Rose, D. D., & Grande, C. (1998). A Historical Overview and Military Perspective on Fluid Resuscitation, Blood Salvaging Techniques, and Blood Substitutes. *Seminars in Anesthesia, Perioperative Medicine and Pain*, 239-251.

Salhanick, M., Corneille, M., Higgins, R., Olson, J., Michalek, J., Harrison, C., . . . Dent, D. (2011). Autotransfusion of hemothorax blood in tramua patients: is it the same as fresh whole blood? *The American Journal of Surgery*, 817-822.

Schoenfeld, A. J., Dunn, J. C., Bader, J. O., & Belmont Jr, P. J. (2013). The nature and extent of war injuries sustained by combat specialty personnel killed and wounded in

Afghanistan and Iraq, 2003–2011. *Journal of Trauma and Acute Care Surgery*, 287-291.

Schulman, C. (2003). Critical Care: Is Your Patient Fully Resuscitated? *Nursing Management*, 44-47.

Spahn, D. R., & Casutt, M. (2000). Eliminating Blood Transfusions: New Aspects and Perspectives. *Anesthesiology*, 242-255.

Spinella, P. C. (2008). Warm fresh whole blood transfusion for severe hemorrhage: U.S. military and potential civilian applications. *Crit Care Med*, S340-S345.

Spinella, P. C. (2013). *Whole Blood vs Components for Hemorrhagic Shock.* UC Denver.

Spinella, P. C., Carroll, C. L., Staff, I., Gross, R., & Mc Quay, J. (2009). Duration of red blood cell storage is associated with increased. *Critical Care*.

Spinella, P. C., Perkins, J. G., Grathwohl, K. W., & Beekley, A. C. (2009). Warm Fresh Whole Blood Is Independently Associated With Improved Survival for Patients With Combat-Related Traumatic Injuries. *J Trauma*, S69-S76.

Spinella, P. C., Perkins, J. G., Grathwohl, K. W., Repine, T., Beekley, A. C., Sebesta, J., . . . Holcomb, J. B. (2007). Risks associated with fresh whole blood and red blood cell transfusions in a combat support hospital. *Crit Care Med*, 2576-2581.

Test Standard Labs. (2014). *ABS Material Data Sheet.* Retrieved from teststandard.com: http://teststandard.com/data_sheets/ABS_Data_sheet.pdf

Topfer, L. A. (2015). *Hemosep: A New System for Ultrafiltration and Blood Conservation in Cardiac Surgery.* Ottawa: Canadian Agency for Drugs and Technologies in Health.

University of Strathclyde. (n.d.). *Rapid Prototyping and Manufacturing Facilities*. Retrieved from strath.ac.uk/dmem: http://www.strath.ac.uk/dmem/businessandindustry/rapidprototypingandmanufacturingfacilities/rapidprototyping/

# Appendix

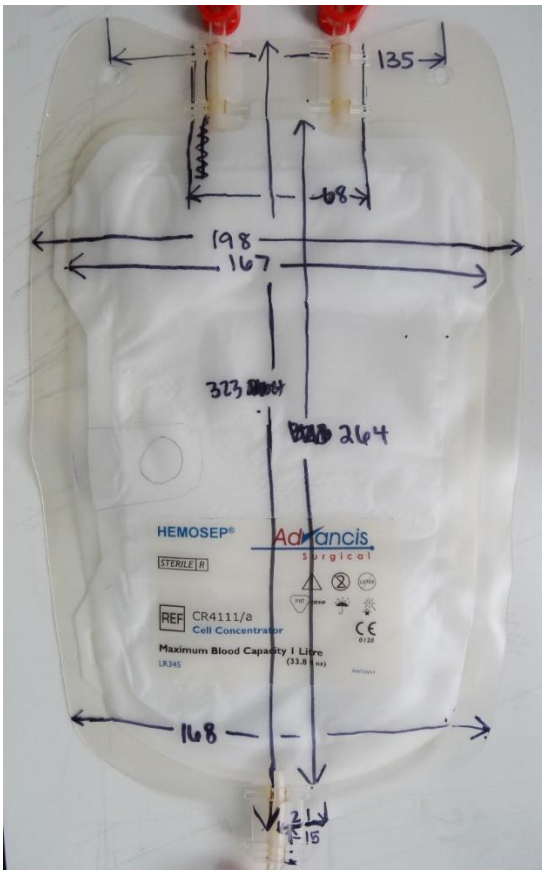


**Photo of dimensioned Hemosep® bag used to build bag within Inventor®**

| | 1 | 2 | 3 | 4 | 5 |
|---|---|---|---|---|---|
| A | 0.212 | 1.377 | 0.182 | 0.280 | 0.046 |
| B | 0.046 | 0.046 | 0.047 | 0.046 | 0.049 |
| C | 0.047 | 0.046 | 0.047 | 0.046 | 0.046 |
| D | 0.047 | 0.047 | 0.047 | 0.047 | 0.047 |
| E | 0.047 | 0.047 | 0.047 | 0.047 | 0.047 |
| F | 0.046 | 0.047 | 0.047 | 0.047 | 0.047 |
| G | 0.047 | 0.048 | 0.047 | 0.047 | 0.047 |
| H | 0.047 | 0.047 | 0.047 | 0.047 | 0.048 |

**Screen image of spectrophotometer results**

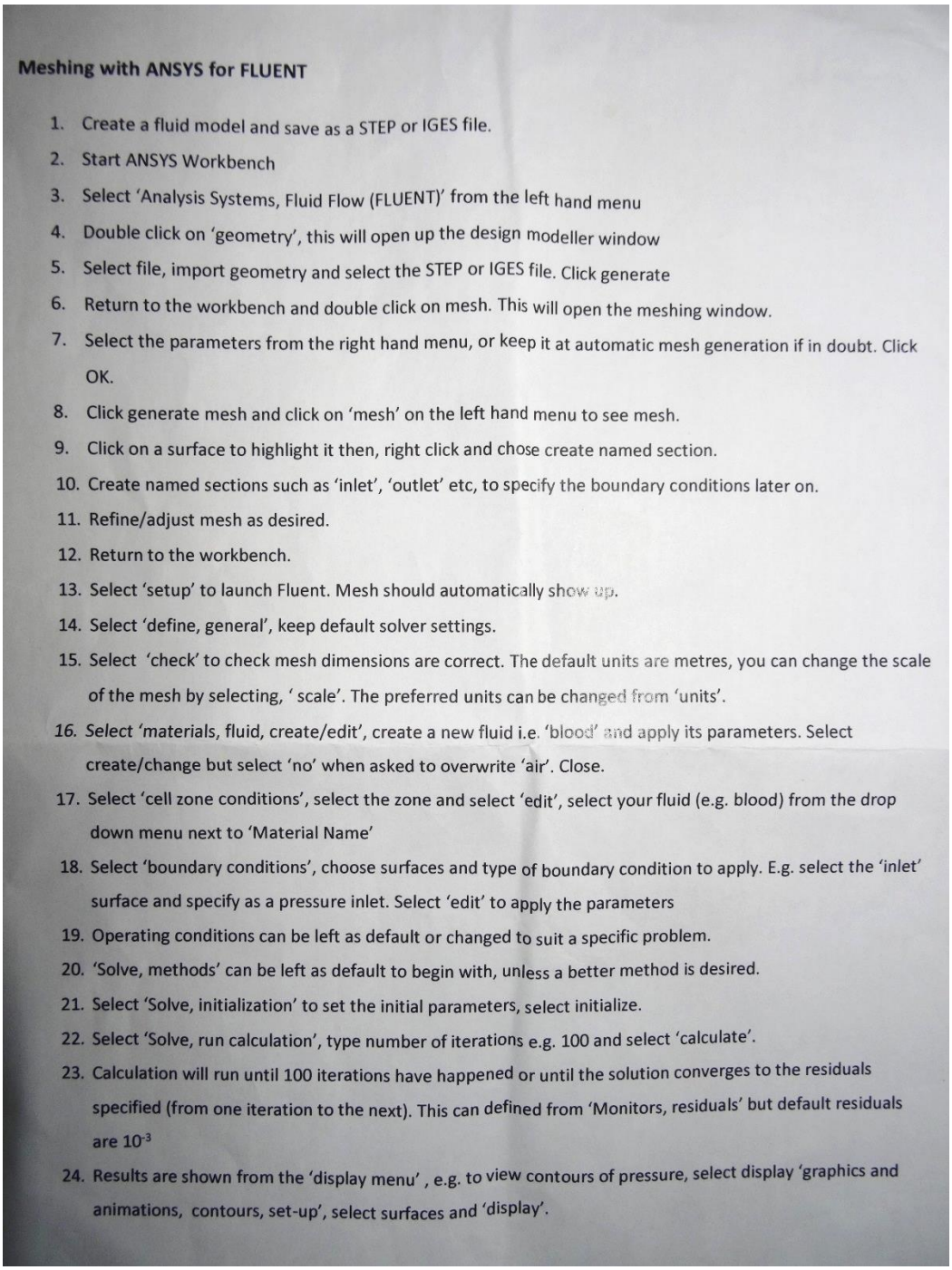

**Meshing with ANSYS for FLUENT**

1. Create a fluid model and save as a STEP or IGES file.
2. Start ANSYS Workbench
3. Select 'Analysis Systems, Fluid Flow (FLUENT)' from the left hand menu
4. Double click on 'geometry', this will open up the design modeller window
5. Select file, import geometry and select the STEP or IGES file. Click generate
6. Return to the workbench and double click on mesh. This will open the meshing window.
7. Select the parameters from the right hand menu, or keep it at automatic mesh generation if in doubt. Click OK.
8. Click generate mesh and click on 'mesh' on the left hand menu to see mesh.
9. Click on a surface to highlight it then, right click and chose create named section.
10. Create named sections such as 'inlet', 'outlet' etc, to specify the boundary conditions later on.
11. Refine/adjust mesh as desired.
12. Return to the workbench.
13. Select 'setup' to launch Fluent. Mesh should automatically show up.
14. Select 'define, general', keep default solver settings.
15. Select 'check' to check mesh dimensions are correct. The default units are metres, you can change the scale of the mesh by selecting, ' scale'. The preferred units can be changed from 'units'.
16. Select 'materials, fluid, create/edit', create a new fluid i.e. 'blood' and apply its parameters. Select create/change but select 'no' when asked to overwrite 'air'. Close.
17. Select 'cell zone conditions', select the zone and select 'edit', select your fluid (e.g. blood) from the drop down menu next to 'Material Name'
18. Select 'boundary conditions', choose surfaces and type of boundary condition to apply. E.g. select the 'inlet' surface and specify as a pressure inlet. Select 'edit' to apply the parameters
19. Operating conditions can be left as default or changed to suit a specific problem.
20. 'Solve, methods' can be left as default to begin with, unless a better method is desired.
21. Select 'Solve, initialization' to set the initial parameters, select initialize.
22. Select 'Solve, run calculation', type number of iterations e.g. 100 and select 'calculate'.
23. Calculation will run until 100 iterations have happened or until the solution converges to the residuals specified (from one iteration to the next). This can defined from 'Monitors, residuals' but default residuals are $10^{-3}$
24. Results are shown from the 'display menu' , e.g. to view contours of pressure, select display 'graphics and animations, contours, set-up', select surfaces and 'display'.

**Basic instructions for Fluent® modelling**

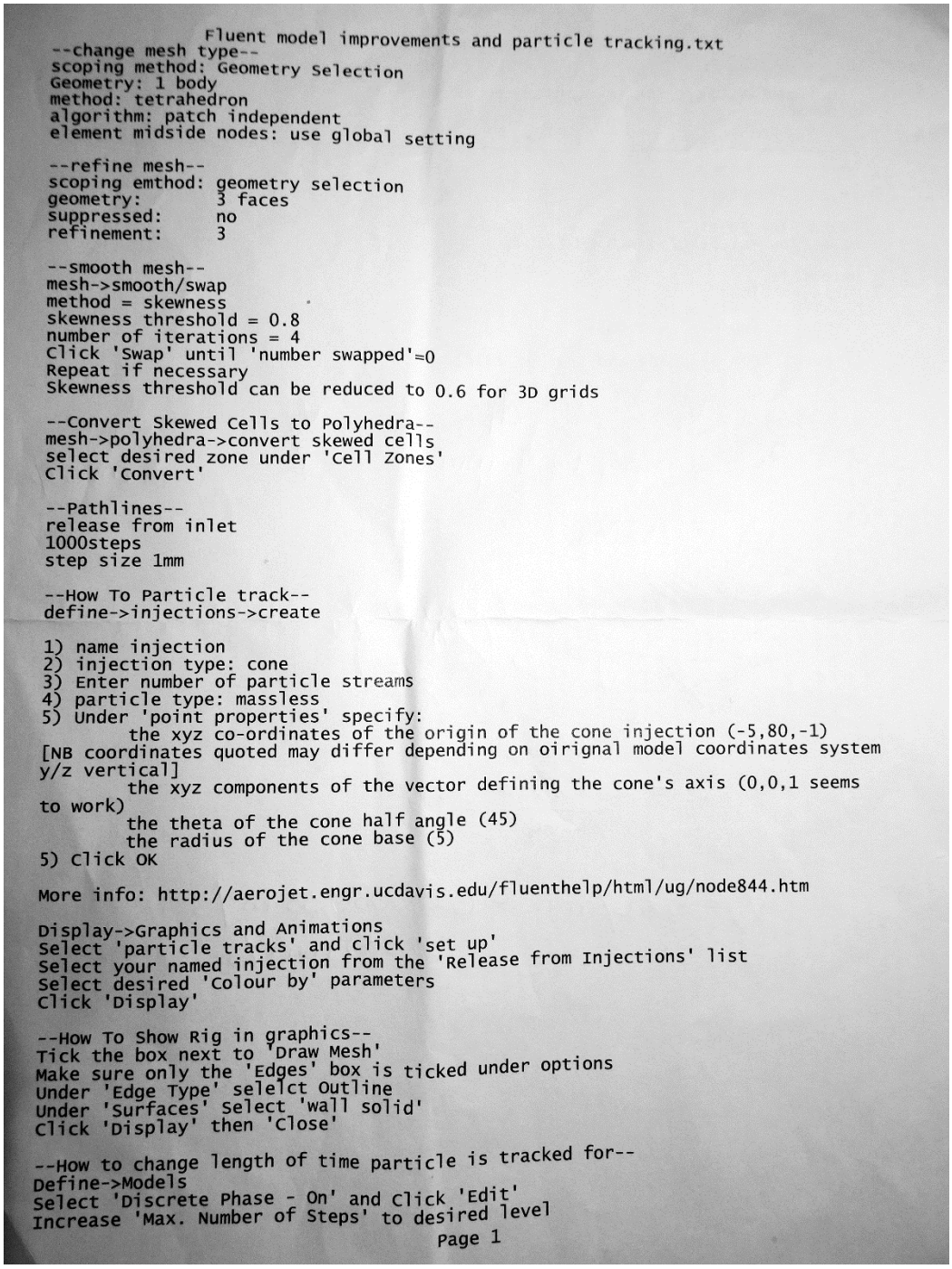

Fluent model improvements and particle tracking.txt

--change mesh type--
scoping method: Geometry Selection
Geometry: 1 body
method: tetrahedron
algorithm: patch independent
element midside nodes: use global setting

--refine mesh--
scoping emthod: geometry selection
geometry: 3 faces
suppressed: no
refinement: 3

--smooth mesh--
mesh->smooth/swap
method = skewness
skewness threshold = 0.8
number of iterations = 4
Click 'Swap' until 'number swapped'=0
Repeat if necessary
Skewness threshold can be reduced to 0.6 for 3D grids

--Convert Skewed Cells to Polyhedra--
mesh->polyhedra->convert skewed cells
select desired zone under 'Cell Zones'
Click 'Convert'

--Pathlines--
release from inlet
1000steps
step size 1mm

--How To Particle track--
define->injections->create

1) name injection
2) injection type: cone
3) Enter number of particle streams
4) particle type: massless
5) Under 'point properties' specify:
the xyz co-ordinates of the origin of the cone injection (-5,80,-1)
[NB coordinates quoted may differ depending on oirignal model coordinates system
y/z vertical]
the xyz components of the vector defining the cone's axis (0,0,1 seems
to work)
the theta of the cone half angle (45)
the radius of the cone base (5)
5) Click OK

More info: http://aerojet.engr.ucdavis.edu/fluenthelp/html/ug/node844.htm

Display->Graphics and Animations
Select 'particle tracks' and click 'set up'
Select your named injection from the 'Release from Injections' list
Select desired 'Colour by' parameters
Click 'Display'

--How To Show Rig in graphics--
Tick the box next to 'Draw Mesh'
Make sure only the 'Edges' box is ticked under options
Under 'Edge Type' selelct Outline
Under 'Surfaces' Select 'wall solid'
Click 'Display' then 'Close'

--How to change length of time particle is tracked for--
Define->Models
Select 'Discrete Phase - On' and Click 'Edit'
Increase 'Max. Number of Steps' to desired level

Page 1

**Fluent® model improvements and alteration suggestions**


**Epoxy glue and primer used to attach sparger pieces**

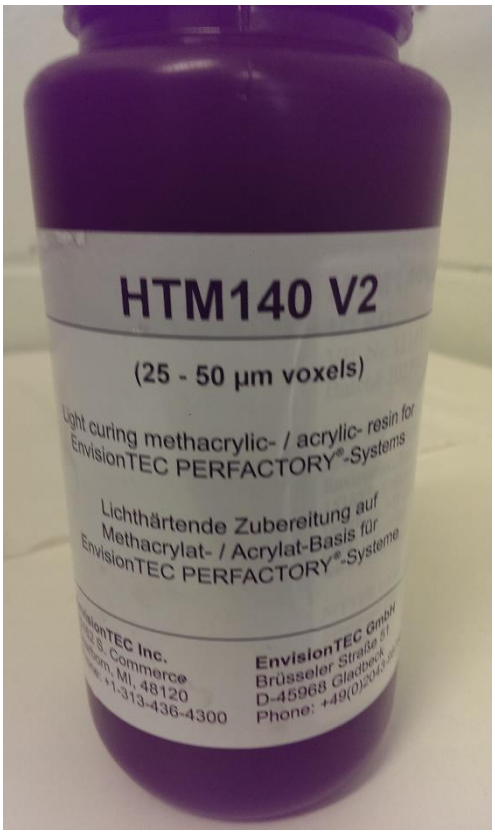


**HTM140 high temperature photopolymer (material used in EnvisionTEC® printing)**